

Unitarity and On-Shell Recursion Methods for Scattering Amplitudes

by

Kasper Risager

Submitted for the degree of Ph.D. in Physics from the
Niels Bohr Institute, Faculty of Science,
University of Copenhagen.

November 2007
(April 2008)

Abstract

This thesis describes some of the recent (and some less recent) developments in calculational techniques for scattering amplitudes in quantum field theory. The focus is on on-shell recursion relations in complex momenta and on the use of unitarity methods for loop calculations. In particular, on-shell recursion is related to the MHV rules for computing tree-level gauge amplitudes and used to extend the MHV rules to graviton scattering. Combinations of unitarity cut techniques and recursion are used to argue for the “No-Triangle Hypothesis” in $\mathcal{N} = 8$ supergravity which is related to its UV behaviour. Finally, combinations of unitarity and recursion are used to demonstrate the full calculation of a one-loop amplitude involving a Higgs particle and four gluons in the limit of large top mass. The present version is edited to incorporate some of the comments and suggestions of the evaluation committee, but has not been updated for developments in the meantime.

Contents

1	Introduction	5
1.1	Scattering Amplitudes in Theory and Experiment	5
1.1.1	Background Processes at the LHC	6
1.1.2	Approaching Quantum Gravity?	7
1.2	Scattering Amplitudes in the Complex Plane	7
1.2.1	The Unitary and Analytic S -Matrix	8
1.2.2	Generalizing from Loops to Trees	10
1.2.3	Full Amplitudes from Trees	11
1.3	About This Thesis	12
1.3.1	Omissions	12
1.3.2	Outline	12
1.4	Conclusion and Outlook	13
1.4.1	A Competitor in the Calculation Race	13
1.4.2	Understanding Quantum Field Theories	14
2	Preliminaries	15
2.1	Colour Ordering	15
2.2	Spinor Helicity Notation	16
2.3	Tree-Level Structure of Yang–Mills Theory	19
2.3.1	MHV Amplitudes	19
2.3.2	Supersymmetry	20
2.3.3	Limit Behaviour	22
2.4	Gravity as a Quantum Field Theory	23
2.4.1	The KLT Relations	23
2.4.2	The $\mathcal{N} = 8 / \mathcal{N} = 4$ Relation	24
3	Tree Level Methods	27
3.1	Earlier Methods	27
3.2	MHV Rules	28
3.2.1	Basic Construction	28
3.2.2	Gravity: A Puzzling Failure	31
3.2.3	Fermions, Higgses, and Vector Bosons	32
3.3	On-Shell Recursion Relations	33

3.3.1	Using Cauchy’s Theorem on Yang–Mills Amplitudes	34
3.3.2	Three-Point Amplitudes (and an Example)	35
3.3.3	Asymptotic Behaviour of the Deformed Amplitude	37
3.3.4	Some Consequences of BCFW on-shell recursion	38
3.3.5	Extension to Other Theories and Deformations	38
4	MHV Rules from Recursion	41
4.1	MHV Rules in Light of Recursion Relations	41
4.2	The NMHV Case	42
4.3	The NNMHV and General Cases	43
4.4	MHV Rules for Gravity	47
4.5	Large z Properties of the MHV Rule Shift	49
5	Loop-Level Methods	51
5.1	Structure of One-Loop Amplitudes	51
5.1.1	Integral Reduction	51
5.1.2	Massless Integral Basis in Four Dimensions	52
5.1.3	Supersymmetric Decomposition	53
5.1.4	Limits and Singularities	54
5.2	Unitarity Cuts	55
5.2.1	Ordinary $D = 4$ Unitarity Cuts	55
5.2.2	Generalized Unitarity	57
5.2.3	Unitarity in $D = 4 - 2\epsilon$	58
5.3	MHV Rules for Loops: The BST Prescription	58
5.4	Quadruple Cuts	60
5.4.1	Basic idea in $\mathcal{N} = 4$	61
5.4.2	A Simple Example	62
5.4.3	Box Coefficients in Other Theories	64
5.4.4	Generalized Unitarity in Complexified Minkowski Space	64
5.5	Recursion at Loop Level	65
6	One-Loop Amplitudes in $\mathcal{N} = 4$ Super-Yang–Mills	69
6.1	MHV Constructibility	69
6.2	NMHV Amplitudes	73
6.2.1	3 Mass Boxes, Gluons Only	73
6.2.2	NMHV SWIs	77
6.2.3	3 Mass Boxes with Two Fermions	78
6.2.4	Beyond Two Fermions	82
6.2.5	Beyond Three-Mass Boxes	83
7	One-Loop Amplitudes in $\mathcal{N} = 8$ Supergravity	85
7.1	One-Loop Structure of Maximal Supergravity	85
7.2	Evidence for the No-Triangle Hypothesis	86
7.2.1	Box Coefficients and Soft Divergences	87

7.2.2	Ruling Out Bubbles	88
7.2.3	Ruling Out Three-Mass Triangles	92
7.2.4	Factorization and Rational Terms	93
7.3	Conclusions	94
8	Amplitude with a Higgs	97
8.1	Higgs in the Large Top Mass Limit	97
8.2	A One-Loop Higgs Amplitude	99
8.2.1	Cut-Constructible Pieces	99
8.2.2	Rational Pieces	106
8.2.3	Tests	110
A	Integral Functions	115
B	Solutions of Quadruple Cut Constraints	119
C	Passarino–Veltman Reduction of Cuts	123

Chapter 1

Introduction

1.1 Scattering Amplitudes in Theory and Experiment

Ever since Physics arose as an empirical science, one of its main objectives has been the identification and understanding of the fundamental principles and constituents of Nature. Over time, fundamental principles have changed or been extended, and constituents regarded as fundamental have been found to contain even more fundamental parts. For the last 100 years, this hunt for the fundamental has been tied to the principles of quantum mechanics which governs Nature at the fundamental level.

Particle physics as we know it today studies objects which are so small and intangible that they can rarely be held in one place for study, either because they are massless and move at the speed of light, or because they simply decay too fast. At the same time, the measurement apparatus cannot possibly be small enough to explore a fundamental particle without being a particle itself. Thus, the only viable method of exploration is to study the interactions between pairs of particles that collide by identifying the consequences of this collision: What comes out where, and how fast.

The physical quantity that describes this is the scattering cross section. It specifies the area within which one particle must hit the other for a specific process to take place, or rather, the area where the particles do collide times the quantum mechanical probability (density) that the given process will occur if the particles collide. Such quantum mechanical probability densities always arise as the absolute value squared of a quantum mechanical amplitude, which is in this case called a scattering amplitude.

A scattering amplitude can receive contributions from different processes which are indistinguishable in the quantum sense, that is, processes which look the same to the measurement apparatus. To form a scattering cross section, all these processes have to be summed before squaring. Thus, if we wish to say something meaningful about a theory with certain particles but not all of those we know to exist, we should not start squaring the amplitude as we would be

missing interference terms from the other processes. This point is made to argue that the scattering amplitude is the furthest one can calculate in a theory without taking into account other physical processes or experimental conditions. In that sense, the scattering amplitude is the most proper way to describe a result in any reductionist approach to particle physics.

Scattering amplitudes are normally calculated by perturbation theory as power series in coupling constants. The lowest order results are easily accessible with today’s methods, but already the next order is an analytical and numerical challenge. This is unfortunate because, as we shall see, more precise (approximate or exact) results are in high demand.

1.1.1 Background Processes at the LHC

For the next many years, particle physics will be dominated by the experimental programme at CERN, where the Large Hadron Collider (LHC) is being built. This machine will collide (for the most part) protons on protons with a center-of-mass energy of 14 TeV. This is hoped to produce an array of novel particles, such as supersymmetric partners of all the known particles, and expected to produce decisive statistical evidence for the existence of the Higgs boson.

These interesting results will, however, be hiding behind massive amounts of particle reactions that we already know and love from earlier investigations of QCD and electroweak interactions. A good knowledge of the production rates of these well-known events is essential because they contaminate the interesting events and need to be subtracted. Knowing only these background processes to the lowest order in the coupling constants is likely to introduce large theoretical uncertainties, some of them prohibitively large.

process ($V \in \{Z, W, \gamma\}$)	relevant for
1. $pp \rightarrow V V \text{ jet}$	$t\bar{t}H$, new physics
2. $pp \rightarrow t\bar{t} b\bar{b}$	$t\bar{t}H$
3. $pp \rightarrow t\bar{t} + 2 \text{ jets}$	$t\bar{t}H$
4. $pp \rightarrow V V b\bar{b}$	$\text{VBF} \rightarrow H \rightarrow VV, t\bar{t}H$, new physics
5. $pp \rightarrow V V + 2 \text{ jets}$	$\text{VBF} \rightarrow H \rightarrow VV$
6. $pp \rightarrow V + 3 \text{ jets}$	various new physics signatures
7. $pp \rightarrow V V V$	SUSY trilepton

Table 1.1: The LHC “priority” wishlist, extracted from [65].

Theorists and phenomenologists working on the LHC have issued a prioritized wishlist of next-to-leading order calculations they want done before the LHC

turns on [65] (scheduled for Spring 2008 at the time of writing) included as table 1.1. At the time of writing, only the first and the last seem to be close to solved [70, 75, 106]. In principle, it is known how to calculate all these, but the conventional methods seem to have hit a roadblock; the calculational complexity of the required calculations is rising faster than the available resources, be they human or electronic. Decisive progress in this area must come from both improved methods of calculation and a strengthened effort.

1.1.2 Approaching Quantum Gravity?

Apart from the prosaic undertaking of extracting useful results from a multi-billion Euro experiment, scattering amplitudes also play a role in the theoretical understanding of quantum field theories. Amplitudes express and reveal both the internal symmetries of a theory and its internal inconsistencies.

One inconsistency plays a special role in the problems defining a quantum theory of gravity, namely that of non-renormalizability. In contrast to other quantum field theories where infinities that pop up in intermediate results can be arranged to vanish in physical quantities, gravity theories normally require more and more new terms in their defining equations to counter the infinities which necessarily appear.

However, it so happens that the maximally supersymmetric ($\mathcal{N} = 8$) quantum field theory of gravity does not seem to have such infinities. Calculation of the necessary scattering amplitudes in this theory (and others) of gravity are unfortunately extremely cumbersome and evidence is only accumulating slowly that this may indeed be the case.

This understanding is driven by new methods of calculating amplitudes. Thus, it may just be that such new methods can give a glimpse of something which, without being a true description of all known particles and interactions, can be called a consistent quantum theory of gravity.

1.2 Scattering Amplitudes in the Complex Plane

Scattering amplitudes are usually calculated perturbatively using Feynman rules. Feynman rules are derived directly from an action principle, are understood by all particle physicists alike, and have well-studied mathematical properties. A calculation done with Feynman rules is rarely called in question, save for the pointing out of simple algebraic errors. This makes Feynman rules the preferred choice of almost everyone in the community, and with good reason.

Unfortunately, there are some issues with Feynman rules that make them unfit in several situations. The first is the issue of complexity: Since the rules work by summing over contributions from all graphs of certain kinds, the complexity of the calculation is factorial in the number of participating particles. When going beyond leading order in coupling constants, there are integrals whose complexities are also factorial in the number of particles. This leads to the roadblock

mentioned earlier. The second issue is that of unphysical singularities: The results of the calculation are most often quoted in a form where some singularities have to cancel between terms. When evaluating such expressions numerically, roundoff error may introduce apparent effects which are not really there.

A contributing factor to these problems is that Feynman rules throw out information in exchange for more mechanical calculations. The prime example of this is non-abelian gauge theories, where gauge invariance enforces a particular structure of the three and four-point interactions. In the actual calculations, however, no reference is made to the gauge invariance, which might as well not have been there. In the end, the constrained form of the Feynman rules ensure that the amplitude is gauge invariant, but this has been obscured by the intermediate calculation. This is just one of several pieces of information which may be used to circumvent Feynman rules and obtain amplitudes faster, in more compact forms, and with fewer unphysical singularities.

1.2.1 The Unitary and Analytic S -Matrix

The focus of this thesis will be the use of methods of complex analysis and methods derived from such considerations. Although most of the methods described here have been developed since 2004, the idea itself is by no means new. In some sense, it can be traced back to the so-called S -matrix programme of the 60's.

The S -matrix is the evolution operator and is conventionally decomposed into a unit piece (which describes no scattering) and into the rest (which describes the actual scattering).

$$S = 1 + iT. \tag{1.1}$$

The scattering operator iT sandwiched between a state of particles coming in from the infinite past and a state of particles coming out at infinite future, gives the scattering amplitude (also known as an S -matrix element if the unit matrix is included). Requiring that the S -matrix be unitary imposes a relation for the T operator commonly known as the optical theorem,

$$2\text{Im}T = TT^\dagger. \tag{1.2}$$

If we insert a complete set of states between T and T^\dagger on the right side, we get the formal diagrammatic expression

$$2\text{Im} \text{---} \text{---} \text{---} \text{---} = \sum \int \text{---} \text{---} \text{---} \text{---} \tag{1.3}$$

where the sum is over all possible insertions of internal states and the integral is over their on-shell momenta. In perturbation theory, the left side could correspond to a one-loop amplitude and the right could correspond to a product of two tree amplitudes.

If we also view the S -matrix as an analytic function of the kinematical variables, we can gain more information. In general, a one-loop amplitude as a complex function of one of the kinematic variables will have a branch cut at real positive values of the variable. The optical theorem can then be twisted to give the discontinuity across the branch cut in terms of the insertions of all possible states between two tree amplitudes, and the hope would be to reconstruct the one-loop amplitude from its branch cut discontinuities. The really interesting thing would then be if this information could somehow be used to bootstrap amplitudes to all orders in perturbation theory.

This was the goal of the S -matrix programme: to produce a theory for the strong interactions (and, in the long run, all of particle physics) from unitarity and analyticity constraints on the S -matrix. That programme failed, partly because a host of other assumptions turned out to be needed for the full reconstruction of the S -matrix, partly because QCD, a Lagrangian quantum field theory, became established as the correct theory of the strong interactions. A review of the methods and motivations of the S -matrix programme can be found in [83].

In the 90's, it was realized that some of the tools of S -matrix theory were more powerful than public opinion in the community had assumed. The power, however, came from the input of facts known from Feynman rules and dimensional regularization, two concepts which were absent in the original S -matrix theory. Bern, Dixon, Dunbar, Kosower and others used the known structure of certain one-loop amplitudes to write them in a form where the discontinuities across branch cuts could be expressed easily so that a (not even complete) computation of the right side of (1.3) would almost completely determine the amplitude [26, 33–35]. We return to a detailed description of these methods in chapter 5.

Although this so-called “unitarity cut technique” produced results which were unthinkable to compute with Feynman graph techniques, and attempted to use all known information as efficiently as possible, it did lack in generality only being useful for some particular cases (some of which were nevertheless relevant to experiment). A central point in these methods is that only on-shell tree amplitudes are used as input for the method, and this hints that we may, after all, be able to bootstrap our way through the perturbative expansion.

This is not as far fetched as it may sound, because there are already results that indicate that this is feasible in principle. The Feynman Tree Theorem [87, 100] gives exactly such a construction. It works by using retarded propagators Δ_R in all propagators in a loop, which set the amplitude to zero because of time ordering. By using that the retarded propagator is the Feynman propagator plus a delta function

$$\Delta_R(P) = \Delta_F(P) - 2\pi i \delta(P^2 - m^2) \theta(-P_0) \tag{1.4}$$

the expression can be rewritten as a sum of ordinary Feynman diagrams where some number of propagators are Feynman and others are set on-shell by the delta function. This construction shows directly that the all-orders perturbative S -matrix can be written as some complicated convolution of the tree-level S -matrix. The Feynman Tree Theorem is discussed in more detail in [55].

1.2.2 Generalizing from Loops to Trees

As we saw above, the use of complex momentum space methods is not a new invention, and at one-loop level, it has been used for some time as a tool for the most efficient evaluation of scattering amplitudes. Most tree-level calculations were still being conducted in real Minkowski space using Feynman diagrams (or related methods) at the turn of the century. The change in affairs would, however, come from a completely different direction.

It had been known since the mid-80's that a certain class of tree amplitudes were considerably simpler than a Feynman diagram calculation would suggest when using the spinor helicity formalism, to which we will turn in chapter 2. These were the so-called Maximally Helicity Violating (MHV) amplitudes where (when all gluons are considered outgoing) two gluons have negative helicity and any number have positive helicity. Building on some critical earlier insight by Nair [115], Witten [133] was able, in 2003, to describe gluon tree-amplitudes from the topological B-model string theory in twistor space, a type of theory not commonly associated to the nuts-and-bolts of scattering calculations. Soon after it was realized that in the same sense that MHV amplitudes are lines in twistor space, tree-amplitudes with more negative helicity gluons were collections of intersecting lines in twistor space. From this, it was only a small leap to conjecture that there existed a formalism for calculating gluon amplitudes whose vertices were MHV amplitudes.

That this was indeed the case was shown by Cachazo, Svrček and Witten in the beginning of 2004 [69]. The construction is commonly known as either MHV rules or CSW rules. This thesis will use the first, knowing that it may cause a bit of confusion (Feynman rules generate Feynman amplitudes; MHV rules *do not* just generate MHV amplitudes). A description of MHV rules and some extensions can be found in chapter 3. A good deal of calculations followed which verified the MHV rules [91, 102, 135, 136]. Brandhuber, Spence and Travaglini were then able to use them for one-loop calculations [57] which was slightly surprising at the time.

All of these events were directly related to the twistor picture of gauge amplitudes, which in itself did not involve complex momenta, but to some extent it did involve momenta in $2 + 2$ dimensions. In that metric signature, Britto, Cachazo and Feng [59] realized that the unitarity cut technique described above can be extended to insert four on-shell internal states rather than just two, basically because the on-shell demand is easier to satisfy with two time directions. When there are four on-shell constraints in a loop integral it becomes trivial because

the four coordinates of loop momentum are fixed. This so-called “Quadruple Cut Technique” allowed *e.g.* the conversion of the calculation of one-loop amplitudes in maximally supersymmetric ($\mathcal{N} = 4$) Yang–Mills to a purely algebraic one in terms of products of tree amplitudes. It was also realized that the constraint of being in 2+2 dimensions could effectively be removed by assuming to be in 4 complex dimensions. We return to this technology in chapter 5.

Since there are relations between tree and one-loop amplitudes in $\mathcal{N} = 4$ super-Yang–Mills [31, 71, 92, 105], this allowed a quartic recursion relation for on-shell tree-level Yang–Mills amplitudes [128], but with complex momenta. Britto, Cachazo and Feng [60] were then able to rewrite this as a quadratic recursion relation, but they also showed together with Witten [61] that it resulted from taking the external momenta seriously as complex and using simple complex analysis. Moreover, they showed that these recursion relations could be iterated such that only complex three-point amplitudes contributed; in other words, the four-point vertex in Yang–Mills can be thought of purely as an artifact of gauge invariance necessary for Feynman rule calculations. These results will be presented in chapter 3.

The remarkable developments described here have presented a completely new view on the calculation of scattering amplitudes, and tie together concepts across loop order in ways which are still not properly understood. The consequences of treating scattering amplitude calculations as complex analysis is, at its essence, the topic of this thesis.

1.2.3 Full Amplitudes from Trees

The concept of on-shell recursion relations derived from complex-momentum methods have numerous applications. Most obvious are concrete tree-level calculations which come out in a form which is more compact than the form from Feynman rules. Another tree-level application is to show how the MHV rules mentioned above can be viewed from recursion as a particular reorganization of the Feynman rule calculation. The connection between MHV rules and on-shell recursion will be explored in detail in chapter 4.

Another use of on-shell recursion is for the calculation of one-loop amplitudes. Parts of one-loop amplitudes can be computed using the unitarity cut technique, and exactly the parts that are missed in that technique are rational ones which have similarities to tree amplitudes. This means that they are also computable by recursion relations [38–40] although in a slightly more involved form. Such a determination of a one-loop amplitude from unitarity cuts and recursion is presented in chapter 8.

Numerous developments of unitarity combined with recursion have accumulated over the last years and have improved one-loop calculation. Interestingly, some results extend to a higher number of loops, although they are primarily unitarity based. Founded on earlier insight by Anastasiou, Bern, Dixon and Kosower [2], Bern, Dixon and Smirnov [41] have been able to propose a closed

form result for the all-loops $\mathcal{N} = 4$ four and five-point amplitudes. Similarly, there have been calculations up to three loops in $\mathcal{N} = 8$ supergravity which lends credibility to the notion that it is perturbatively UV finite, and hence a (comparably) well-defined theory of gravity outside string theory. The input into the calculations are tree amplitudes and the results are consequences of their structure. These multi-loop results continue to attract attention from outside the circle of specialists.

1.3 About This Thesis

1.3.1 Omissions

The purpose of this thesis is to review some of the central complex momentum methods developed in recent years and to convey the results of the authors own works in this area. As the reader will notice, the review part already takes up a large part of the thesis, but still the topics that are relevant and interesting in this context are so numerous and complex that many of these things have had to be omitted.

Twistors are omitted completely, a choice which could be perceived as radical when the field has such close connections to twistor string theory. In the approach taken here, however, this connection is more historical since complex momentum methods has managed to outrun the twistor methods in many cases, in particular those cases chosen here. Twistor string theory has been well reviewed by Cachazo and Svrček [67] to which the reader is referred. Gauge theories in twistor spaces have been developed by *e.g.* [52].

Another area which is not covered is that dealing with MHV rules as derived from ordinary Yang–Mills in light-cone gauge. In this approach [93,113], the light-cone Lagrangian is rewritten in a form where the MHV rules appear naturally, and this permits extensions to loop calculations. Some important works in this area are [56,86]. The viewpoint taken on MHV rules here is that MHV rules are a special case of recursion relations, a viewpoint which is admittedly too narrow.

There have also been refinements of many of the unitarity and recursions mentioned here which would lead us too far if they were to be explained in detail. These are mentioned in the relevant connections. Within more traditional calculational approaches, there have also been recent advances which will not be covered.

1.3.2 Outline

The thesis is roughly divided in two parts, having to do with tree-level and one-loop level, and is not in historical order. It starts out by explaining some basic results in Yang–Mills theory, some notation, and the concept of gravity as a quantum field theory in chapter 2. Armed with those methods, we can take a look at the two important tree-level developments, namely the MHV rules and on-shell

recursion in chapter 3. Based primarily on the articles [126] by the author and [49] together with Bjerrum-Bohr, Dunbar, Ita and Perkins, chapter 4 describes how MHV rules can appear as a special case of recursion relations, and how that can be used to derive MHV rules for a gravitational theory. This highlights some of the similarities between gravity and Yang–Mills that are obscure in their Lagrangian formulation.

The purpose of chapter 5 is to introduce the loop level methods that will guide us through the rest of the thesis, as well as some related ones, and the remaining three chapters present some more concrete one-loop calculations which serve different purposes. The calculations of chapter 6 serve to explain how amplitudes in $\mathcal{N} = 4$ super-Yang–Mills are computed using a variety of techniques. The part of the calculation which regards amplitudes with other external field content than gluons is based on [127] together with Bidder and Perkins. Chapter 7 contains calculations which elucidate the one-loop structure of maximal ($\mathcal{N} = 8$) supergravity, which is necessary for the understanding of the all-loop structure. As such, it serves to support the notion that $\mathcal{N} = 8$ supergravity is UV finite, and is based on [50] together with Bjerrum-Bohr, Dunbar, Ita and Perkins. The thesis ends on a more prosaic note with the calculation in chapter 8 of the amplitude for a Higgs going to four gluons of particular helicities in the limit where the top mass is large. It is based on work together with Badger and Glover [10], but the treatment is slightly different from the article.

1.4 Conclusion and Outlook

Rather than ending the thesis with a conclusion, we will sum up the main points that the thesis will support, and give an outlook for the future.

1.4.1 A Competitor in the Calculation Race

The combined methods of unitarity and recursion have provided some extremely effective means of calculating one-loop scattering amplitudes. More specifically, they have allowed for the calculation of hitherto unknown six-parton QCD amplitudes, and hold the promise of making the progression to seven-parton QCD amplitudes smoother. As demonstrated in chapter 8, they have also allowed for calculations with fewer external particles to be sufficiently simplified that compact algebraic expressions for amplitudes can be generated without the use of computer algebra. Thus, it has opened up a new frontier for the specialists, and hopefully provided tools for the many smaller groups of physicists with simpler calculations in mind. New twists on these methods seem to keep coming in.

This is not to say that these methods are the only game in town. A purely Lagrangian approach is still favoured by the broad community, and there have been several refinements of conventional technology, both semi-numerical and algebraic, which are reaching a comparable level. One can only hope that a

combined effort of all the methods on the market can have the results in place when they are needed in the near future.

1.4.2 Understanding Quantum Field Theories

The use of complex momentum methods have shown us that perturbative quantum field theory is still far from understood. The investigation of scattering amplitudes as complex functions gives several puzzles. At tree level, the simplest version of on-shell recursion described in chapter 3 is known to work for both Yang–Mills theories and gravity, but more complicated versions, such as those used in chapter 4, are not proven but seem extremely likely to hold. Superficially, the existence of on-shell recursion seems related to the UV behaviour of tree amplitudes, a relation which is not clear either.

Equally, if not more, interesting are the relations *between* loop orders. Using unitarity, statements about loop amplitudes seem to be reformulable as statements about tree amplitudes. In chapter 7, we will see how the existence of on-shell recursion for tree gravity amplitudes comes close to proving that the one-loop structure of $\mathcal{N} = 8$ supergravity is the same as $\mathcal{N} = 4$ super-Yang–Mills. Putting such relations on a firm footing would contribute greatly to both our fundamental understanding of perturbative quantum field theory, as well as our ability to do calculations.

Together with the understanding of the full perturbative expansion of $\mathcal{N} = 4$ Yang–Mills and the prospects for a UV finite theory of gravity, this makes the topic of this thesis most exciting, an excitement that I hope that you, dear reader, will share.

Enjoy!

Chapter 2

Preliminaries

2.1 Colour Ordering

One of the more annoying aspects of doing gauge theory calculations is the proliferation of indices, both for colour and for space-time. A strategy to avoid this is to specify quantum numbers (such as colour) as early as possible in the calculation. This can provide expressions with less index mess, compensated by more expressions to compute. The two chief methods for doing this are colour ordering as described in this section and spinor helicity notation described in the next. The contents of sections 2.1 to 2.3 are also reviewed in [76].

The strategy inherent in colour ordering is to identify the possible colour structures we can obtain when we have finished an on-shell calculation. If we consider adjoint particles only, the colour structures are products of structure constants, f^{abc} , which can be written in terms of traces of $N_C \times N_C$ fundamental colour matrices,

$$f^{abc} = -\frac{i}{\sqrt{2}} \text{Tr}[t^a t^b t^c - t^a t^c t^b], \quad (2.1)$$

where we normalise the matrices as

$$[t^a, t^b] = i\sqrt{2} f^{abc} t^c, \quad \text{Tr}[t^a t^b] = \delta^{ab}. \quad (2.2)$$

By using contraction identities such as (for $SU(N_C)$)

$$(t^a)_i^{\bar{j}} (t^a)_k^{\bar{l}} = \delta_i^{\bar{j}} \delta_k^{\bar{l}} - \frac{1}{N_C} \delta_i^{\bar{j}} \delta_k^{\bar{l}}, \quad (2.3)$$

we can write all colour structures in terms of traces of fundamental colour matrices. Note that when we are contracting structure constants only, the last term of (2.3) will always drop out. Thus, we can write the completeness relation as

$$\text{Tr}[t^a M] \text{Tr}[t^a N] = \text{Tr}[MN] \quad (2.4)$$

where M and N are arbitrary matrix strings.

At the end of the calculation, (the tree-level part of) an amplitude can be written as a linear combination of the distinct trace structures,

$$A_n = \sum_{\{\sigma_i\} \in S_n(1, \dots, n)/Z_n} \text{Tr}[t^{a_{\sigma_1}} t^{a_{\sigma_2}} \dots t^{a_{\sigma_n}}] \mathcal{A}_n(\sigma_1, \sigma_2, \dots, \sigma_n), \quad (2.5)$$

the simplest examples being

$$A_3 = \text{Tr}[t^{a_1} t^{a_2} t^{a_3}] \mathcal{A}_3(1, 2, 3) + \text{Tr}[t^{a_1} t^{a_3} t^{a_2}] \mathcal{A}_3(1, 3, 2) \quad (2.6)$$

and

$$\begin{aligned} A_4 = & \text{Tr}[t^{a_1} t^{a_2} t^{a_3} t^{a_4}] \mathcal{A}_4(1, 2, 3, 4) + \text{Tr}[t^{a_1} t^{a_2} t^{a_4} t^{a_3}] \mathcal{A}_4(1, 2, 4, 3) \\ & + \text{Tr}[t^{a_1} t^{a_3} t^{a_2} t^{a_4}] \mathcal{A}_4(1, 3, 2, 4) + \text{Tr}[t^{a_1} t^{a_3} t^{a_4} t^{a_2}] \mathcal{A}_4(1, 3, 4, 2) \\ & + \text{Tr}[t^{a_1} t^{a_4} t^{a_2} t^{a_3}] \mathcal{A}_4(1, 4, 2, 3) + \text{Tr}[t^{a_1} t^{a_4} t^{a_3} t^{a_2}] \mathcal{A}_4(1, 4, 3, 2). \end{aligned} \quad (2.7)$$

The coefficients of the trace structures are called *colour ordered* amplitudes, because they correspond to a particular ordering of the colour matrices. Instead of calculating the amplitude, using (2.1) to (2.4), and deducing the colour ordered amplitudes we can calculate them directly by using colour ordered Feynman rules. A diagram then contributes to a colour ordered amplitude if the cyclic ordering of the external particles corresponds to that of the wanted colour ordered amplitude.

If we are dealing with particles in the fundamental representation, the strings of matrices will not be traced, because the colour indices of the fundamental particles are free. It is still possible to define a colour ordering, *e.g.*,

$$A_4(q_1^i, \bar{q}_2^{\bar{j}}, 3^{a_3}, 4^{a_4}) = [t^{a_3} t^{a_4}]_j^i \mathcal{A}_4(q_1, 3, 4, \bar{q}_2) + [t^{a_4} t^{a_3}]_j^i \mathcal{A}_4(q_1, 4, 3, \bar{q}_2). \quad (2.8)$$

If we work in an $SU(N_C)$ gauge theory, we now have to take the last term of (2.3) into account. This corresponds to subtracting at each vertex the contribution of a $U(1)$ gauge boson.

At loop level, we will also encounter multi-trace terms which we need to compute. At one-loop level, however, it can be shown that all two-trace terms are permutations of the (“planar”) single-trace terms [33].

2.2 Spinor Helicity Notation

After trading the colour information for more diagrams, we can now trade the use of polarization vectors for yet more diagrams. This consists of writing the amplitudes completely (or rather, to the extent possible) in terms of Weyl spinors of massless particles. We will find that in this notation we can write down explicit polarization vectors corresponding to positive and negative helicity gluons.

We start by deriving some basic facts about Weyl spinors. The Weyl spinors corresponding to a massless momentum can be found by solving the massless Dirac equation

$$p_\mu \gamma^\mu u(p) = \not{p} u(p) = 0 \quad (2.9)$$

where $u(p)$ is a four component vector and γ^μ is a vector of 4×4 matrices obeying

$$\{\gamma^\mu, \gamma^\nu\} = 2g^{\mu\nu} I. \quad (2.10)$$

We use ‘‘Peskin and Schroeder’’ conventions [122] where

$$\gamma^\mu = \begin{pmatrix} 0 & \sigma^\mu \\ \bar{\sigma}^\mu & 0 \end{pmatrix} \quad (2.11)$$

Switching now to Weyl–van der Waerden notation the Dirac spinor can be written as two two-component spinors

$$u(p) = \begin{pmatrix} u_\alpha(p) \\ \tilde{u}^{\dot{\alpha}}(p) \end{pmatrix} \quad (2.12)$$

whose indices are raised and lowered with $\epsilon_{\alpha\beta}$, $\epsilon_{\dot{\alpha}\dot{\beta}}$, *etc.*, using southwest-northeast contraction. We define antisymmetric inner products between spinors,

$$\langle \lambda \eta \rangle = \epsilon_{\alpha\beta} \lambda^\alpha \eta^\beta = \epsilon^{\alpha\beta} \lambda_\alpha \eta_\beta = \lambda^\alpha \eta_\alpha, \quad (2.13)$$

$$[\tilde{\lambda} \tilde{\eta}] = \epsilon_{\dot{\beta}\dot{\alpha}} \tilde{\lambda}^{\dot{\alpha}} \tilde{\eta}^{\dot{\beta}} = \epsilon^{\dot{\beta}\dot{\alpha}} \tilde{\lambda}_{\dot{\alpha}} \tilde{\eta}_{\dot{\beta}} = \tilde{\lambda}_{\dot{\alpha}} \tilde{\eta}^{\dot{\alpha}}, \quad (2.14)$$

thus we are working with the ‘‘QCD’’ sign convention rather than the ‘‘string’’ sign convention. In this notation (2.9) becomes

$$p \cdot \sigma_{\beta\dot{\alpha}} \tilde{u}^{\dot{\alpha}}(p) = p \cdot \sigma^{\dot{\beta}\alpha} u_\alpha(p) = 0, \quad (2.15)$$

which can further be elucidated by noting that $p \cdot \sigma^{\dot{\alpha}\alpha}$ can be decomposed into a product of two two-component spinors because $\det(p \cdot \sigma) = p^2 = 0$:

$$p \cdot \sigma^{\dot{\alpha}\alpha} = \tilde{\lambda}^{\dot{\alpha}}(p) \lambda^\alpha(p), \quad (2.16)$$

which is solved by

$$\lambda^1 = \sqrt{|p_0 + p_3|}, \quad \lambda^2 = \text{sign}(p_0) \frac{p_1 + ip_2}{\sqrt{|p_0 + p_3|}}, \quad (2.17)$$

$$\lambda_1 = \text{sign}(p_0) \frac{p_1 + ip_2}{\sqrt{|p_0 + p_3|}}, \quad \lambda_2 = -\sqrt{|p_0 + p_3|}. \quad (2.18)$$

$$\tilde{\lambda}^{\dot{\alpha}} = \text{sign}(p_0) (\lambda^\alpha)^* \quad (2.19)$$

From the above properties of the two-component spinors it follows immediately that the Dirac spinors satisfying the Dirac equation are spanned by

$$u^+(p) = \begin{pmatrix} \lambda_\alpha(p) \\ 0 \end{pmatrix} \equiv |p\rangle, \quad u^-(p) = \begin{pmatrix} 0 \\ \tilde{\lambda}^{\dot{\alpha}}(p) \end{pmatrix} \equiv [p], \quad (2.20)$$

whose conjugate spinors are

$$\bar{u}^-(p) = \begin{pmatrix} \lambda^\alpha(p) \\ 0 \end{pmatrix}^T \equiv \langle p|, \quad \bar{u}^+(p) = \begin{pmatrix} 0 \\ \tilde{\lambda}_{\dot{\alpha}}(p) \end{pmatrix}^T \equiv [p|. \quad (2.21)$$

The definitions of $|p\rangle$, $|p]$ *etc.*, ensure that $\langle pq\rangle = \langle \lambda(p)\lambda(q)\rangle$ and $[pq] = [\tilde{\lambda}(p)\tilde{\lambda}(q)]$ thereby helping to simplify the algebra significantly. In terms of momenta, the antisymmetric inner products are

$$\langle pq\rangle = -\text{sign}(p_0)\sqrt{\left|\frac{q_0 + q_3}{p_0 + p_3}\right|}(p_1 + ip_2) + \text{sign}(q_0)\sqrt{\left|\frac{p_0 + p_3}{q_0 + q_3}\right|}(q_1 + iq_2), \quad (2.22)$$

$$[pq] = \text{sign}(q_0)\sqrt{\left|\frac{q_0 + q_3}{p_0 + p_3}\right|}(p_1 - ip_2) - \text{sign}(p_0)\sqrt{\left|\frac{p_0 + p_3}{q_0 + q_3}\right|}(q_1 - iq_2), \quad (2.23)$$

which obey

$$\langle pq\rangle[qp] = (p + q)^2 = 2p \cdot q, \quad [qp] = \text{sign}(p_0q_0)\langle pq\rangle^*. \quad (2.24)$$

We will often encounter these spinors strung together using gamma matrices. The following identities can be shown by using standard Dirac algebra:

$$\langle p|\gamma^\mu|q\rangle = [q|\gamma^\mu|p\rangle, \quad (2.25)$$

$$\langle q|\gamma^\mu|q\rangle = 2q^\mu, \quad (2.26)$$

$$\langle p|\gamma^\mu|q\rangle\langle r|\gamma_\mu|s\rangle = -2\langle pr\rangle[qs] \quad (\text{Fierz rearrangement}), \quad (2.27)$$

$$\langle p|\gamma^\mu\gamma^\nu|q\rangle = -\langle q|\gamma^\nu\gamma^\mu|p\rangle, \quad (2.28)$$

$$\langle pq\rangle\langle r| + \langle qr\rangle\langle p| + \langle rp\rangle\langle q| = 0 \quad (\text{Schouten Identity}). \quad (2.29)$$

The last two have equivalent forms with $\langle \cdot | \rightarrow [\cdot]$. We will suppress Feynman slashes in general unless possibilities of misunderstandings arise. In fact, we will quite often write momenta as their slashed versions rather than their vector versions, as the whole point of spinor helicity notation is to get rid of explicit vectors. When we write massless momenta in matrix form we should really write

$$p = |p\rangle[p| + |p]\langle p|, \quad (2.30)$$

but since only one of them avoids being projected out in spinor strings such as $\langle q|p|r\rangle$ or $\langle q|p|r|s\rangle$, we will allow ourselves the sloppiness of writing

$$p = |p\rangle[p| \quad \text{or} \quad p = |p]\langle p|. \quad (2.31)$$

We now know how to treat expressions with Weyl spinors and momenta. The last objects which may occur in a colour ordered scattering amplitude are polarization vectors. We use the two explicit realizations

$$\epsilon_\mu^+(p) = \frac{\langle q|\gamma_\mu|p\rangle}{\sqrt{2}\langle qp\rangle}, \quad \epsilon_\mu^-(p) = \frac{\langle p|\gamma_\mu|q\rangle}{\sqrt{2}[pq]}. \quad (2.32)$$

In both of these, q is some massless reference momentum. Using the rules above it is quite straightforward to verify the standard properties of polarization vectors,

$$\epsilon^\pm(p) \cdot p = 0, \quad \epsilon_\mu^+(p) = (\epsilon_\mu^-(p))^*, \quad (2.33)$$

$$\epsilon^+(p) \cdot \epsilon^-(p) = -1, \quad \epsilon^+(p) \cdot \epsilon^-(p) = 0. \quad (2.34)$$

We can argue that q is an arbitrary (apart from $p \cdot q \neq 0$) gauge vector by considering the difference between two different choices of q :

$$\epsilon_\mu^+(p; q') - \epsilon_\mu^+(p; q) \quad (2.35)$$

$$= \frac{\langle q' | \gamma_\mu | p \rangle}{\sqrt{2} \langle q' p \rangle} - \frac{\langle q | \gamma_\mu | p \rangle}{\sqrt{2} \langle q p \rangle} \quad (2.36)$$

$$= \frac{-\langle q' | \gamma_\mu \gamma_\nu | q \rangle + \langle q | \gamma_\mu \gamma_\nu | q' \rangle}{\sqrt{2} \langle q' p \rangle \langle q p \rangle} p^\nu \quad (2.37)$$

$$= \frac{\langle q | \{ \gamma_\mu, \gamma_\nu \} | q' \rangle}{\sqrt{2} \langle q' p \rangle \langle q p \rangle} p^\nu \quad (2.38)$$

$$= \frac{\sqrt{2} \langle q q' \rangle}{\langle q' p \rangle \langle q p \rangle} p_\mu. \quad (2.39)$$

Thus, the two choices give the same results due to the Ward identity. Finally, we note that the polarization sum is that of a lightlike axial gauge with gauge vector q :

$$\epsilon_\mu^+ \epsilon_\nu^- + \epsilon_\mu^- \epsilon_\nu^+ = -g_{\mu\nu} + \frac{p_\mu q_\nu + q_\mu p_\nu}{p \cdot q}. \quad (2.40)$$

This particular gauge is ghost-free, which will be extremely helpful in later chapters when we deal with loops.

Recently, a Mathematica package for manipulations with spinors in this context called S@M has been published [109], but using slightly different conventions.

2.3 Tree-Level Structure of Yang–Mills Theory

This section collects some facts of Yang–Mills theory that we will need in the future, and is not intended as a review of the subject. We will return to the one-loop structure of Yang–Mills amplitudes in section 5.1.

2.3.1 MHV Amplitudes

It has already been mentioned that Yang–Mills scattering amplitudes take on very simple forms in spinor helicity notation. The most striking example of this

was conjectured by Parke and Taylor [120] and proven by Berends and Giele [16], and states that

$$\begin{aligned}\mathcal{A}(1^+, \dots, n^+) &= 0, \\ \mathcal{A}(1^+, \dots, i^-, \dots, n^+) &= 0, \\ \mathcal{A}(1^+, \dots, i^-, \dots, j^-, \dots, n^+) &= i \frac{\langle ij \rangle^4}{\langle 12 \rangle \langle 23 \rangle \cdots \langle n1 \rangle},\end{aligned}\tag{2.41}$$

where \dots denotes any number of positive helicity gluons. The last of these is called the ‘‘Maximally Helicity Violating’’ amplitude, or MHV amplitude for short. There is a similar expression for the amplitude with two positive and the rest negative helicity obtained by complex conjugation,

$$\mathcal{A}(1^-, \dots, i^+, \dots, j^+, \dots, n^-) = (-1)^n i \frac{[ij]^4}{[12][23] \cdots [n1]},\tag{2.42}$$

called the ‘‘googly MHV amplitude’’¹. These formulas determine all gluon amplitudes up to and including five points, since all those amplitudes are either zero, MHV or googly-MHV.

It should be noted that the ‘‘Maximally’’ in MHV becomes a misnomer at loop level since the two first equations of (2.41) cease to hold in non-supersymmetric theories.

2.3.2 Supersymmetry

Tree-level amplitudes in Yang–Mills theory have an apparent supersymmetry [104, 119] because, say, a gluino and any adjoint fermion have the same Feynman rules. Also, at the level of individual colour ordered amplitudes fundamental and adjoint fermions are really indistinguishable since their colour ordered Feynman rules are the same. The difference only shows when we compute amplitudes with non-adjacent fermions where the fundamental fermion amplitude must vanish. The actual supersymmetry only reveals itself at loop level where the number of particle species becomes important.

The tree-level supersymmetry can be exploited to constrain tree amplitudes by ‘‘Supersymmetric Ward Identities’’, SWI’s [95, 96], which relate amplitudes of different external particle content but with the same momenta and the same sum of helicities. Following [76], SWI’s are obtained by writing the amplitude as a string of operators Φ_i creating helicity eigenstates by acting on the vacuum

$$\langle 0 | \Phi_1 \Phi_2 \cdots \Phi_n | 0 \rangle.\tag{2.43}$$

We now introduce the spinorial supercharge Q_α and contract it as $Q(q, \theta) = \theta q^\alpha Q_\alpha$ where θ is a Grassmann parameter and q^α is the Dirac spinor of some

¹The word ‘‘googly’’ is a cricket reference often used in twistor theory. In cricket it denotes a ball bowled with the opposite spin of the normal, thrown by a right-handed bowler.

lightlike momentum. The inclusion of θ makes $Q(q, \theta)$ a bosonic operator. Since Q_α annihilates the vacuum, we can write

$$0 = \langle 0 | [Q(q, \theta), \Phi_1 \Phi_2 \cdots \Phi_n] | 0 \rangle = \sum_{i=1}^n \langle 0 | \Phi_1 \cdots [Q(q, \theta), \Phi_i] \cdots \Phi_n | 0 \rangle, \quad (2.44)$$

where the last expression must represent a sum over amplitudes where Q has exchanged one particle with another. If one computes all the commutators, one will get

$$\begin{aligned} [Q(q, \theta), g^+(k)] &= \theta[kq]f^+, \\ [Q(q, \theta), f^+(k)] &= \theta\langle kq \rangle g^+, \\ [Q(q, \theta), f^-(k)] &= \theta[qk]g^-, \\ [Q(q, \theta), g^-(k)] &= \theta\langle qk \rangle f^-. \end{aligned} \quad (2.45)$$

This permits us to prove the two first formulas of (2.41). The second can be proven by acting on $\langle 0 | g_1^- f_2^+ g_3^+ \cdots g_n^+ | 0 \rangle$,

$$0 = \langle q1 \rangle \mathcal{A}(f_1^-, f_2^+, \dots) - \langle q2 \rangle \mathcal{A}(g_1^-, g_2^+, \dots), \quad (2.46)$$

and choosing $q = 1$ to eliminate the first term. Notice that the amplitudes with two f^+ 's are zero because of the requirement of conservation of fermion helicity.

We can also extend the formula for MHV gluon amplitudes to amplitudes with a fermion pair by acting on an amplitude with two negative helicity gluons at 1 and i and a positive helicity fermion at j and the rest positive helicity gluons. This gives the SWI

$$0 = \langle q1 \rangle \mathcal{A}(f_1^-, g_i^-, f_j^+) + \langle qi \rangle \mathcal{A}(g_1^-, f_i^-, f_j^+) - \langle qj \rangle \mathcal{A}(g_1^-, g_i^-, g_j^+), \quad (2.47)$$

and choosing $q = 1$ reduces this to

$$\mathcal{A}(g_1^-, f_i^-, f_j^+) = \frac{\langle 1j \rangle}{\langle 1i \rangle} \mathcal{A}(g_1^-, g_i^-, g_j^+) = i \frac{\langle 1j \rangle \langle 1i \rangle^3}{\langle 12 \rangle \langle 23 \rangle \cdots \langle n1 \rangle}. \quad (2.48)$$

This can be explained as moving a half unit of negative helicity from i to j , thereby exchanging a factor of $\langle 1i \rangle$ with a factor of $\langle 1j \rangle$.

SWI's can be extended to describe other supersymmetries. For example, $\mathcal{N} = 2$ supersymmetry would contain a scalar and thus allow (2.48) to be extended to include those. The $\mathcal{N} = 4$ supersymmetry algebra will be of special importance to us since that theory enters at both tree and loop level in several places below. It has a gluon g^\pm , four fermions f_a^\pm , six real scalars $s_{ab} = -s_{ba}$, and the algebra

$$\begin{aligned} [Q_a(q, \theta), g^+(k)] &= \theta[kq]f_a^+, \\ [Q_a(q, \theta), f_b^+(k)] &= \theta\delta_{ab}\langle kq \rangle g^+ + \theta[kq]s_{ab}, \\ [Q_a(q, \theta), s_{bc}(k)] &= \theta\delta_{ab}\langle kq \rangle f_c^+ - \theta\delta_{ac}\langle kq \rangle f_b^+ + \theta[qk]\epsilon_{abcd}f_d^-, \\ [Q_a(q, \theta), f_b^-(k)] &= \theta\delta_{ab}[qk]g^- + \frac{1}{2}\theta\langle qk \rangle\epsilon_{abcd}s_{cd} \\ [Q_a(q, \theta), g^-(k)] &= \theta\langle qk \rangle f_a^-. \end{aligned} \quad (2.49)$$

Notice that we might as well have used $\tilde{s}_{ab} = \frac{1}{2}\epsilon_{abcd}s_{cd}$. Using these, we can deduce SWT's for theories with several different fermions and scalars, as well as SWT's for $\mathcal{N} = 4$ amplitudes to any loop order. In particular, we can deduce the exact form of all tree-level MHV amplitudes in $\mathcal{N} = 4$ SYM by a procedure like (2.48).

2.3.3 Limit Behaviour

We will also briefly touch on the behaviour of Yang–Mills tree amplitudes in different limits. In a limit where a multi-particle kinematic invariant (and thus a propagator) goes on-shell, the residue factorizes into two on-shell amplitudes, summed over possible internal states. In the pure-gluon case we have

$$\mathcal{A}(\dots) \rightarrow \sum_{h=\pm} \frac{\mathcal{A}(\dots, P^h)\mathcal{A}(-P^{-h}, \dots)}{P^2} \quad (2.50)$$

as $P^2 \rightarrow 0$. This factorization is present in most theories described by Feynman rules and not just Yang–Mills.

When two-particle kinematic invariants go on-shell the situation is different in massless Yang–Mills theory. Because of kinematics we should really be looking at the limit where two colour adjacent momenta become collinear. In this limit, the amplitude factorizes into the amplitude with one fewer external state times a so-called splitting amplitude which depends on the particles going collinear and the internal state which is going on-shell. Again, considering only gluons we have, when $a \rightarrow zP$ and $b \rightarrow (1-z)P$,

$$\mathcal{A}(\dots, a^{h_a}, b^{h_b}, \dots) \rightarrow \sum_{h_i=\pm} \mathcal{A}(\dots, P^{-h_i}, \dots)\text{Split}_{h_i}(z, a^{h_a}, b^{h_b}). \quad (2.51)$$

The splitting amplitudes for gluons are

$$\begin{aligned} \text{Split}_-^{\text{tree}}(a^-, b^-) &= 0, \\ \text{Split}_-^{\text{tree}}(a^+, b^+) &= \frac{1}{\sqrt{z(1-z)}\langle ab \rangle}, \\ \text{Split}_+^{\text{tree}}(a^+, b^-) &= \frac{(1-z)^2}{\sqrt{z(1-z)}\langle ab \rangle}, \\ \text{Split}_-^{\text{tree}}(a^+, b^-) &= -\frac{z^2}{\sqrt{z(1-z)}[ab]}, \end{aligned} \quad (2.52)$$

from which the remaining can be deduced by parity. Similarly, one can deduce splitting functions involving fermions and scalars from the corresponding MHV amplitudes. The one-loop limits and singularities will be considered in section 5.1.4.

2.4 Gravity as a Quantum Field Theory

It is well known that General Relativity has serious problems when implemented as a quantum field theory. It has a dimensionful coupling which means that it is non-renormalizable. At each loop order one has to introduce new counterterms to cancel divergences, and since nothing prevents finite parts of those counterterms, we automatically introduce infinitely many coupling constants into the theory.

Because of this, the “conventional wisdom” is that a QFT version of GR is non-sensical. The situation, however, is not as bad as one may think. Gravity can be treated as an effective field theory [131], where the theory is only renormalized to the loop order needed. This is legal because we know that an all-orders renormalized calculation can still be Taylor expanded around zero coupling. As long as the coupling constant is small, we can expect tree-level computations to be close to the actual result, and even at loop level the counterterms contribute to local interactions but not to *e.g.* long range corrections to the gravitational potential [47, 78, 79]. One could also remark that Yang–Mills theory in more than four dimensions is also non-renormalizable, a fact which neither does nor should deter people from working with the theory.

Another problem plaguing quantum gravity theories is that of algebra. When the Einstein–Hilbert action,

$$S_{EH} = \frac{1}{2\kappa^2} \int d^4x \sqrt{-g} R, \quad (2.53)$$

is written out in terms of a perturbation around flat

$$g_{\mu\nu} = \eta_{\mu\nu} + \kappa h_{\mu\nu} \quad \text{or curved} \quad g_{\mu\nu} = g_{\mu\nu}^0 + \kappa h_{\mu\nu} \quad (2.54)$$

space, it contains vertices to all orders, and even the lowest order terms suffer from severe congestion of indices. The three-point Feynman vertex takes up about half a page in condensed notation, the four point requires one or two. This means that only amplitudes where gravitons enter in the simplest manner can be calculated analytically. The only computational point we will make here is that of polarization tensors: Gravitons are spin 2 particles which have two on-shell helicity states with traceless polarization tensors $\epsilon_{\mu\nu}^\pm$. It so happens that one can use products of gluon polarization,

$$\epsilon_{\mu\nu}^\pm = \epsilon_\mu^\pm \epsilon_\nu^\pm. \quad (2.55)$$

With the choices of polarization vectors described in section 2.2, we may even choose different reference momenta for ϵ_μ^\pm and ϵ_ν^\pm .

2.4.1 The KLT Relations

What one *can* do to compute tree-level amplitudes in quantum gravity is to use a result from string theory by Kawai, Lewellen and Tye [99], the KLT relations.

These are obtained by rewriting the string computation for closed string scattering in terms of products of open string scatterings, and by taking the $\alpha' \rightarrow 0$ limit, they make a statement about a relation between graviton and gluon scattering amplitudes. The relation is valid on-shell at tree-level in any number of dimensions. The first three are (setting irrelevant factors to 1)

$$\begin{aligned}
\mathcal{M}(1, 2, 3) &= \mathcal{A}(1, 2, 3)\tilde{\mathcal{A}}(1, 2, 3) \\
\mathcal{M}(1, 2, 3, 4) &= s_{12}\mathcal{A}(1, 2, 3, 4)\tilde{\mathcal{A}}(1, 2, 4, 3) \\
\mathcal{M}(1, 2, 3, 4, 5) &= s_{12}s_{34}\mathcal{A}(1, 2, 3, 4, 5)\tilde{\mathcal{A}}(1, 4, 3, 5, 2) \\
&\quad + s_{13}s_{24}\mathcal{A}(1, 3, 2, 4, 5)\tilde{\mathcal{A}}(1, 4, 2, 5, 3).
\end{aligned} \tag{2.56}$$

The \mathcal{M} 's are graviton amplitudes and the \mathcal{A} and $\tilde{\mathcal{A}}$ are colour ordered gauge amplitudes. In fact, there are many forms of these relations since an (irrelevant) relabeling on the gravity side gives another combination of orderings on the gauge side. The simplest non-trivial example is the four graviton amplitude in four dimensions which is

$$\begin{aligned}
\mathcal{M}(1^-, 2^-, 3^+, 4^+) &= s_{12}\mathcal{A}(1^-, 2^-, 3^+, 4^+)\mathcal{A}(1^-, 2^-, 4^+, 3^+) \\
&= \langle 34 \rangle [43] \frac{\langle 12 \rangle^3}{\langle 23 \rangle \langle 34 \rangle \langle 41 \rangle} \frac{\langle 12 \rangle^3}{\langle 24 \rangle \langle 43 \rangle \langle 31 \rangle} \\
&= \frac{[43] \langle 12 \rangle^7}{\langle 12 \rangle \langle 23 \rangle \langle 34 \rangle \langle 41 \rangle \langle 24 \rangle \langle 13 \rangle}.
\end{aligned} \tag{2.57}$$

The KLT relations also imply that graviton states decompose into a tensor product of two gluon states. Since the proof of the KLT relations does not rely on the particular string theory in question, we may imagine that there are more states than gravitons on the gravity side and gluons on the gauge side and that the gravity states are tensor products of two gauge states. The two gauge theories need not be the same. If we imagine the gravity side to be a heterotic string theory, the one gauge theory corresponds to the right moving sector and the other corresponds to the left moving sector [22].

2.4.2 The $\mathcal{N} = 8 / \mathcal{N} = 4$ Relation

At this point we can take a closer look at one of the main themes of this thesis, namely the relation between the maximally supersymmetric gravity and gauge theories in four dimensions. At tree level, the KLT relations give us a correspondence between the two theories both at the level of the states of the two theories (something which is independent of the loop order) and between the actual amplitudes.

The spectrum (and Lagrangian) of $\mathcal{N} = 8$ supergravity [72, 73] can be derived by dimensionally reducing 11 dimensional $\mathcal{N} = 1$ supergravity [74] and contains a graviton, eight Rarita-Schwinger gravitini, 28 vectors, 56 Majorana fermions and 70 real scalars, a total of 256 states when helicities are taken into account. The $\mathcal{N} = 4$ multiplet has a gluon, four (Majorana or Weyl) fermions and six real

scalars, a total of 16 states. By the KLT relation, any state in $\mathcal{N} = 8$ supergravity can be seen as a tensor product of two $\mathcal{N} = 4$ states such that the sum of the two $\mathcal{N} = 4$ state helicities add up to the $\mathcal{N} = 8$ state helicity. Supergravity can have the same construction as we saw for supersymmetric gauge theories above where the states are related by supersymmetry charges. In that sense, four of the $\mathcal{N} = 8$ charges map to the charges of one of the $\mathcal{N} = 4$ theories and the remaining four to the other.

This, however, does not account for all the symmetry on the gauge side. The symmetry of Yang–Mills theory at tree level is the same as $\mathcal{N} = 4$ SYM at loop level, namely the superconformal symmetry. Since the spectrum, the supersymmetry and the amplitudes are directly related to tree-level $\mathcal{N} = 8$ supergravity, one might guess that there is an additional symmetry in gravity theories which mirrors the additional conformal symmetry in Yang–Mills. We will return to the relations between $\mathcal{N} = 8$ and $\mathcal{N} = 4$ at loop level in chapter 7.

Chapter 3

Tree Level Methods

3.1 Earlier Methods

Calculation of tree-level scattering amplitudes is normally done by applying the Feynman rules. This procedure is completely safe, in the sense that it is completely mechanical and results are trusted. The expressions generated in this way are known not to be the most compact, but they also avoid unphysical singularities which may cause problems for numerical evaluation. For calculations by hand, however, they become impractical beyond five-particle processes because the number of diagrams becomes too big. Taking as an example the $n + 2$ point gluon amplitude, the number of diagrams increases factorially, as shown in the table below [101, 112].

n	2	3	4	5	6	7	8
# of diagrams	4	25	220	2485	34300	559405	10525900

Table 3.1: The number of Feynman diagrams contributing to the scattering process $gg \rightarrow n g$. Extracted from [112].

The problem of the number of diagrams can, to a large extent, be solved by implementing Feynman rules (or an equivalent recursive formulation) on a computer, where the running time for generating an amplitude and evaluating it at a specific kinematical point is not prohibitively long even for a number of points of the order of 15. There are several programs that can do such calculations [98, 103, 110, 111, 123].

Problems may still arise if we want to generate a *large* number of events with many final states, since reevaluating the amplitude many times is time consuming. On the other hand, deriving the amplitude analytically and subsequently inserting numbers is also problematic since the analytic expressions from Feynman rules are extremely large. What we would ideally like to have is some means

of computing the amplitude in a form which is compact and well suited for insertions of numerical values.

One method for this, based on Feynman rules, is Berends–Giele recursion [16]. It uses colour ordering and the spinor helicity formalism and in addition keeps as little off-shell information as possible. In this way it takes advantage of gauge invariance and other on-shell conditions to simplify intermediate results instead of waiting till the end. Berends–Giele recursion for gluon amplitudes works by introducing the off-shell n -point gluon current J_n^μ which is the (gauge dependent) off-shell amplitude for n -gluon scattering with $n-1$ legs taken on-shell by multiplying in polarization vectors and using $k^2 = 0$. By looking back into the way J_n^μ was calculated, we see that the off-shell leg had to be attached to either a three or a four vertex. Whatever was at the other legs of that vertex would sum up exactly to some J_m^μ where $m < n$. This allows us to write down a cubic recursion relation for J_n^μ , which can be terminated by setting the momentum of the off-shell leg on-shell and multiplying by the polarization. We can either try to solve the recursion relation exactly or implement it on a computer. A good description of Berends–Giele recursion can be found in [76].

Even though this sort of recursion can speed up the calculation of amplitudes, it still suffers from very long expressions, although less severely than the traditional application of Feynman rules. 2004 saw the invention of two methods which, in their separate ways, have contributed to both more compact results and theoretical insight into the structure of gauge theory amplitudes. We now turn to them in historical order.

3.2 MHV Rules

3.2.1 Basic Construction

As described in the introduction, the analysis of Yang–Mills amplitudes in twistor space led to an intuitive picture of MHV vertices connected by propagators. The MHV vertex, however, was not a well defined concept since it is only well defined on-shell where the momenta are all light-like. To make the MHV picture concrete, it was necessary to construct an off-shell continuation of the MHV amplitude. This was achieved by Cachazo, Svrček, and Witten [69] in March of 2004. The rules presented below were not derived as such, but rather proposed and subsequently motivated. For multi-gluon amplitudes, the rules state:

1. Draw all possible graphs (“MHV diagrams”)
 - where external lines represent external gluons and have their helicity marked,
 - where internal lines have opposite helicities (\pm) at each end,
 - where each vertex has exactly two edges of negative helicity—and at least one of positive helicity—attached,

- and which is planar and respects the colour ordering of the external gluons.

2. For each graph, assign

- to each external line the outgoing momentum of the respective gluon,
- off-shell momenta P_i to the internal lines by assuming conservation of momentum at each vertex,
- holomorphic spinors to internal lines as

$$|P_i^b\rangle = |P_i\eta] \quad (3.1)$$

where the same (almost arbitrary) anti-holomorphic spinor $|\eta]$ must be used for all internal lines of all graphs.

3. For each graph, multiply,

- for each internal line of momentum P_i ,

$$\frac{1}{P_i^2}, \quad (3.2)$$

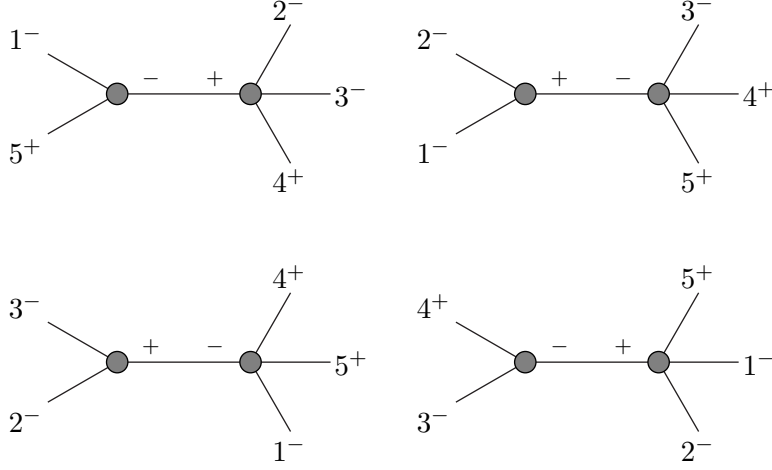
- for each vertex, the MHV formula using $|P_i^b\rangle$ for the holomorphic spinors of the internal lines.

4. Add the contributions of all graphs.

The combinatorics of these rules are similar to that of Feynman rules, but with a somewhat gentler sprawl of diagrams. It is simple to show that an MHV diagram with p negative helicity external gluons will have $p - 1$ MHV vertices and $p - 2$ propagators; significantly fewer than for Feynman rules. For fixed p , the number of diagrams grows polynomially in the number of external gluons, thus presenting a significant simplification over Feynman rules, but if we need all helicity configurations (and thus all p up to half the number of gluons) *e.g.* for computing an unpolarized cross section, the asymptotic behaviour of the number of MHV diagrams is again factorial, thus not providing a significant advantage over Feynman rules for many external gluons.

For few gluons, however, the simplification is remarkable. By taking advantage of parity, a six gluon amplitude can be computed with the use of only 32 diagrams (depending on how you count) three of which are MHV and thus trivial.

To gain some familiarity with the rules, let us consider the simplest non-trivial case of $A(1^-, 2^-, 3^-, 4^+, 5^+)$. It is of course slightly trivial because it is a googly-MHV amplitude, but it will be a welcome first check to verify that the rules obey parity. Having three negative helicity gluons, this amplitude is called “Next-to-MHV”, or NMHV, and the diagrams must have two vertices and one propagator. There are four permitted diagrams,



Following the rules above, we get the contribution of the first diagram,

$$\frac{\langle 1(-P_{51}^b) \rangle^3}{\langle (-P_{51}^b)5 \rangle \langle 51 \rangle} \frac{1}{P_{51}^2} \frac{\langle 23 \rangle^3}{\langle 34 \rangle \langle 4P_{51}^b \rangle \langle P_{51}^b 2 \rangle} \quad (3.3)$$

$$= \frac{\langle 1P_{51}\eta \rangle^3}{\langle 5P_{51}\eta \rangle \langle 51 \rangle} \frac{1}{[15] \langle 51 \rangle} \frac{\langle 23 \rangle^3}{\langle 34 \rangle \langle 4P_{51}\eta \rangle \langle 2P_{51}\eta \rangle} \quad (3.4)$$

$$= \frac{[5\eta]^3 \langle 23 \rangle^3}{[1\eta][51] \langle 34 \rangle \langle 4(5+1)\eta \rangle \langle 2(5+1)\eta \rangle}. \quad (3.5)$$

At this point we can make a choice of $|\eta\rangle$ if we like. The choice $|\eta\rangle = |5\rangle$ will immediately set the diagram to zero, whereas the choices $|\eta\rangle = |1\rangle$, $|(5+1)4\rangle$, $|(5+1)2\rangle$ will render it undefined. The latter three correspond to unphysical poles which cancel among the diagrams. If we continue with $|\eta\rangle = |5\rangle$, the three other diagrams contribute

$$- \frac{\langle 34 \rangle^2 [45]^3}{[12][51] \langle 45 \rangle [52] \langle 5P_{12}5 \rangle}, \quad (3.6)$$

$$- \frac{\langle 14 \rangle^2 [45]^3}{[23][51] \langle 45 \rangle [52] \langle 15 \rangle [53]} \quad (3.7)$$

and,

$$- \frac{\langle 12 \rangle^2 [45]^3}{[34][51] \langle 15 \rangle [53] \langle 5P_{34}5 \rangle}, \quad (3.8)$$

which adds up to the expected result,

$$- \frac{[45]^3}{[12][23][34][51]}. \quad (3.9)$$

Though the result of this calculation was already known to be fairly simple, it is remarkable that we can compute a five point amplitude using only three contributing diagrams of such limited complexity.

A comment on the choice of the off-shell extension (3.1) is in order here. Because internal lines must have opposite helicities at each end, every diagram is invariant under scaling of internal spinors. In other words, the requirement (3.1) should really read

$$|P_i^b\rangle \sim |P_i\eta\rangle. \quad (3.10)$$

As noted by Kosower [102] such a relation can be achieved by defining

$$P_i^{b\mu} = P_i^\mu + \alpha\eta^\mu \quad (3.11)$$

and choosing α such that P_i^b is lightlike. This results in

$$P_i^{b\mu} = P_i^\mu - \frac{P_i^2}{2P_i \cdot \eta} \eta^\mu \quad (3.12)$$

$$|P_i^b\rangle [P_i^b] = \frac{|P_i\eta\rangle \langle \eta P_i|}{\langle \eta P_i \eta \rangle} \quad (3.13)$$

In the Yang–Mills MHV rules, only the holomorphic spinor is used, so in a sense, the above rewriting adds information which is not used in practise.

3.2.2 Gravity: A Puzzling Failure

The success of MHV rules for Yang–Mills theory immediately raised the question of whether MHV rules existed for gravity. Even though such rules were not directly implied by the KLT relationship, the possibility was not excluded by them, nor by any other known principle. The main obstacle, however, was that graviton MHV amplitudes were not holomorphic (*cf.* (2.56)) and thus the extension $|P_i^b\rangle \sim |P_i\eta\rangle$ was insufficient. As an example, take the graviton equivalent of the diagram treated in detail above. MHV rules would give that this diagram was

$$M(5^+, 1^-, -P_{51}^{b-}) \frac{1}{P_{51}^2} M(2^-, 3^-, 4^+, P_{51}^{b+}), \quad (3.14)$$

where the graviton amplitudes can be obtained from the KLT relations. For that we would need P_{23}^2 or, equivalently, $(P_4 + P_{51}^b)^2$, but these are not obviously the same because we are now “inside the MHV vertex” where we must use P_{51}^b rather than P_{51} . For this to be consistent, we must have

$$\langle 4P_{51}^b 4 \rangle = \langle 4P_{51} 4 \rangle + P_{51}^2 \quad (3.15)$$

$$\frac{\langle 4P_{51}\eta \rangle \langle \eta P_{51} 4 \rangle}{\langle \eta P_{51} \eta \rangle} = \langle 4P_{51} 4 \rangle + P_{51}^2 \quad (3.16)$$

$$-P_{51}^2 \frac{\langle 4\eta \rangle [\eta 4]}{\langle \eta P_{51} \eta \rangle} = P_{51}^2 \quad (3.17)$$

$$\langle \eta P_{451} \eta \rangle = 0 \quad (3.18)$$

$$\langle \eta(2+3)\eta \rangle = 0. \quad (3.19)$$

The last requirement states that η^μ must be a lightlike momentum orthogonal to the time-like momentum P_{23} . By going to the rest frame of P_{23} it can be seen clearly that no such (non-zero) η^μ exists. Thus, any gravitational attempt at MHV rules along these lines seems impossible.

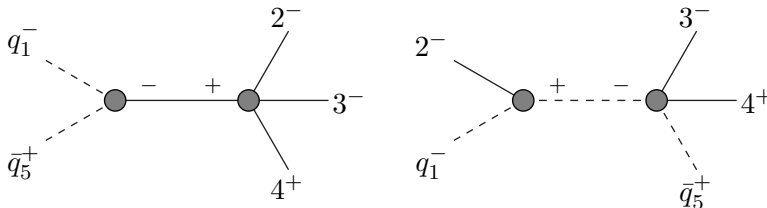
Although it seems that the problem at hand is rooted in the non-holomorphic character of graviton MHV amplitudes, it is in fact much deeper. The amplitude $M(2^-, 3^-, 4^+, P_{51}^{b+})$ is ill-defined because we have taken P_{51} away from its real value without compensating in other places; the amplitude isn't just off-shell, it disobeys conservation of momentum. Had this been an amplitude proper, the implicit delta function in the momenta would have set it to zero before we even started. And this argument relates as much to Yang–Mills as to gravity.

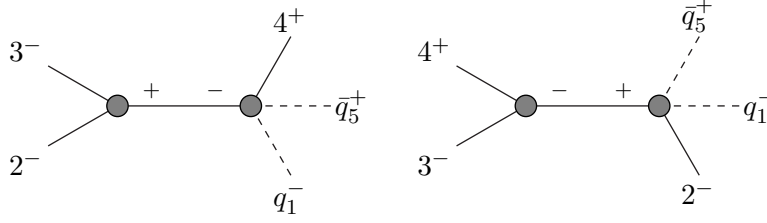
In this light, the fact that Yang–Mills MHV rules *do* work becomes even more puzzling. It gives the impression of being an inherently ill-defined procedure which magically becomes meaningful for theories with holomorphic MHV amplitudes. The missing ingredient to understand why the situation is significantly brighter than this, will appear in section 3.3, and the puzzle will be resolved in the next chapter.

3.2.3 Fermions, Higgses, and Vector Bosons

Meanwhile, we can turn to some of the additional successes of MHV rules. As described above, the success of the MHV rules seemed to rely somewhat on the holomorphic nature of MHV amplitudes, so similar theories with holomorphic MHV amplitudes ought to have associated MHV rules.

The primary example of this is Yang–Mills theory with coloured (adjoint or fundamental) massless scalars and fermions [90, 91, 134, 135]. As described in section 2.3.2, replacing gluons with fermions or scalars in an MHV amplitude only changes the numerator, and there is nothing preventing us from extending the MHV rules with fermionic and scalar internal lines. Particles in the fundamental representation are handled by requiring them to be adjacent at all times. If, for instance, we wanted to compute the NMHV amplitude $A_5(q_1^-, 2^-, 3^-, 4^+, \bar{q}_5^+)$, the diagrams would be similar to those of our previous example, just with some of the gluons being replaced by fermions denoted by dashed lines,





The contribution of the second diagram would be

$$\frac{\langle 12 \rangle^3 \langle (-P_{12}^b) 2 \rangle}{\langle 12 \rangle \langle 2(-P_{12}^b) \rangle \langle (-P_{12}^b) 1 \rangle} \frac{1}{P_{12}^2} \frac{\langle 3P_{12}^b \rangle^3 \langle 35 \rangle}{\langle P_{12}^b 3 \rangle \langle 34 \rangle \langle 45 \rangle \langle 5P_{12}^b \rangle} \quad (3.20)$$

$$= -\frac{\langle 12 \rangle^2}{\langle 1P_{12}^b \rangle} \frac{1}{P_{12}^2} \frac{\langle 3P_{12}^b \rangle^2 \langle 35 \rangle}{\langle 34 \rangle \langle 45 \rangle \langle 5P_{12}^b \rangle}, \quad (3.21)$$

which differs from the corresponding gluon diagram by the factor

$$\frac{\langle 2P_{12}^b \rangle \langle 35 \rangle}{\langle 21 \rangle \langle 3P_{12}^b \rangle} = \frac{[1\eta] \langle 35 \rangle}{\langle 3P_{12}\eta \rangle}. \quad (3.22)$$

If we now try to compute $A_5(s_1, 2^-, 3^-, 4^+, s_5)$ we will again have four diagrams similar to those above and for the one treated we would obtain the factor

$$\left(\frac{[1\eta] \langle 35 \rangle}{\langle 3P_{12}\eta \rangle} \right)^2 \quad (3.23)$$

relative to the gluon result.

Another case where MHV rules apply is one to which we will turn in chapter 8, namely that of a massive, uncoloured particle H (such as a Higgs) which couples to a gauge field through the term $CHF_{\mu\nu}F^{\mu\nu}$ in the Lagrangian.

The last case is that of the coupling of gauge fields to electroweak vector boson currents. The formalism is somewhat involved, and rather than trying to explain it here, we refer the reader to the original article on the matter [44].

3.3 On-Shell Recursion Relations

As was discussed in the introduction, a decisive turn came with the realization that spinors could be taken away from 3+1 dimensions, in which λ_a and $\tilde{\lambda}_{\dot{a}}$ are related by complex conjugation, to complexified Minkowski space \mathbb{C}^4 where they are complex and independent. This allows for the use of standard methods of complex analysis, in particular Cauchy's Theorem. Although on-shell recursion relations were first discovered as the combined consequence of $\mathcal{N} = 4$ IR consistency conditions and the quadruple cut method [60], we will take the complex analysis viewpoint introduced by Britto, Cachazo, Feng, and Witten (BCFW) [61]. We will, however, also touch on the connection with IR consistency conditions in later chapters.

3.3.1 Using Cauchy's Theorem on Yang–Mills Amplitudes

BCFW on-shell recursion works by deforming a tree-level amplitude \mathcal{A} by a complex parameter z to $\hat{\mathcal{A}}(z)$ by choosing two external particles i and j and deforming their spinors

$$|\hat{i}\rangle = |i\rangle + z|j\rangle, \quad |\hat{j}\rangle = |j\rangle - z|i\rangle. \quad (3.24)$$

This deformation obeys conservation of momentum since

$$\hat{p}_i + \hat{p}_j = |i\rangle\langle\hat{i}| + |\hat{j}\rangle\langle j| = |i\rangle\langle i| + z|i\rangle\langle j| + |j\rangle\langle j| - z|i\rangle\langle j| = p_i + p_j, \quad (3.25)$$

so $\hat{\mathcal{A}}(z)$ is a well defined amplitude in \mathbf{C}^4 .

For now, we assume that $\hat{\mathcal{A}}(z) \rightarrow 0$ as $z \rightarrow \infty$. This allows us to use Cauchy's Theorem to write

$$0 = \frac{1}{2\pi i} \oint_{\mathcal{C}_\infty} \frac{dz}{z} \hat{\mathcal{A}}(z) = \hat{\mathcal{A}}(0) + \sum_{\text{poles } p} \frac{\text{Res}_p \hat{\mathcal{A}}(z)}{z_p} \quad (3.26)$$

The poles of tree amplitudes are well known; they correspond to the Feynman propagators of internal momenta going on-shell, and the ‘‘residue’’ is given by

$$\lim_{P_{k,m}^2 \rightarrow 0} \left[P_{k,m}^2 \mathcal{A} \right] = \sum_{h=\pm 1} \mathcal{A}(k, \dots, m, -P_{k,m}^{-h}) \mathcal{A}(P_{k,m}^h, m+1, \dots, k-1). \quad (3.27)$$

If $i \in \{k, \dots, m\}$ and $j \notin \{k, \dots, m\}$ (or vice versa) there will be a corresponding pole in z because

$$\hat{P}_{k,m}(z)^2 = (P_{k,m} + z|i\rangle\langle j|)^2 = P_{k,m}^2 + z\langle iP_{k,m}j\rangle, \quad (3.28)$$

thus

$$z_{k,m} = -\frac{P_{k,m}^2}{\langle iP_{k,m}j\rangle}. \quad (3.29)$$

The residue of this pole is

$$\begin{aligned} & \lim_{z \rightarrow z_{k,m}} \left[z \mathcal{A} \right] \\ &= \frac{1}{\langle iP_{k,m}j\rangle} \lim_{P_{k,m}^2 \rightarrow 0} \left[P_{k,m}^2 \mathcal{A} \right] \\ &= \sum_{h=\pm 1} \frac{\mathcal{A}(k, \dots, m, -\hat{P}_{k,m}^{-h}(z_{k,m})) \mathcal{A}(\hat{P}_{k,m}^h(z_{k,m}), m+1, \dots, k-1)}{\langle iP_{k,m}j\rangle}. \end{aligned} \quad (3.30)$$

Combining this with (3.26) leads to

$$\mathcal{A} = \sum_{\substack{k \in \{j+1, \dots, i\} \\ m \in \{i, \dots, j-1\} \\ k \neq m, m+2 \\ h = \pm 1}} \frac{\mathcal{A}(k, \dots, m, -\hat{P}_{k,m}^{-h}(z_{k,m})) \mathcal{A}(\hat{P}_{k,m}^h(z_{k,m}), m+1, \dots, k-1)}{P_{k,m}^2}. \quad (3.31)$$

In human language, the conditions under the sum state that we must sum over all internal momenta affected by the deformation. We can draw this as a diagram consisting of two deformed amplitudes and an internal propagator, together with the sum,

$$\sum_{\text{all such diagrams}} \quad \begin{array}{c} \widehat{i} \\ \diagup \quad \diagdown \\ \text{---} \bigcirc \quad \pm \quad \mp \quad \bigcirc \text{---} \\ \diagdown \quad \diagup \\ \widehat{j} \end{array} \quad \widehat{P}_{k,m}$$

$\widehat{P}_{k,m}$ is on-shell and has the form

$$\widehat{P}_{k,m} = P_{k,m} - \frac{P_{k,m}^2}{\langle iP_{k,m}j \rangle} |i\rangle[j] = \frac{|P_{k,m}j\rangle \langle iP_{k,m}|}{\langle iP_{k,m}j \rangle}. \quad (3.32)$$

Very often this recursion relation is used with i and j adjacent, *e.g.* $(i, j) = (n, 1)$ in an n -point amplitude. This simplifies the above relation to

$$\mathcal{A}_n = \sum_{m=2}^{n-2} \sum_{h=\pm 1} \frac{\mathcal{A}(m+1, \dots, n, \widehat{P}_{1,m}^{-h}(z_m)) \mathcal{A}(-\widehat{P}_{1,m}^h(z_m), 1, \dots, m)}{P_{1,m}^2} \quad (3.33)$$

where

$$z_m = \frac{P_{1,m}^2}{\langle nP_{1,m}1 \rangle}, \quad \widehat{P}_{1,m} = \frac{|P_{1,m}n\rangle \langle 1P_{1,m}|}{\langle 1P_{1,m}n \rangle} = \frac{|P_{n,m}n\rangle \langle 1P_{2,m}|}{\langle 1P_{1,m}n \rangle}. \quad (3.34)$$

Before we can go and apply this decomposition on poles to the calculation of real gluon amplitudes, there are two subtleties to consider, having to do with three-point amplitudes and the behaviour of $\widehat{\mathcal{A}}(z)$ as $z \rightarrow \infty$.

3.3.2 Three-Point Amplitudes (and an Example)

In real Minkowski space, three-point gauge amplitudes are zero. This basically stems from the fact that in order for the three momenta to be light-like, they must also be orthogonal,

$$0 = p_3^2 = (-p_1 - p_2)^2 = \langle 12 \rangle [21], \quad \Rightarrow \quad \langle 12 \rangle = [12]^* = 0, \quad \textit{etc.} \quad (3.35)$$

$$\Rightarrow p_1 \sim p_2 \sim p_3. \quad (3.36)$$

When we move away from real Minkowski space, however, the restriction that $\lambda_a = \widetilde{\lambda}_a$ is lifted and the on-shell constraints have two solutions,

$$|1\rangle \sim |2\rangle \sim |3\rangle \quad \text{or} \quad |1\rangle \sim |2\rangle \sim |3\rangle. \quad (3.37)$$

These each allow one of the two helicity configurations to be non-zero because the expressions

$$\frac{[12]^3}{[23][31]} \quad \text{and} \quad \frac{\langle 12 \rangle^3}{\langle 23 \rangle \langle 31 \rangle}, \quad (3.38)$$

respectively, are well-defined and contribute to (3.31).

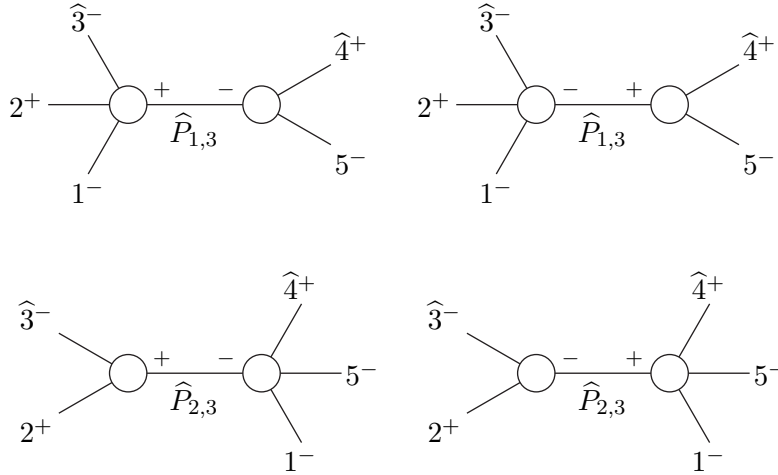
We can illustrate the method and the considerations about three-point amplitudes with the calculation of the googly-MHV five-point amplitude $\mathcal{A}(1^-, 2^+, 3^-, 4^+, 5^-)$. We define the deformation by taking

$$|\widehat{3}\rangle = |3\rangle + z|4\rangle, \quad |\widehat{4}\rangle = |4\rangle - z|3\rangle. \quad (3.39)$$

The internal momenta affected by this deformation are $P_{1,3}$ and $P_{2,3}$ each corresponding to a pole in z at

$$z_{1,3} = -\frac{P_{1,3}^2}{\langle 3P_{1,34} \rangle} = \frac{\langle 45 \rangle}{\langle 35 \rangle}, \quad z_{2,3} = -\frac{P_{2,3}^2}{\langle 3P_{2,34} \rangle} = -\frac{[23]}{[24]}. \quad (3.40)$$

Summing also over internal helicities gives four diagrams



with the contributions

$$\begin{aligned} & \frac{\mathcal{A}(1^-, 2^+, \widehat{3}^-(z_{1,3}), -\widehat{P}_{1,3}^+(z_{1,3}))\mathcal{A}(\widehat{P}_{1,3}^-(z_{1,3}), \widehat{4}^+(z_{1,3}), 5^-)}{P_{1,3}^2} \\ & \frac{\mathcal{A}(1^-, 2^+, \widehat{3}^-(z_{1,3}), -\widehat{P}_{1,3}^-(z_{1,3}))\mathcal{A}(\widehat{P}_{1,3}^+(z_{1,3}), \widehat{4}^+(z_{1,3}), 5^-)}{P_{1,3}^2} \\ & \frac{\mathcal{A}(2^+, \widehat{3}^-(z_{2,3}), -\widehat{P}_{2,3}^+(z_{2,3}))\mathcal{A}(\widehat{P}_{2,3}^-(z_{2,3}), \widehat{4}^+(z_{2,3}), 5^-, 1^-)}{P_{2,3}^2} \\ & \frac{\mathcal{A}(2^+, \widehat{3}^-(z_{2,3}), -\widehat{P}_{2,3}^-(z_{2,3}))\mathcal{A}(\widehat{P}_{2,3}^+(z_{2,3}), \widehat{4}^+(z_{2,3}), 5^-, 1^-)}{P_{2,3}^2}. \end{aligned} \quad (3.41)$$

Two of these contributions can be discarded immediately. Number 2 and 3 contain an amplitude of the form $\mathcal{A}(- - +)$ which is zero. In contribution number 1, $z_{1,3}$ is found by requiring that

$$\widehat{P}_{1,3}^2 = \langle \widehat{45} \rangle [54] = 0, \quad \text{or} \quad |\widehat{4}\rangle \sim |5\rangle, \quad (3.42)$$

so the three-point MHV amplitude in that contribution is zero, even in complex momenta. The corresponding condition in the last contribution is $|\widehat{3}\rangle \sim |2\rangle$ which kills the googly-MHV three-point but not the MHV three-point we need. Thus it gives the only contribution, for which we need the solutions

$$|\widehat{4}\rangle = |4\rangle + \frac{[23]}{[24]} |3\rangle = \frac{[P_{3,4}2]}{[42]}, \quad \widehat{P}_{23} = \frac{|P_{2,3}4\rangle \langle 3P_{2,3}|}{\langle 3P_{2,3}4\rangle} = \frac{|P_{2,4}4\rangle [2]}{[24]}. \quad (3.43)$$

This allows us to compute

$$\begin{aligned} & \frac{\langle 3(-\widehat{P}_{2,3}) \rangle^3}{\langle (-\widehat{P}_{2,3})2 \rangle \langle 23 \rangle} \frac{1}{P_{2,3}^2} \frac{\langle 51 \rangle^3}{\langle 1\widehat{P}_{2,3} \rangle \langle \widehat{P}_{2,3}4 \rangle \langle \widehat{45} \rangle} \\ &= \frac{\langle 51 \rangle^3 \langle 3\widehat{P}_{2,3} \rangle^3}{\langle 23 \rangle^2 [32] \langle \widehat{45} \rangle \langle 2\widehat{P}_{2,3} \rangle \langle 1\widehat{P}_{2,3} \rangle \langle \widehat{4}\widehat{P}_{2,3} \rangle} \\ &= \frac{\langle 51 \rangle^3 \langle 3P_{2,3}4 \rangle^3 [24]^2}{\langle 23 \rangle^2 [32] [2P_{3,4}5] \langle 2P_{2,3}4 \rangle \langle 1P_{2,3}4 \rangle [2P_{3,4}P_{2,3}4]} \\ &= \frac{\langle 51 \rangle^3 \langle 32 \rangle^3 [24]^5}{\langle 23 \rangle^2 [32] [21] \langle 15 \rangle \langle 23 \rangle [34] \langle 15 \rangle [54] [24] \langle 51 \rangle [15]} \\ &= -\frac{[24]^4}{[12][23][34][45][51]}, \end{aligned} \quad (3.44)$$

which is, of course, the known expression for a five-point googly-MHV amplitude.

3.3.3 Asymptotic Behaviour of the Deformed Amplitude

Until now we postponed the issue of whether $\lim_{z \rightarrow \infty} \widehat{\mathcal{A}}(z) = 0$. For certain choices of the spinors to deform we can immediately argue that this must be the case by looking at the calculation from Feynman diagrams and tracking the dependence on z . Every propagator in a Feynman diagram affected by the deformation must asymptotically contribute z^{-1} , and every three vertex affected by the deformation must contribute z^1 . The “worst case scenario” for the asymptotic z dependence will be when the deformation only affects three-vertices. Before multiplying by the external polarizations, such a diagram will go as z^1 .

If we make the deformation (3.24) the dependences of ϵ_i^μ and ϵ_j^μ on z will depend on their helicities. For i the reaction to the deformation is

$$\widehat{\epsilon}_i^{\mu+} = \frac{\langle q\gamma^\mu \widehat{i} \rangle}{\sqrt{2}\langle iq \rangle} \sim z^1, \quad \widehat{\epsilon}_i^{\mu-} = \frac{\langle i\gamma^\mu q \rangle}{\sqrt{2}[\widehat{i}q]} \sim z^{-1}, \quad (3.45)$$

and for j the asymptotic behaviour is the opposite. This leads us to conclude that the worst behaviour of $\widehat{\mathcal{A}}(z)$ as $z \rightarrow \infty$ for helicities (h_i, h_j) is

$$(-, +) \sim z^{-1}, \quad (+, +), (-, -) \sim z^1, \quad (+, -) \sim z^3. \quad (3.46)$$

This tells us that using BCFW on-shell recursion relations is always justified when we deform the antiholomorphic spinor of a negative helicity particle and the holomorphic spinor of a positive helicity particle.

In practice, however, the behaviour may be more benign. If we consider the MHV amplitude $\mathcal{A}(1^-, 2^-, \dots, n^+)$, the choice $(i, j) = (1^-, 2^-)$ goes as z^{-1} and so does *e.g.* the choice $(3^+, 4^+)$ while $(2^-, 4^+)$ and $(3^+, 5^+)$ go as z^{-2} . This shows us that we can often expect an actual behaviour which is a few powers of z better than the worst case. This is another expression of the fact that Feynman rules are not taking advantage of all the available symmetries of the theory.

3.3.4 Some Consequences of BCFW on-shell recursion

Two points are worth making at this point. First, since we have rigorously proven that we can always perform on-shell recursion with the choice $(-, +)$ it follows that any tree amplitude can, by successive recursion, be reduced to three-amplitudes. In this perspective, the four gluon vertex can be completely neglected for practical calculations, and its presence in the Lagrangian is only required for gauge invariance.

Second, the existence of on-shell recursion shows that other formalisms that claim to reproduce Yang–Mills amplitudes are correct if they have the right singularity structure (3.27) and Lorentz covariance. This was proven together with the proposal of the MHV rules [69], thus, BCFW recursion provides an indirect proof that the MHV rules are correct.

Both of these points are elaborated on in the original article [61].

3.3.5 Extension to Other Theories and Deformations

The deformation (3.24) chosen by BCFW is by no means unique. For instance, one may choose three gluons i, j, k and deform them to [39]

$$|\widehat{i}\rangle = |i\rangle + z|j\rangle + \alpha z|k\rangle, \quad |\widehat{j}\rangle = |j\rangle - z|i\rangle, \quad |\widehat{k}\rangle = |k\rangle - \alpha z|i\rangle, \quad (3.47)$$

which also obeys momentum conservation for any α . In general one will have to redo the derivations of section 3.3.1, but most features of the relations persist. Using extended deformations may be helpful for improved $z \rightarrow \infty$ behaviour and for constructing relations to the MHV rules as done in the next chapter.

The methods of deriving on-shell recursion relations are clearly very generic, relying mostly on the fact that the theory at hand is an ordinary quantum field theory. Gauge invariance or colour ordering may be practical tools for obtaining simpler expressions, but are not required as such for doing on-shell recursion in this way. One extension is to allow other states than gluons to participate,

such as charged scalars and fermions (massless, massive, D -dimensional) [7, 9, 107, 108, 125], another is to take a completely different theory, such as QED [117], gravity [12, 68], or more exotic theories [15]. The challenge in most of these cases is to prove the appropriate $z \rightarrow \infty$ behaviour, which is sometimes done and sometimes left to faith. Especially in gravity, where the “worst case scenario” analysis gives very bad asymptotic behaviour, the on-shell recursion relations were used for quite some time on this faith until a proof appeared [14].

The applications to loop-level calculations will be reviewed in section 5.5.

Chapter 4

MHV Rules from Recursion

In the present chapter we will connect the two subjects of the previous chapter and show how MHV rule constructions follow from on-shell recursion. The original articles are [126] for the Yang–Mills case and [49] for the gravity case.

4.1 MHV Rules in Light of Recursion Relations

The MHV rules as described in section 3.2 distance themselves from recursion relations in one obvious way: recursion relations have one unshifted propagator, while the MHV rules have several. This immediately tells us that a simple derivation of the MHV rules from recursion is not obtainable, but also that the NMHV case can serve as an initial test case. With this in mind, we can note four features of MHV rules that will guide us:

1. An internal momentum is shifted on-shell in a manner close to that of recursion relations. Setting

$$P^b = P - \frac{P^2}{2P \cdot \eta} \eta, \quad (4.1)$$

is practically the same as shifting P as

$$\hat{P} = P - z\eta, \quad (4.2)$$

setting $\hat{P}^2 = 0$, and solving for z .

2. The asymmetry between holomorphic and anti-holomorphic spinors is deeply rooted. The attempt to construct MHV rules for gravity by choosing $|\eta\rangle = (|\eta])^*$ failed because it produced non-Lorentz invariant results, thereby providing a hint that η is a complex momentum whose holomorphic and anti-holomorphic spinors are unrelated. Admittedly, there is a bit of hindsight in this argument, since the existence of MHV rules for gravity was not guaranteed.

3. If η is a complex momentum, we might as well continue all momenta. If we do that, all the anti-holomorphic spinors of the external momenta are unspecified by the MHV rules, just as $|\eta\rangle$. In fact, $|\eta\rangle$ may even differ between different internal momenta.
4. The MHV rules contain MHV three-point vertices and no googly three-point vertices. The easiest way of ensuring this would be to shift only anti-holomorphic spinors. This fits well the fact that these do not show up in the MHV rules anyway.

This leads us to conclude that if MHV rules can be proven from recursion relations, the proof must involve a non-minimal shift of anti-holomorphic spinors, and all these shifts must be proportional to the (otherwise unspecified) $|\eta\rangle$.

4.2 The NMHV Case

We first apply the above considerations to the calculation of the amplitude $\mathcal{A}_n(m_1^-, \dots, m_2^-, \dots, m_3^-, \dots)$ where the \dots have helicity $+$. If we choose to shift only the three negative helicity gluons, the shift is unique up to a constant,

$$|\widehat{m}_1\rangle = |m_1\rangle + z|\eta\rangle\langle m_2 m_3\rangle, \quad (4.3)$$

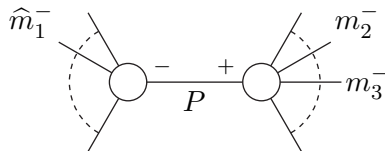
$$|\widehat{m}_2\rangle = |m_2\rangle + z|\eta\rangle\langle m_3 m_1\rangle, \quad (4.4)$$

$$|\widehat{m}_3\rangle = |m_3\rangle + z|\eta\rangle\langle m_1 m_2\rangle, \quad (4.5)$$

where conservation of momentum follows from the Schouten identity

$$|m_1\rangle\langle m_2 m_3\rangle + |m_2\rangle\langle m_3 m_1\rangle + |m_3\rangle\langle m_1 m_2\rangle = 0. \quad (4.6)$$

We will postpone the proof of the legality of this shift to section 4.5. With the above shift, the z dependent internal momenta are those that have at least one of $m_{1,2,3}$ at each end, *e.g.*



The opposite helicity assignment for the inner line does not contribute, so we have split the amplitude into two (shifted) MHV amplitudes. The solution for z is found by setting

$$\widehat{P}^2 = (P - z|m_1\rangle\langle m_2 m_3\rangle[\eta])^2 = P^2 - z\langle m_2 m_3\rangle\langle m_1 P \eta\rangle = 0 \quad (4.7)$$

$$\widehat{P} = \frac{|P\eta\rangle\langle m_1 P|}{\langle m_1 P\eta\rangle} \quad |\widehat{P}\rangle \sim |P\eta\rangle \quad (4.8)$$

It should now be clear that we have reproduced the NMHV version of the MHV rules for Yang–Mills: We must sum over all diagrams that split the amplitude into two MHV vertices. For the external momenta we must use the shifted spinors (but because the MHV amplitude only involves holomorphic spinors, it makes no difference) and for the internal we must use $|\widehat{P}\rangle \sim |P\eta\rangle$.

We have, however, obtained more than just the Yang–Mills MHV rules. We have obtained the full expression for the shifted momenta, allowing us to construct MHV rules for theories with other MHV amplitudes than Yang–Mills; most notably gravity. We will return to the MHV rules for gravity in section 4.4 after treating the general case with more than three negative helicity particles.

4.3 The NNMHV and General Cases

From the above discussion, it should be clear that setting up a recursion by shifting the anti-holomorphic spinors of all negative helicity gluons by the same reference spinor $|\eta\rangle$ allows a description where a) the left and right amplitudes both have fewer negative helicity gluons than the full amplitude, b) there are no three-point googly amplitudes, and c) the spinor to be used for the internal line is the same as in the MHV rules. The remaining problem is that there are several propagators in each MHV diagram while the recursion relations can only provide one.

The solution will be to perform similar shifts one after the other and to reach a representation which can subsequently be proven to be equivalent to the MHV rules. Starting with an NNMHV amplitude, we can choose a set $c_i^{(1)}$ and shift

$$|\widehat{m}_i\rangle = |m_i\rangle + z c_i^{(1)} |\eta\rangle. \quad (4.9)$$

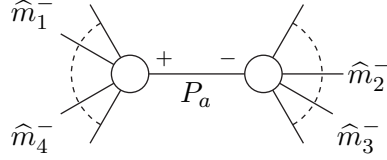
For conservation of momentum, the c 's must be chosen such that

$$\sum_{i=1}^4 c_i^{(1)} \langle m_i | = 0. \quad (4.10)$$

If we label the possible internal lines by a , we can write the result of the recursion as

$$\mathcal{A}_n(m_{1\dots A}^-) = \sum_a \frac{\mathcal{A}(\widehat{m}^-, \widehat{P}_a^\pm) \mathcal{A}(\widehat{m}^-, -\widehat{P}_a^\mp)}{P_a^2}, \quad (4.11)$$

where $|\widehat{P}_a\rangle = |P_a\eta\rangle$, and there is an implicit summation over helicities where relevant. The two sub amplitudes are MHV and NMHV, respectively. Such contributions can be depicted as



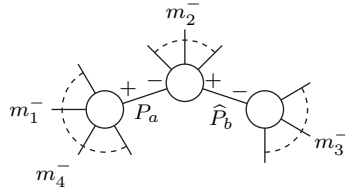
To uncover a second propagator, we can set up a similar recursion for each term in the above sum. However, we have the constraint on those recursions that we should not uncover the same propagator $1/P_a^2$ again, or we would not have progressed. Thus, for each a we choose a set $c_{a,i}^{(2)}$ and set up the recursion as

$$|\widehat{m}_i] = [m_i] + z c_{a,i}^{(2)}[\eta] \quad (4.12)$$

such that $\widehat{P}_a^2 = P_a^2$. This gives one additional constraint on the $c_{a,i}^{(2)}$ apart from conservation of momentum. Performing the recursion for all terms in the sum (4.11), we arrive at

$$\mathcal{A}_n(m_{1\dots 4}^-) = \sum_a \sum_{b \neq a} \frac{\mathcal{A}(\widehat{m}^-, \widehat{P}_a^\pm) \mathcal{A}(\widehat{m}^-, -\widehat{P}_a^\mp, \widehat{P}_b^\pm) \mathcal{A}(\widehat{m}^-, -\widehat{P}_b^\mp)}{P_a^2 \widehat{P}_b^2} \quad (4.13)$$

where the terms in the sum can be drawn as (placement of m 's and \pm 's can differ)



Since our recursion cannot split MHV amplitudes, it is clear that all three amplitudes in the numerator must be MHV and thus that the helicities of the internal lines are fixed by the external helicities. Moreover, if we write the twice shifted $|m]$'s as

$$|\widehat{m}_i] = |m_i] + r_i[\eta] \quad (4.14)$$

and remind ourselves that the coefficients were constructed to obey momentum conservation and $\widehat{P}_a^2 = \widehat{P}_b^2 = 0$ we can fix the $|\widehat{m}_i]$ uniquely as a function of a and b . This solution is independent of which of these was uncovered first, so we can collect terms in (4.13) two by two and write it as

$$\mathcal{A}_n(m_{1\dots 4}^-) = \sum_{\{a,b\}} \mathcal{A}(\widehat{m}^-, \widehat{P}_a^\pm) \mathcal{A}(\widehat{m}^-, -\widehat{P}_a^\mp, \widehat{P}_b^\pm) \mathcal{A}(\widehat{m}^-, -\widehat{P}_b^\mp) \quad (4.15)$$

$$\times \left(\frac{1}{P_a^2 \widehat{P}_{b(a)}^2} + \frac{1}{P_b^2 \widehat{P}_{a(b)}^2} \right) \quad (4.16)$$

where $\widehat{P}_{b(a)}$ means P_b shifted using $c_i^{(1)}$ as to put P_a on-shell. The last factor, however, is exactly what we would get if we took

$$\frac{1}{P_a^2 P_b^2} \quad (4.17)$$

and did recursion on it using $c_i^{(1)}$. In terms of diagrams, what we are arguing is that

$$=$$

Thus, we can write the amplitude as

$$\mathcal{A}_n(m_{1..4}^-) = \sum_{\{a,b\}} \frac{\mathcal{A}(\widehat{m}^-, \widehat{P}_a^\pm) \mathcal{A}(\widehat{m}^-, -\widehat{P}_a^\mp, \widehat{P}_b^\pm) \mathcal{A}(\widehat{m}^-, -\widehat{P}_b^\mp)}{P_a^2 P_b^2}. \quad (4.18)$$

This is exactly the MHV rules for NNMHV amplitudes.

It should now be clear how to proceed with the general case. To uncover the first propagator in an N^p MHV amplitude, a , use the shift

$$|\widehat{m}_i] = |m_i] + z c_i^{(1)} |\eta]. \quad (4.19)$$

For each a , uncover the next propagator b by using the shift

$$|\widehat{\widehat{m}}_i] = |\widehat{m}_i] + z c_{i,a}^{(2)} |\eta] \quad (4.20)$$

where $c_{i,a}^{(2)}$ is chosen such that $\widehat{\widehat{P}}_a^2 = 0$. The third propagator c can now be uncovered by using the shift

$$|\widehat{\widehat{\widehat{m}}}_i] = |\widehat{\widehat{m}}_i] + c_{i,a,b}^{(3)} |\eta] \quad (4.21)$$

where $c_{i,a,b}^{(3)}$ is chosen such that $\widehat{\widehat{P}}_a^2 = \widehat{\widehat{P}}_b^2 = 0$. We can evidently continue in this way until we have uncovered p propagators, at which point we have shifted the $|m_i|$ to $|m_i| + r_i|\eta|$ and required that the shifted momenta of the uncovered propagators are on-shell. The latter, together with conservation of momentum, fixes r_i independently of the order in which the propagators were uncovered. Writing the amplitude formally as

$$\mathcal{A}_n = \sum_{\substack{\text{ordered} \\ \text{sets of } p \\ \text{propagators}}} \frac{\mathcal{A}^{\text{MHV}} \mathcal{A}^{\text{MHV}} \dots \mathcal{A}^{\text{MHV}}}{P_a^2 \widehat{\widehat{P}}_b^2 \widehat{\widehat{P}}_c^2 \dots}, \quad (4.22)$$

this allows the formal rewriting

$$\mathcal{A}_n = \sum_{\substack{\text{unordered} \\ \text{sets of } p \\ \text{propagators}}} \mathcal{A}^{\text{MHV}} \mathcal{A}^{\text{MHV}} \dots \mathcal{A}^{\text{MHV}} \sum_{\text{orderings}} \frac{1}{P_a^2 \widehat{\widehat{P}}_b^2 \widehat{\widehat{P}}_c^2 \dots}. \quad (4.23)$$

The last sum is exactly what one would get by considering

$$\frac{1}{P_a^2 P_b^2 P_c^2 \dots} \quad (4.24)$$

and applying recursion, first using $c_i^{(1)}$, then, depending on which propagator was uncovered, applying recursion using $c_{i,a}^{(2)}$ and then (depending on a and b) applying recursion using $c_{i,a,b}^{(3)}$, *etc.* In other words,

$$\mathcal{A}_n = \sum_{\substack{\text{unordered} \\ \text{sets of } p \\ \text{propagators}}} \frac{\mathcal{A}^{\text{MHV}} \mathcal{A}^{\text{MHV}} \dots \mathcal{A}^{\text{MHV}}}{P_a^2 P_b^2 P_c^2 \dots}, \quad (4.25)$$

We can now state what we have derived: To compute an amplitude,

1. Draw all permitted MHV diagrams,
2. For each diagram, shift the negative helicity particles according to

$$|m_i^b] = |m_i] + r_i|\eta] \quad (4.26)$$

and solve for r_i under the condition that all shifted internal momenta P_a^b are on-shell, and under the condition of conservation of momentum,

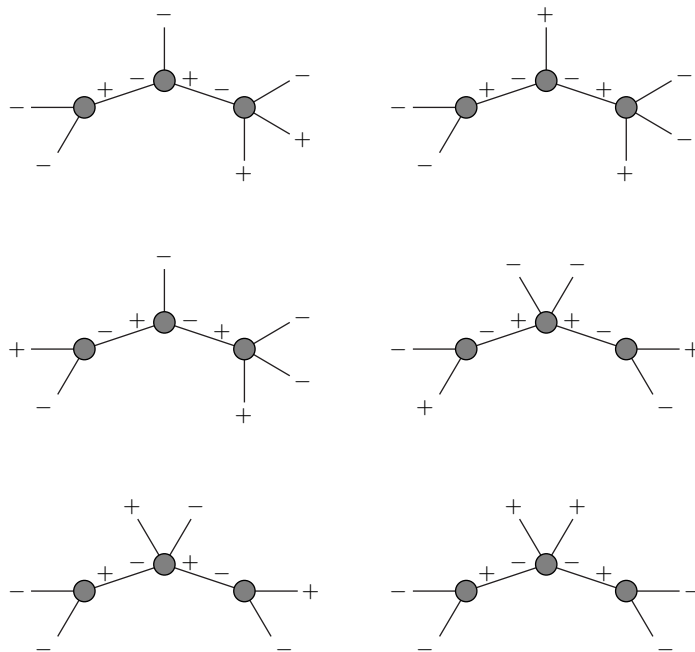
$$\sum_i r_i \langle m_i | = 0. \quad (4.27)$$

3. For each MHV vertex, multiply by the amplitude as a function of the shifted momenta.
4. For each internal line with unshifted momentum P_a , multiply by $1/P_a^2$.

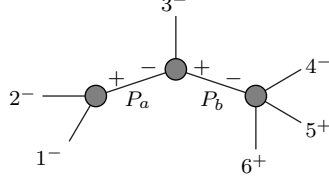
For pure Yang–Mills, step 2 is irrelevant because it only provides information on the anti-holomorphic spinors. For internal momenta, $|P^b\rangle \sim |P\eta\rangle$ is independent of the actual values of the r_i . In the gravity application of these rules, to which we now turn, this step becomes crucial.

4.4 MHV Rules for Gravity

Postponing again the question of the required large z behaviour, we can apply the above version of the MHV rules to gravity amplitudes. We will do so through the example of the amplitude $M_6(1^-, 2^-, 3^-, 4^-, 5^+, 6^+)$, which is N^2 MHV, but also googly MHV, a fact which will not concern us here. This amplitude has a total of 90 MHV diagrams that are permutations of six basic ones,



To compute the contribution of a representative of the first basic diagram,



we first write down the conditions for the on-shell'ness of the shifted internal momenta,

$$\begin{aligned} (P_a^b)^2 &= (P_a + r_1|1\rangle[\eta] + r_2|2\rangle[\eta])^2 = P_a^2 + r_1\langle 1P_a\eta\rangle + r_2\langle 2P_a\eta\rangle \\ &= \langle 12\rangle([\eta] + r_1[2\eta] + r_2[\eta 1]) = 0, \end{aligned} \quad (4.28)$$

$$(P_b^b)^2 = (P_b + r_4|4\rangle[\eta])^2 = P_b^2 + r_4\langle 4(5+6)\eta\rangle = 0. \quad (4.29)$$

Two additional conditions can be obtained by hitting the conservation of momentum equation with two spinors (here we choose 3 and 4):

$$r_1\langle 13\rangle + r_2\langle 23\rangle + r_4\langle 43\rangle = 0 \quad (4.30)$$

$$r_1\langle 14\rangle + r_2\langle 24\rangle + r_3\langle 34\rangle = 0. \quad (4.31)$$

The solution is

$$r_1 = -\frac{\langle 4(5+6)1\rangle}{\langle 4(5+6)\eta\rangle}, \quad |1^b\rangle = \frac{|(5+6)4\rangle[\eta 1]}{[\eta(5+6)4]}, \quad (4.32)$$

$$r_2 = -\frac{\langle 4(5+6)2\rangle}{\langle 4(5+6)\eta\rangle}, \quad |2^b\rangle = \frac{|(5+6)4\rangle[\eta 2]}{[\eta(5+6)4]}, \quad (4.33)$$

$$r_3 = -\frac{\langle 4(5+6)3\rangle}{\langle 4(5+6)\eta\rangle}, \quad |3^b\rangle = \frac{|(5+6)4\rangle[\eta 3]}{[\eta(5+6)4]}, \quad (4.34)$$

$$r_4 = -\frac{(4+5+6)^2}{\langle 4(5+6)\eta\rangle}, \quad |4^b\rangle = -\frac{|(5+6)(4+5+6)\eta\rangle}{\langle 4(5+6)\eta\rangle}, \quad (4.35)$$

such that

$$P_a^b = \frac{|(1+2)\eta\rangle\langle 4(5+6)|}{\langle 4(5+6)\eta\rangle}, \quad (4.36)$$

$$P_b^b = \frac{|(4+5+6)\eta\rangle\langle 4(5+6)|}{\langle 4(5+6)\eta\rangle}. \quad (4.37)$$

The contribution of this diagram is thus

$$\begin{aligned} &M_3^{\text{MHV}}(1^{b-}, 2^{b-}, -P_a^{b+}) \frac{1}{P_a^2} \\ &\quad \times M_3^{\text{MHV}}(P_a^{b-}, 3^{b-}, P_b^{b+}) \frac{1}{P_b^2} M_4^{\text{MHV}}(-P_b^{b-}, 4^{b-}, 5^+, 6^+) \end{aligned} \quad (4.38)$$

$$= \frac{\langle 12\rangle^6}{\langle 2P_a^b\rangle^2 \langle P_a^b 1\rangle^2} \frac{1}{P_a^2} \frac{\langle P_a^b 3\rangle^6}{\langle 3P_b^b\rangle^2 \langle P_b^b P_a^b\rangle^2} \frac{1}{P_b^2} \frac{[56]\langle P_b^b 4\rangle^6}{\langle 56\rangle\langle 45\rangle\langle 6P_b^b\rangle\langle 46\rangle\langle 5P_b^b\rangle} \quad (4.39)$$

$$\begin{aligned}
&= \frac{\langle 12 \rangle^2}{[1\eta]^2 [\eta 2]^2} \frac{1}{\langle 12 \rangle [21]} \frac{[\eta(1+2+3)3]^6}{\langle 3(4+5+6)\eta \rangle^2 [\eta(4+5+6)(1+2)\eta]^2} \\
&\quad \times \frac{1}{(4+5+6)^2} \frac{[56][\eta(5+6)4]^6}{\langle 45 \rangle \langle 56 \rangle \langle 46 \rangle \langle 6(4+5)\eta \rangle \langle 5(4+6)\eta \rangle} \tag{4.40}
\end{aligned}$$

$$= \frac{\langle 12 \rangle [56] \langle 3P_b \eta \rangle^2 \langle 4P_b \eta \rangle^6}{[1\eta]^2 [2\eta]^2 [3\eta]^2 [21] \langle 45 \rangle \langle 56 \rangle \langle 46 \rangle \langle 6P_b \eta \rangle \langle 5P_b \eta \rangle P_b^2}. \tag{4.41}$$

Though the procedure to obtain one out of six contributions to the amplitude is in itself quite complicated, it is nothing in comparison to the Lagrangian approach. But again, the on-shell recursion relations for gravity will produce results faster.

Rather than computational speed, the interesting thing here is that it is possible to formulate MHV rules for a gravity theory. This highlights one of the mysterious connections between Yang–Mills theory and gravity which is not properly understood. In this case, the MHV rules for YM drop out of a description in twistor space, and such a description does not seem likely for gravity, although there have been attempts which reproduce the correct spectrum [1] but not the correct dynamical theory [116]. Thus, an explanation outside of on-shell recursion relations is still an outstanding problem.

4.5 Large z Properties of the MHV Rule Shift

The question of the $z \rightarrow \infty$ behaviour of deformed amplitudes should now be addressed. To see what behaviour we need, consider the very last step of the successive recursions where, for an N^n MHV amplitude, we have uncovered $n - 1$ propagators. To uncover the last propagator, the last shift must have the amplitude go as z^{-1} . When we get to this point, the antiholomorphic spinors have already been shifted many times,

$$|m_i] \rightarrow |m_i] + (s_i + t_i z)|\eta] \tag{4.42}$$

where s_i are the consequences of all the previous shifts and the t_i impose conservation of momentum and the vanishing of the z dependence of all propagator terms we have already uncovered. Had we not imposed this, every propagator already uncovered would have contributed z^{-1} to the large z limit. In other words, had the t_i been unconstrained (apart from momentum conservation) the large z behaviour of the final shift would be z^{-n} . The dependence on the s_i is subleading in z and mainly a consequence of the $c_{i,\dots}^{(\cdot)}$'s chosen along the way, so their presence should not disturb this conclusion for generic external momenta. This leads us to conclude that the condition for the MHV rules to hold as described here is that under the shift

$$|m_i] \rightarrow |m]_i + \tilde{t}_i z |\eta] \tag{4.43}$$

where \tilde{t}_i impose momentum conservation but are otherwise free, an N^n MHV amplitude must go as z^{-n} as $z \rightarrow \infty$.

For gluon amplitudes in Yang–Mills this can be proven directly by looking at the worst possible Feynman diagram. In such a diagram, the $n + 2$ external negative helicity gluons must be connected by some number v of three-vertices and $v - 1$ propagators. Since three-vertices go as z^1 and propagators go as z^{-1} , these internal parts of the diagram go as z^1 . The dependence of the polarizations is z^{-1} each, because we are shifting the antiholomorphic spinor of a negative helicity gluon, so the polarizations together go as $z^{-(n+2)}$. In total the whole amplitude goes as $z^{-(n+1)}$ which is one power better than required. This forms the last ingredient of the on-shell recursive proof of the MHV rules for gluons.

For gravitons it is a different story. If we do the same analysis as above, we find that the v vertices contribute z^{2v} , the propagators contribute z^{-v+1} and the external polarizations contribute $z^{-2(n+2)}$. This gives in total z^{v-2n-3} . The maximal number of vertices that may have z dependence in an m -point amplitude is $m-2$, so the worst possible Feynman diagram has the behaviour z^{m-2n-5} where we require z^{-n} . An analysis using the above result for Yang–Mills together with the KLT relations gives the same estimate.

Luckily, these types of arguments are known to be way off for gravity. If we do the same analysis for the BCFW shift (3.24) of an m -point amplitude we would obtain z^{m-5} , where the real result is known to be z^{-2} [5, 14]. Cancellations of this order of magnitude in the shifts used here should in general ensure that the MHV rules for gravity are justified. In the original article on gravity MHV rules [49], the NMHV six and seven point amplitudes were found to go as z^{-5} which is two powers better than needed, and four and five powers, respectively, better than the worst expectation. If we allow ourselves some speculation, this hints that the actual $z \rightarrow \infty$ behaviour is z^{-n-4} , implying that $m - n + 1$ powers are removed by obscure symmetries in the gravity theory.

Chapter 5

Loop-Level Methods

Until now we have mostly concerned ourselves with tree-level amplitudes. For most practical applications though, amplitudes at one or more loops are required for interesting results. This chapter will review four general tools out of strict historical order. For loop-level calculations it is often necessary (or just useful) to use combinations of them.

5.1 Structure of One-Loop Amplitudes

First, however, we will start out by reviewing what is known in general about one-loop amplitudes, mostly in Yang–Mills theory, but also more generally.

5.1.1 Integral Reduction

When doing one-loop calculations with Feynman rules, one will encounter integrals with arbitrary numbers of propagators and tensors depending on the loop momentum of arbitrary rank. In Yang–Mills theory, an n -point calculation will give up to n loop propagators and up to rank n tensors, while *e.g.* a gravity calculation will give up to n loop propagators and rank $2n$ tensors in the loop momentum. Such integrals are impossible to do directly, so one will normally do some sort of integral reduction.

The most important of these is Passarino–Veltman reduction [121], which reduces the powers of loop momentum appearing in the numerator by using the knowledge that the result must be writable as a Lorentz tensor, together with the knowledge of which Lorentz tensors it can depend on. As a simple example, take the integral

$$\int d^D L \frac{L^\mu L^\nu}{(L^2 + i\epsilon)((L + P)^2 + i\epsilon)}. \quad (5.1)$$

Since this integral can only depend on $g_{\mu\nu}$ and P^μ , it must be writable as

$$A(P)g^{\mu\nu} + B(P)P^\mu P^\nu. \quad (5.2)$$

By contracting with $g_{\mu\nu}$ and P_μ on both sides of this equation and using similar results from simpler integrals, one can find expressions for A and B in terms of integrals fewer powers of loop momentum in the numerator and the same number of, or fewer, loop propagators. Iterating this procedure can remove all dependence on the loop momentum in the numerator and leave us with scalar integrals only.

Depending on the dimension of spacetime, the scalar integrals may be reduced further. Take for instance the massless hexagon integral in four dimensions (with implicit $i\epsilon$'s)

$$\int d^4L \frac{1}{L^2(L+K_1)^2(L+K_2)^2(L+K_3)^2(L+K_4)^2(L+K_5)^2}. \quad (5.3)$$

Because the external momenta are “twice” linearly dependent in four dimensions, we can always adjust constants a_0 through a_5 such that

$$a_0L^2 + \sum_{i=1}^5 a_i(L+K_i)^2 = 1, \quad (5.4)$$

which allows us to split the hexagon integral into six pentagons. Notice that this depends on the dimension in which the external momenta live; dimensionally regulating the loop momentum does not change this.

By using these types of integral reduction, one can arrive at expressions for the wanted amplitudes which contain a reduced set of integrals that are possible to compute, or more often, look up.

5.1.2 Massless Integral Basis in Four Dimensions

For four dimensional theories with massless states running in the loop, there is an additional identity that allows pentagons to be written in terms of lower point integrals [36]. This leaves a basis for all one-loop amplitudes consisting of scalar box integrals, triangle integrals, bubble integrals, and 1¹. The integrals are defined as (implicit $i\epsilon$'s)

$$\begin{aligned} I_4(P_1, P_2, P_3) &= -i\mu^{2\epsilon} \int \frac{d^{4-2\epsilon}L}{(2\pi)^{4-2\epsilon}} \\ &\quad \times \frac{1}{L^2(L+P_1)^2(L+P_1+P_2)^2(L+P_1+P_2+P_3)^2}, \\ I_3(P_1, P_2) &= i\mu^{2\epsilon} \int \frac{d^{4-2\epsilon}L}{(2\pi)^{4-2\epsilon}} \frac{1}{L^2(L+P_1)^2(L+P_1+P_2)^2}, \\ I_2(P) &= -i\mu^{2\epsilon} \int \frac{d^{4-2\epsilon}L}{(2\pi)^{4-2\epsilon}} \frac{1}{L^2(L+P)^2}, \end{aligned} \quad (5.5)$$

These integrals (and 1) have coefficients which are rational functions of the external spinors and momenta. In addition, box and triangle integrals come out as

¹Remember that massless tadpoles vanish in dimensional regularization

expressions of mass dimension -2ϵ , divided by their respective Gram determinants which may or may not be rational. This prompts us to define the box and triangle *integral functions* F_4 and F_3 where the Gram determinant is taken into the coefficient instead, where we will often find that it is cancelled.

Box and triangle integrals are classified according to which of their external momenta are massless. For triangles there are zero-mass through three-mass ($0m$, $1m$, $2m$, $3m$) while for boxes there zero-, one-, three-, and four-mass together with the so-called two-mass-easy ($2me$) and two-mass-hard ($2mh$) configurations where the massless corners are opposite and adjacent, respectively. The integral functions and Gram determinants are given in appendix A.

5.1.3 Supersymmetric Decomposition

When calculating gauge theory amplitudes, the answer depends on the number of massless fermions and scalars in the gauge theory because they can run in the loop. There are particular choices for these numbers that give dramatically simpler answers, namely those corresponding to supersymmetric theories. It is standard to use the “basis” for the particle content consisting of an $\mathcal{N} = 4$ multiplet (1 gluon, 4 fermions, 3 complex scalars), an $\mathcal{N} = 1$ chiral multiplet (1 fermion, 1 complex scalar), and the so-called $\mathcal{N} = 0$ multiplet containing just a complex scalar. A theory with n_f adjoint fermions and n_s adjoint scalars can thus be written as

$$(\mathcal{N} = 4) - [4 - n_f](\mathcal{N} = 1) + [1 - n_f + n_s](\mathcal{N} = 0). \quad (5.6)$$

If the fermions or scalars are in the fundamental representation, $n_{f,s}$ should be substituted with $n_{f,s}/N_C$ where N_C is the number of colours.

In background field gauge, it can be shown explicitly that there are diagram-by-diagram cancellations that remove four powers of loop momentum in the numerator for $\mathcal{N} = 4$ and two powers for $\mathcal{N} = 1$. When those results are Passarino–Veltman reduced, they can only give rise to boxes in the $\mathcal{N} = 4$ case and only to boxes, triangles and bubbles (that is, no additional rational terms) in $\mathcal{N} = 1$. For $\mathcal{N} = 0$ there are no such cancellations, but the calculation is made simpler by the reduced number of Lorentz indices for a scalar running in the loop as compared to a gluon.

Supersymmetric decompositions can be used in other theories as well, however, without a formal handle on the cancellation of numerator loop momentum. Since the expression of the supersymmetry at tree level is the same as in gauge theory (*e.g.* SWI’s, *cf.* section 2.3.2) and tree level results are recycled in most loop calculations, it is generally believed that the same regularity holds for other theories, in particular gravity. For arbitrary \mathcal{N} it is believed that an even \mathcal{N} multiplet will have \mathcal{N} cancellations of loop momenta in the numerator while an odd \mathcal{N} multiplet will have $\mathcal{N} + 1$ [21].

5.1.4 Limits and Singularities

To aid in both checking and construction expressions for one-loop amplitudes, it becomes important to look at these expressions in certain limits. The tree-level limiting behaviour was studied in section 2.3.3 and this is extended here to one-loop level.

The multiparticle poles of Yang–Mills amplitudes can occur in the same way as at tree-level when a non-loop propagator goes on shell and splits the diagram in two, the loop being on one side or the other. We may also have a singularity coming from other parts of the calculation which has a more messy interpretation, though. This gives the multiparticle limit [30]

$$\begin{aligned} \mathcal{A}^{1\text{-loop}}(\dots) \rightarrow \sum_{h=\pm} & \left(\frac{\mathcal{A}^{\text{tree}}(\dots, P^h) \mathcal{A}^{1\text{-loop}}(-P^{-h}, \dots)}{P^2} \right. \\ & + \frac{\mathcal{A}^{1\text{-loop}}(\dots, P^h) \mathcal{A}^{\text{tree}}(-P^{-h}, \dots)}{P^2} \\ & \left. + \mathcal{F} \frac{\mathcal{A}^{\text{tree}}(\dots, P^h) \mathcal{A}^{\text{tree}}(-P^{-h}, \dots)}{P^2} \right) \end{aligned} \quad (5.7)$$

as $P^2 \rightarrow 0$, where \mathcal{F} is a function depending (in a cut-containing and non-factorized way) on all incoming momenta, but not on the helicities. It also depends on the particle content of the theory.

Another type of singularity that Yang–Mills theory has, is collinear singularities. Again, we get something similar to the tree-level case, only now we have to introduce 1-loop splitting amplitudes which depend on the particle content of the theory. We have

$$\begin{aligned} \mathcal{A}^{1\text{-loop}}(a^{h_a}, b^{h_b}, \dots) \rightarrow \sum_{h=\pm} & \left[\text{Split}_h^{\text{tree}}(z, a^{h_a}, b^{h_b}) \mathcal{A}^{1\text{-loop}}(P^{-h}, \dots) \right. \\ & \left. + \text{Split}_h^{1\text{-loop}}(z, a^{h_a}, b^{h_b}) \mathcal{A}^{\text{tree}}(P^{-h}, \dots) \right] \end{aligned} \quad (5.8)$$

as $a \rightarrow zP$, $b \rightarrow (1-z)P$. The one-loop splitting functions for both gluons and fermions are given in [33] (and to all orders in ϵ in [32]). The pure-gluon splitting functions are

$$\begin{aligned} \text{Split}_+^{1\text{-loop}}(a^+, b^+) &= -\frac{1}{48\pi^2} \left(1 - \frac{n_f}{N} + \frac{n_s}{N} \right) \sqrt{z(1-z)} \frac{[ab]}{\langle ab \rangle^2} \\ \text{Split}_-^{1\text{-loop}}(a^+, b^+) &= c_\Gamma \text{Split}_-^{\text{tree}}(a^+, b^+) \left[U + \frac{1}{3} \left(1 - \frac{n_f}{N} + \frac{n_s}{N} \right) z(1-z) \right] \\ \text{Split}_+^{1\text{-loop}}(a^\pm, b^\mp) &= c_\Gamma \text{Split}_+^{\text{tree}}(a^\pm, b^\mp) U \end{aligned} \quad (5.9)$$

where

$$U = -\frac{1}{\epsilon^2} \left(\frac{\mu^2}{z(1-z)(-s_{ab})} \right)^\epsilon + 2 \log z \log(1-z) - \frac{\pi^2}{6} \quad (5.10)$$

and c_Γ is defined in (A.3).

The general form of infrared divergences in Yang–Mills is also known from general arguments. This imposes the constraint that [71, 92, 105]

$$\mathcal{A}^1 = -\frac{c_\Gamma}{\epsilon^2} A^0 \sum_{i=1}^4 \left(\frac{\mu^2}{-s_{i,i+1}} \right)^\epsilon + \mathcal{O}(\epsilon^0). \quad (5.11)$$

This imposes some quite stringent constraints on coefficients of box and triangle functions because there needs to be complete cancellation of *e.g.* terms of the kind

$$\frac{1}{\epsilon^2} \left(\frac{\mu^2}{-t\dots} \right)^\epsilon \quad (5.12)$$

where $t\dots$ is any multiparticle kinematic invariant [31]. In one-loop gravity, a similar relation holds [81],

$$\mathcal{M}^{1\text{-loop}} = \frac{i}{(4\pi)^2} \left[\frac{\sum_{i<j} s_{ij} \log[-s_{ij}]}{2\epsilon} \right] \mathcal{M}^{\text{tree}} + \mathcal{O}(\epsilon^0) \quad (5.13)$$

with similar consequences [48] to be explored further in chapter 7.

5.2 Unitarity Cuts

As mentioned in the introduction, the concepts of unitarity and analyticity of the S -matrix came to play a large role again in the 90's. That was primarily because the insights of the previous section were sufficient to fill in the missing parts of the puzzle, the parts which (helped by experimental evidence) sent S -matrix theory out in the cold.

5.2.1 Ordinary $D = 4$ Unitarity Cuts

Instead of trying to directly reconstruct the one-loop amplitude from its cut discontinuities—a procedure which is often ambiguous—it is possible to use all the insights of the previous section to come up with an ansatz for the result and match cuts on both sides of the equation to arrive at an answer. This was first used by Bern, Dixon, Dunbar and Kosower to compute the one-loop MHV amplitudes in $\mathcal{N} = 4$ Yang–Mills [33] as follows: It is known that the $\mathcal{N} = 4$ amplitude only contains boxes, so we can write

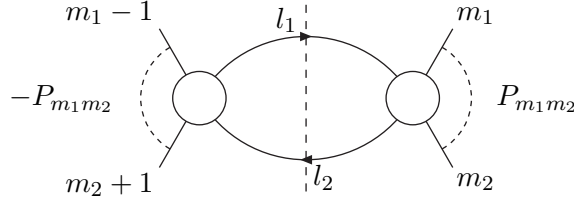
$$\mathcal{A}_{\text{MHV}}^{1\text{-loop}}(i^-, j^-) = \sum_{a \in \text{boxes}} c_a I_a. \quad (5.14)$$

On both sides we can pick out the discontinuity in P_{m_1, m_2}^2 by replacing the loop propagators between m_1 and $m_1 + 1$ and between $m_2 - 1$ and m_2 by delta functions in the square of the loop momenta. On the left side of (5.14) we get an integral

over the product of two tree amplitudes, possibly summed over internal helicities in the loop,

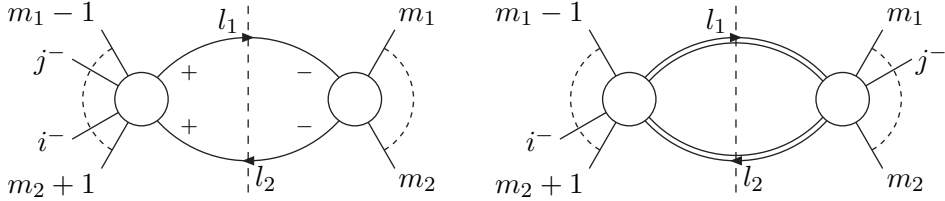
$$\begin{aligned} & \Delta_{m_1, m_2} \mathcal{A}^{1-loop} \\ &= \sum_{h, h'} \int d^D l_1 d^D l_2 \delta(l_1^2) \delta(l_2^2) \delta^{(D)}(l_1 - l_2 - P_{m_1, m_2}) \\ & \quad \times \mathcal{A}(m_2 + 1, \dots, m_1 - 1, l_1^h, (-l_2)^{-h'}) \mathcal{A}(m_1, \dots, m_2, l_2^{h'}, (-l_1)^{-h}). \end{aligned} \quad (5.15)$$

Pictorially, this becomes



where the dashed line denotes the cutting of the two internal lines. In Lorentz invariant gauges such as Feynman gauge, we would have to include a ghost loop, but by using the spinor-helicity formalism, which is implicitly in a light-like axial gauge as mentioned at the end of section 2.2, we can avoid them.

For the two tree amplitudes to be non-zero, they must both be MHV. Then, if i and j are both on the left [right] side we have $(h, h') = (1, -1) [(-1, 1)]$ while if they are on opposite sides $h = h'$ can take any value in the $\mathcal{N} = 4$ multiplet and we need to do an actual summation. These two distinct cases can be drawn as



The summation over the $\mathcal{N} = 4$ multiplet, however, gives exactly the same result as when both i and j are on the same side, namely that the integrand can be written as

$$\mathcal{A}^{\text{tree}}(i^-, j^-) \frac{\langle (m_1 - 1) m_1 \rangle \langle l_1 l_2 \rangle \langle m_2 (m_2 + 1) \rangle \langle l_2 l_1 \rangle}{\langle (m_1 - 1) l_1 \rangle \langle l_1 m_1 \rangle \langle m_2 l_2 \rangle \langle l_2 (m_2 + 1) \rangle}. \quad (5.16)$$

This can again be rewritten as

$$\frac{1}{2} \mathcal{A}^{\text{tree}} \left[\frac{P_{m_1, m_2}^2 P_{m_1-1, m_2+1}^2 - P_{m_1-1, m_2}^2 P_{m_1, m_2+1}^2}{(l_1 + (m_1 - 1))^2 (l_2 - (m_2 + 1))^2} \right]$$

$$\begin{aligned}
& + \frac{P_{m_1, m_2-1}^2 P_{m_1-1, m_2}^2 - P_{m_1-1, m_2-1}^2 P_{m_1, m_2}^2}{(l_1 + (m_1 - 1))^2 (l_2 + m_2)^2} \\
& + \frac{P_{m_1+1, m_2}^2 P_{m_1, m_2+1}^2 - P_{m_1, m_2}^2 P_{m_1+1, m_2+1}^2}{(l_1 - m_1)^2 (l_2 - (m_2 + 1))^2} \\
& + \frac{P_{m_1+1, m_2-1}^2 P_{m_1, m_2}^2 - P_{m_1, m_2-1}^2 P_{m_1+1, m_2}^2}{(l_1 - m_1)^2 (l_2 + m_2)^2} \Big], \tag{5.17}
\end{aligned}$$

plus terms that vanish when we integrate. In this way all the dependence on the loop momenta has been confined to two propagators in each of the four terms. That, however, is exactly what one would get by cutting four particular 2-mass easy boxes. And even better, the coefficients (apart from $\mathcal{A}^{\text{tree}}$) are the respective Gram determinants, so this is a sum of cuts of four box functions (F 's) with the same coefficient. In equations,

$$\begin{aligned}
\Delta_{m_1, m_2} \mathcal{A}^{1\text{-loop}} = \mathcal{A}^{\text{tree}} \Delta_{m_1, m_2} & \left(F_4(m_1 - 1, P_{m_1, m_2}, m_2 + 1) \right. \\
& + F_4(m_1 - 1, P_{m_1, m_2-1}, m_2) \\
& + F_4(m_1, P_{m_1+1, m_2}, m_2 + 1) \\
& \left. + F_4(m_1, P_{m_1+1, m_2-1}, m_2) \right). \tag{5.18}
\end{aligned}$$

This suggests that the one-loop amplitude can be written roughly as the tree amplitude times the sum of all 2-mass easy box functions. The 'roughly' comes in through careful considerations of which choices of m_1 and m_2 are allowed and independent. The result can now be checked using other means such as collinear limits and it does indeed hold up.

Staying inside Yang–Mills theory there are two extensions we can make on this [34]. Firstly, we can consider the $\mathcal{N} = 1$ or the $\mathcal{N} = 0$ theory where triangle and bubble integrals are introduced on the right side of (5.14). This complicates the calculation by giving integrands whose numerators depend on the cut loop momenta while there may be one less propagator. This then requires integral reduction *a la* Passarino–Veltman (section 5.1.1) with some simplifying conditions on the loop momenta. For the $\mathcal{N} = 0$ theory there is the additional complication that the rational terms are not picked up by four-dimensional unitarity cuts. As we will see later, it can still be quite useful to know the cut-containing parts of the amplitude. Secondly, we can go beyond MHV amplitudes where the integrand does not immediately have the nice decomposition into boxes as *e.g.* in (5.17). Still, some $\mathcal{N} = 4$ six-point results can be obtained.

Inspired by the recent revival of unitarity arguments, some improvements have been made on the technology which allows for quite efficient extraction of integral coefficients [58, 63].

5.2.2 Generalized Unitarity

The process of computing a unitarity cut where two propagators are put on-shell has a clear interpretation as the discontinuity across a cut in the amplitude as a

complex function of the kinematic variables. In the way it is applied, however, this interpretation of the cut is not used. Although the interpretation of the cutting of more than two loop propagators may not be as clear, it seems just as reasonable to use it to constrain an amplitude.

The problem is that many integrals cut on more than two propagators turn out to be zero because there are no solutions in Minkowski space for the cut momenta. A triple cut is only non-zero when applied to three-mass triangles and three- and four-mass boxes, while a quadruple cut is only non-zero for four-mass boxes. Higher cuts are zero because they over-constrain the four-dimensional loop momentum. There are some situations where generalized unitarity does come in handy in Minkowski space; the NMHV $\mathcal{N} = 4$ amplitude has been calculated to all n in this way [31, 37].

Since the comments here apply only to amplitudes in real Minkowski space, they will be altered completely when we move to complex momenta below.

5.2.3 Unitarity in $D = 4 - 2\epsilon$

If we want to know a full one-loop amplitude we must do the dimensional regularization properly. This involves taking the loop momentum to be $4 - 2\epsilon$ -dimensional rather than four-dimensional. This poses a very deep problem when using the spinor helicity formalism as it is tied to exactly four dimensions. One solution could be to use spinor helicity notation for all non-loop quantities and ordinary Lorentz notation for loop quantities. This comes at the expense of the compact form of tree amplitudes.

When computing gluon scattering amplitudes, the easiest way to proceed is to use the fact that only the $\mathcal{N} = 0$ component can have rational terms, and thus we only need the less compact amplitudes for scalar particles in the loop [26, 35]. In this way issues of summing over polarization states are also avoided. The cut momentum of the scalar is written as

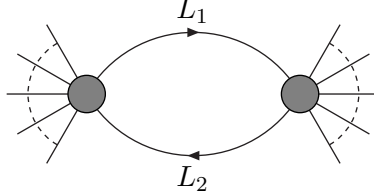
$$L_{(4-2\epsilon)} = L_{(4)} + \mu e_{(-2\epsilon)}, \quad (5.19)$$

where $L_{(4)}$ is a four-dimensional momentum of mass μ and $e_{(-2\epsilon)}$ is a -2ϵ -dimensional unit vector. The integration will then split into an integral over a massive scalar and an integral over the mass. Using the unitarity method, this can be used to write the amplitude in terms of loop integrals whose rational parts as $\epsilon \rightarrow 0$ are known. Recent versions of such methods are developed in [3, 4, 62].

5.3 MHV Rules for Loops: The BST Prescription

When the MHV rules were conceived, the perspective for their use at loop level was rather dim. It was argued that the loops would necessarily contain states of conformal supergravity, a theory which is non-unitary. Not everyone was deterred by this argument, at least not Brandhuber, Spence and Travaglini (BST) who decided to recalculate the one-loop $N = 4$ MHV amplitude using MHV rules [57].

Their prescription consists of drawing all diagrams with two MHV vertices and two internal lines to form a loop,



The momenta L_1, L_2 of these internal lines are off-shell, so on-shell continuations of them are required for use in the MHV vertices. This is performed by taking the integration measure

$$d^4 L_1 d^4 L_2 \frac{\delta^{(4)}(L_1 - L_2 + P)}{(L_1^2 + i\epsilon)(L_2^2 + i\epsilon)} \quad (5.20)$$

and changing variables to $l_{1,2}$ and $z_{1,2}$ such that $l_{1,2}$ are lightlike and

$$L_{1,2} = l_{1,2} + z_{1,2}\eta \quad (5.21)$$

where η is an arbitrary lightlike vector. As shown in [55], the combination $z_1 + z_2$ can be integrated out by standard (albeit involved) methods of complex analysis, while the combination $z_1 - z_2$ can be replaced by $P_z^2 = (P + z_1\eta - z_2\eta)^2$. This yields the measure

$$2\pi i d^4 l_1 d^4 l_2 \delta^{(+)}(l_1^2) \delta^{(+)}(l_2^2) \frac{dP_z^2 \theta(P_z^2)}{P_z^2 - P^2 - i\epsilon} \delta^{(4)}(l_1 - l_2 + P_z). \quad (5.22)$$

where the $(+)$ on the delta functions impose that l_1 and l_2 must have positive energy.

For $\mathcal{N} = 4$ matter running in the loop, BST found that the product of the two MHV vertices (summed over the multiplet) became—in a way similar to the unitarity example above—a sum over terms of the kind

$$\mathcal{A}^{\text{tree}} \frac{(P_z + m_1)^2 (P_z - m_2)^2 - P_z^2 (P_z + m_1 - m_2)^2}{2(l_1 + m_1)^2 (l_2 + m_2)^2}. \quad (5.23)$$

At this point the loop momenta are described as 4-momenta rather than spinors, and that permits a dimensional regularization by taking the number of dimensions to be $4 - 2\epsilon$ as usual.

With sufficient hard work, the integration of (5.23) with the measure (5.22) can be performed and terms (four of each) which have the same numerator in (5.23) combine to form two-mass easy box functions. The proof relies in part on an identity between nine dilog functions and in this way gives a different form of the two-mass easy function derived earlier by Duplanić and Nizić [82] but not widely known.

There are generalizations to the cases with $\mathcal{N} = 1$ [13, 124] and scalar matter [11] in the loop which require triangle and bubble functions. In the scalar case there are additional rational pieces which are not predicted by this version of the loop MHV rules because they contain cuts almost by construction. These rational terms, however, appear to be generated in the light-cone reformulation of the MHV rules with a particular non-dimensional regularization [56].

In spite of the successful application to several one-loop calculations of MHV (and similar [6, 10]) amplitudes, the BST prescription appears to be unpractical for higher numbers of negative helicity gluons than two. Although the formal correctness of the prescription has been proven using the Feynman Tree Theorem [55] for any number of negative helicity gluons, there have been no concrete calculations, mainly because the method has been superseded by others mentioned in this chapter.

The prescription also inherits a formal problem from the tree-level MHV rules, namely the one mentioned in section 3.2.2 that the vertices do not obey momentum conservation. From that perspective, it may be seen as odd that the right results appear, as any (momentum conserving) rewriting of the vertices will change the results to something wrong. Resolution of this problem comes either from formulating the loop-level MHV rules in a light-cone form or by noting that any cutting of internal lines (as in the Feynman Tree Theorem mentioned in the introduction) reduces the amplitude to integrals over on-shell tree amplitudes where the conservation-of-momentum problem was resolved by viewing the rules as coming from recursion relations in complexified Minkowski space (chapter 4).

5.4 Quadruple Cuts

The unitarity method of section 5.2 employed cuts on two internal states, partly because the cut conditions are guaranteed to have solutions for which the internal momenta are real in Minkowski space. Clearly, there is nothing wrong with applying more cuts in principle, but the cut conditions often turn out not to allow any real solutions, thereby setting the cut to zero and rendering its information useless.

While working with twistor methods, first described in 2+2 dimensions where the spinors are real and independent, Britto, Cachazo and Feng realized [59] that working in that signature (or, more generally, in complexified Minkowski space) would allow simultaneous solutions to the constraints of four cuts. Since the loop momentum is four dimensional this would fix it completely, reducing the problem of finding the coefficient of a box function to a purely algebraic one. This is particularly useful for calculating $\mathcal{N} = 4$ amplitudes which only contain box integrals.

5.4.1 Basic idea in $\mathcal{N} = 4$

Consider first a one-loop amplitude and choose four internal lines to take on-shell. There is, of course, a one-to-one correspondence between the boxes and the sets of four internal lines, so there is no double counting issue. The chosen box with coefficient c is

$$c \int \frac{d^4 L}{(2\pi)^4} \frac{1}{[L^2 + i\epsilon][(L + K_1)^2 + i\epsilon][(L + K_1 + K_2)^2 + i\epsilon][(L - K_4)^2 + i\epsilon]} \quad (5.24)$$

which is cut to

$$c \sum_{\text{soln.}} \int d^4 L \delta^{(+)}[L^2] \delta^{(+)}[(L + K_1)^2] \delta^{(+)}[(L + K_2)^2] \delta^{(+)}[(L - K_4)^2]. \quad (5.25)$$

The constraints have two solutions which give rise to the same Jacobian for the integral. The Jacobian is inversely proportional to the Gram determinant but will otherwise not concern us. The result of the cutting is now

$$2c \text{Jac}(K_1, K_2, K_4). \quad (5.26)$$

We can do the same considerations for each Feynman diagram in the calculation of the one-loop amplitude. Adding up contributions from all diagrams that cut our four chosen internal lines will give

$$\begin{aligned} & \int d^4 L \sum_{\text{soln.,states}} \mathcal{A}(\dots, -L, L + K_1) \mathcal{A}(\dots, -L - K_1, L + K_1 + K_2) \\ & \quad \times \mathcal{A}(\dots, -L - K_1 - K_2, L - K_4) \mathcal{A}(\dots, -L + K_4, L) \\ & \quad \times \delta^{(+)}[L^2] \delta^{(+)}[(L + K_1)^2] \delta^{(+)}[(L + K_2)^2] \delta^{(+)}[(L - K_4)^2], \end{aligned} \quad (5.27)$$

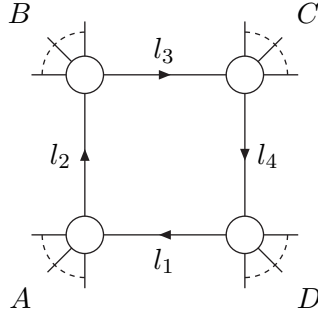
where the summation over states refers to the possibility that different particles may have those momenta, and that we must sum over all possibilities. In the same way as above, this gives

$$\left(\sum_{\text{soln.,states}} \mathcal{A}_A \mathcal{A}_B \mathcal{A}_C \mathcal{A}_D \right) \text{Jac}(K_1, K_2, K_4), \quad (5.28)$$

or,

$$c = \frac{1}{2} \sum_{\text{soln.,states}} \mathcal{A}_A \mathcal{A}_B \mathcal{A}_C \mathcal{A}_D. \quad (5.29)$$

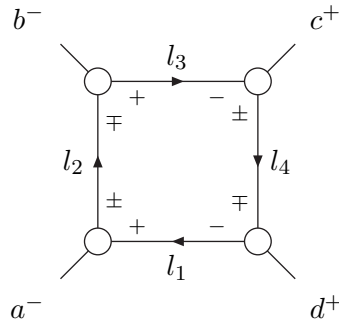
In other words, the coefficient is given by products of four on-shell tree amplitudes in four dimensions. The quadruple cut can be depicted as a box with four corner tree amplitudes connected by the (implicitly cut) loop propagators,



In concrete examples the internal momenta have helicity labels if there is only one helicity configuration which gives non-vanishing contributions.

5.4.2 A Simple Example

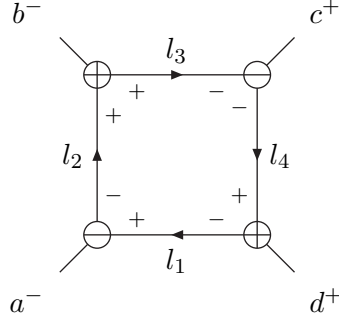
As a first example, we may try to calculate the one-loop $(- - ++)$ amplitude. This has only one quadruple cut, namely



There are two solutions for the internal momenta l_1 through l_4 . The first is

$$\begin{aligned}
 l_1 &= |d\rangle \frac{\langle ba \rangle}{\langle bd \rangle} [a], & l_2 &= |b\rangle \frac{\langle da \rangle}{\langle bd \rangle} [a], \\
 l_3 &= |b\rangle \frac{\langle dc \rangle}{\langle db \rangle} [c], & l_4 &= |d\rangle \frac{\langle bc \rangle}{\langle db \rangle} [c],
 \end{aligned}
 \tag{5.30}$$

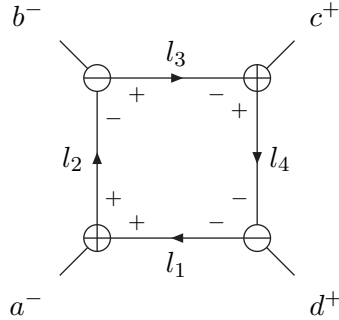
with the consequence that MHV three-point amplitudes at corners B and D are zero while googly-MHV three-point amplitudes at corners A and C are zero. Thus, the only non-vanishing assignment of internal states is



giving the contribution²

$$\begin{aligned}
& \frac{1}{2} \frac{\langle al_2 \rangle^3}{\langle l_2(-l_1) \rangle \langle (-l_1)a \rangle} \frac{[l_3(-l_2)]^3}{[(-l_2)b][bl_3]} \frac{\langle l_4(-l_3) \rangle^3}{\langle (-l_3)c \rangle \langle cl_4 \rangle} \frac{[(-l_4)d]^3}{[dl_1][l_1(-l_4)]} \\
&= \frac{1}{2} \frac{\langle al_2 \rangle^3}{\langle al_1 \rangle \langle l_1 l_2 \rangle} \frac{[l_2 l_3]^3}{[l_2 b][bl_3]} \frac{\langle l_3 l_4 \rangle^3}{\langle l_3 c \rangle \langle cl_4 \rangle} \frac{[l_4 d]^3}{[l_4 l_1][l_1 d]} \\
&= \frac{1}{2} \frac{\langle da \rangle^2 \langle dc \rangle^2 \langle bc \rangle^2}{\langle bd \rangle^6} \frac{\langle ab \rangle^3}{\langle al_1 \rangle \langle l_1 b \rangle} \frac{[ac]^3}{[ab][bc]} \frac{\langle bd \rangle^3}{\langle bc \rangle \langle bd \rangle} \frac{[cd]^3}{[cl_1][l_1 d]} \\
&= \frac{1}{2} \frac{\langle da \rangle^2 \langle dc \rangle^2 \langle bc \rangle^2}{\langle bd \rangle^4 \langle ab \rangle^2} \frac{\langle ab \rangle^3}{\langle ad \rangle \langle db \rangle} \frac{[ac]^3}{[ab][bc]} \frac{\langle bd \rangle^3}{\langle bc \rangle \langle bd \rangle} \frac{[cd]^3}{[ca][ad]} \\
&= -\frac{1}{2} st \mathcal{A}^{\text{tree}}, \tag{5.31}
\end{aligned}$$

where s and t are the normal Mandelstam variables. The other solution for the internal momenta comes about by 'flipping' $|\cdot\rangle \leftrightarrow |\cdot]$ in (5.30) and appropriately reversing the conclusions about the helicity assignments to get



Notice how the symbols \ominus and \oplus are used for three-point MHV and googly-MHV corner amplitudes, respectively. Since $\mathcal{A}^{\text{tree}}$ is invariant under flipping we get the same result as before. The one-loop amplitude then becomes

$$\mathcal{A}^{1\text{-loop}} = -st \mathcal{A}^{\text{tree}} I_4(a, b, c) = 2\mathcal{A}^{\text{tree}} F_4(a, b, c). \tag{5.32}$$

²Remember that $|(-k)\rangle = |k\rangle$ and $|(-k)] = -|k]$.

In practice, a calculation will be a good deal more involved as it may include more complicated corner amplitudes, especially non-MHV amplitudes, and summing over the full $\mathcal{N} = 4$ multiplet possibly running in the loop. Such an example (pieces of which were calculated in the original article on quadruple cuts [59]) is presented in the next chapter.

To aid our calculations in the remainder of this thesis, the solutions of the internal constraints have been assembled in Appendix B.

5.4.3 Box Coefficients in Other Theories

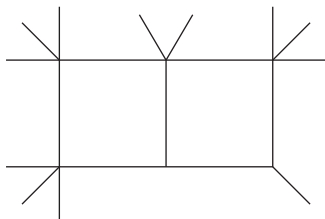
The quadruple cut method extends smoothly to other theories, but without being “complete” in the sense that the entire amplitude can be found from that method. What it does calculate is the contribution to the amplitude from box functions, since the quadruple cut singles out the boxes. When calculating a general Yang–Mills one-loop amplitude, the contributions to boxes from the $\mathcal{N} = 1$ chiral multiplet running in the loop can be calculated just by adjusting the internal states. As is done in chapter 8, the method may also be used where some (massive) external states do not run in the loop. Another extension is to gravity theories such as $\mathcal{N} = 8$ supergravity, where it is possible in general to use the KLT relations between tree amplitudes to construct KLT-like relations between the box coefficients. The use of quadruple cuts in gravity will be considered in more detail in chapter 7.

5.4.4 Generalized Unitarity in Complexified Minkowski Space

As briefly mentioned in section 5.2.2, taking quadruple cuts was not a genuine new idea in itself, rather it was the use of internal momenta in complexified Minkowski space. Thus, the method also allows for wider use of the triple cut. This leads to different methods for obtaining the cut-containing parts of amplitudes [51, 85, 88, 118].

Also, both triple and quadruple cuts can be done with massive particles or, equivalently (*cf.* section 5.2.3) with massless particles exactly in $4 - 2\epsilon$ dimensions to yield also the rational parts of amplitudes [54, 114]

The idea of generalized unitarity can be extended to higher loop orders, where cutting a large portion of the propagators can reveal information as to the structure of both the momentum-dependent numerator and any other coefficients, and can likewise provide useful checks of higher loop unitarity cut calculation where a more conventional generalized unitarity approach is taken. An amusing case [64], which unfortunately does not seem to generalize, is $\mathcal{N} = 4$ two-loop integral coefficients up to and including six external gluons where completely cut integrals such as



have an additional propagator-like singularity coming from the Jacobian of the right box. This singularity can again be cut providing a total of eight constraints which fix the integration completely and gives the coefficient as a product of tree amplitudes. This, however, requires that there is a box which is two-mass hard or one-mass; otherwise the Jacobian is not propagator-like.

Recently, Cachazo and Skinner has shed some additional light on the use of cutting procedures at higher loops [66].

5.5 Recursion at Loop Level

Up till now, this chapter has been concerned with deriving one-loop amplitudes from tree amplitudes. In that perspective it should come as no surprise that recursion can also play a role here. Indeed it does play a role in determining coefficients of the integral functions [29, 51], although it does not seem to be as strong a tool as at tree level.

The problem of determining integral coefficients is, however, not our main objective in this section. Rather, it is the calculation of the rational parts of non-supersymmetric one-loop amplitudes directly in four dimensions without appealing to D -dimensional (generalized) unitarity. The methods described here were developed by Bern, Dixon and Kosower, first for amplitudes with no cut-containing parts [38, 39] and later for amplitudes with cut-containing parts [40]. Since this section is more intended as background material for chapter 8 than a review of advanced topics, the treatment will be adapted to that case and other complications will only be mentioned briefly.

As in the tree case, on-shell recursion starts out by deforming two external momenta with a complex parameter z and writing the $z = 0$ result as an integral along a closed contour enclosing the origin,

$$\mathcal{A}^{1\text{-loop}} = \frac{1}{2\pi i} \oint_{\text{around } 0} \frac{dz}{z} \widehat{\mathcal{A}}^{1\text{-loop}}(z). \quad (5.33)$$

If $\widehat{\mathcal{A}}^{1\text{-loop}}(z) \rightarrow 0$ as $z \rightarrow \infty$, we can write this formally as a sum over integrations around all singularities of $\widehat{\mathcal{A}}^{1\text{-loop}}(z)$, which may be both poles and branch cuts,

$$\begin{aligned} \mathcal{A}^{1\text{-loop}} &= -\frac{1}{2\pi i} \sum_{\text{singularities } i} \oint_{\text{around } i} \frac{dz}{z} \widehat{\mathcal{A}}^{1\text{-loop}}(z) \\ &= -\sum_{\text{poles } i} \frac{\text{Res}_i \widehat{\mathcal{A}}^{1\text{-loop}}(z)}{z_i} - \int_B \frac{dz}{z} \text{Disc}_B \mathcal{A}^{1\text{-loop}}(z) \end{aligned} \quad (5.34)$$

where B is a branch cut and Disc_B is the discontinuity across it. In the first term, the residues are given by the appropriate multiparticle or collinear factorization and depend on lower-point one-loop amplitudes or splitting functions. Since we assume that the cut-containing parts of the amplitude can be calculated by other methods described in this chapter, it makes sense to split all one-loop amplitudes and one-loop splitting functions into their cut-containing³ and rational parts. Then it can be argued that cut-containing parts can be deduced from the cut-containing parts of lower-point one-loop amplitudes and splitting functions, and that rational parts can be deduced from the rational parts of them.

This removes the complication of cuts in the amplitude, but introduces a new one. When we make the split of an amplitude into cut-containing and rational parts

$$\mathcal{A}^{1\text{-loop}} = C + R, \quad (5.35)$$

we cannot trust that C and R individually only have physical (*i.e.* multiparticle and collinear) singularities. In fact, the cut containing parts will often contain terms like

$$\frac{\log(s/t)}{(s-t)^n}, \quad (5.36)$$

which do not correspond to physical singularities of $\mathcal{A}^{1\text{-loop}}$. To handle this, we add and subtract a rational *cut-completion* term CR ,

$$\mathcal{A}^{1\text{-loop}} = (C + CR) + (R - CR) \quad (5.37)$$

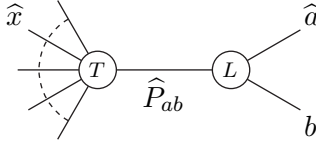
which has (minus) the same unphysical singularities as C . The singularities of $R - CR$ are poles (single or double) in kinematic invariants, so we can do the usual on-shell recursion trick (again, assuming $R(z) - CR(z) \rightarrow 0$ as $z \rightarrow \infty$),

$$R - CR = - \sum_{\text{poles } i} \frac{\text{Res}_i(R(z) - CR(z))}{z_i}, \quad (5.38)$$

where the poles are those that arise from known singularities of $\mathcal{A}^{1\text{-loop}}$. The terms coming from R and CR are known as the direct recursive DR and overlap O terms, respectively. The latter can be computed directly from $CR(z)$ while the former is more intricate.

If the one-loop splitting functions had only single poles, we could interpret them—in the same way as tree splitting functions—as recursion diagrams of the type

³Rational terms proportional to π^2 are included with the cut-containing part.



Drawing it like that, we can now use the rational parts of the splitting functions (5.9) for a gluon in the loop,

$$\begin{aligned}
\text{Split}_{\pm}^{1\text{-loop,R}}(x, a^+, b^-) &= 0, \\
\text{Split}_{+}^{1\text{-loop,R}}(x, a^+, b^+) &= -\frac{c_{\Gamma}}{3} \sqrt{x(1-x)} \frac{[ab]}{\langle ab \rangle^2}, \\
\text{Split}_{-}^{1\text{-loop,R}}(x, a^+, b^+) &= \frac{c_{\Gamma}}{3} \frac{\sqrt{x(1-x)}}{\langle ab \rangle}
\end{aligned} \tag{5.39}$$

to say something about the contribution of such a diagram. Firstly, if a and b have opposite helicities, there is no contribution. This is also the case if all three helicities sitting on the three-point “vertex” and a had its antiholomorphic spinor shifted, since the requirement of \hat{a} and b being collinear is $[\hat{a}b] = 0$; conversely, if a had its holomorphic spinor shifted the all-minus splitting function would give zero.

If the holomorphic spinor of a is shifted and we have to deal with an all-plus splitting amplitude, we immediately see that it has a double pole in z . This poses a serious problem because finding the residue requires us to separate the pure double pole from any single pole which may be hiding underneath it. However, Bern, Dixon and Kosower found a way to circumvent this by introducing a slightly different three-point vertex which seems to do the job in certain cases. Lastly, the complex factorization of the last splitting amplitude above is quite murky, and it should generally be avoided [39].

Keeping these matters in mind, we can obtain the direct recursive terms as

$$\begin{aligned}
DR = \sum_{i,h=\pm} & \left(\frac{\mathcal{A}^{\text{tree}}(\dots, -P_i^h) R(P_i^{-h}, \dots)}{P_i^2} + \frac{R(\dots, -P_i^h) \mathcal{A}^{\text{tree}}(P_i^{-h}, \dots)}{P_i^2} \right. \\
& \left. + \mathcal{F}_R \frac{\mathcal{A}^{\text{tree}}(\dots, -P_i^h) \mathcal{A}^{\text{tree}}(P_i^{-h}, \dots)}{P_i^2} \right)
\end{aligned} \tag{5.40}$$

where i runs over all channels affected by the shift, R are the rational parts of lower-point amplitudes or properly defined three-point loop vertices and \mathcal{F}_R is the rational part of the factorization function. Summing up, the rational part of the amplitude we are after is

$$R = DR + CR - O. \tag{5.41}$$

A last complication is that of the $z \rightarrow \infty$ behaviour of the amplitudes. It is not always possible to find a shift which is both zero as $z \rightarrow \infty$ and avoids problematic splitting functions. However, it has been shown [19] that all problems can be circumvented with imaginative combinations of shifts. This means that any one-loop amplitude in massless QCD is in principle obtainable by the combination of unitarity methods for the cut-constructible parts and recursion for the rational part. A computer program under the name of *BlackHat* which performs such calculations is under development [18]. In chapter 8 we will turn to a complete calculation of a particular one-loop amplitude in QCD with an effective coupling to the Higgs particle.

Chapter 6

One-Loop Amplitudes in $\mathcal{N} = 4$ Super-Yang–Mills

In this chapter we take a closer look at the calculation of one-loop amplitudes in $\mathcal{N} = 4$ Yang–Mills. As described in section 5.4, these amplitudes can be written as linear combinations of scalar Feynman integrals, where the coefficients are essentially products of four tree amplitudes. Here we will calculate some concrete one-loop amplitudes as a demonstration of the technique. The first calculation, of the one-loop MHV amplitude, is primarily included for demonstrational purposes. The part of the calculation of the one-loop NMHV amplitude where scalars and fermions in external states are taken into account is based on [127].

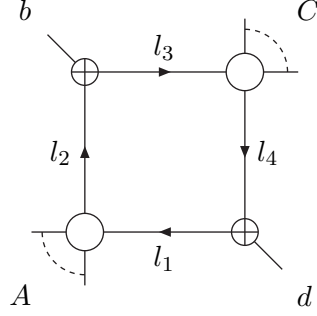
6.1 MHV Constructibility

Although the quadruple cut method allows for the efficient numerical evaluation of one-loop amplitudes from tree amplitudes, there are many analytic simplifications to exploit. The most important of these is the combination with the simple all- n expression for MHV tree amplitudes. For certain configurations of external helicities, and for some box coefficients, the required tree amplitudes are all either MHV or googly-MHV, leading to easily obtainable all- n expressions. A box coefficient with only MHV and googly-MHV corners is called *MHV constructible*.

The simplest class of MHV constructible box coefficients are those of the MHV one-loop amplitude. They were first computed by the unitarity method of section 5.2 by Bern, Dixon and Kosower [33], but we will review the calculation from the quadruple cut perspective here for the sake of familiarity with the method.

As in any quadruple cut calculation, we must start by determining which box functions contribute. This can often be reduced to a matter of counting pluses and minuses: The MHV amplitude has two external minuses. Inside the cut box there are four internal lines with one minus each. Thus, the four tree-level corner amplitudes must have a total of six minuses. The only way these can be distributed without giving zero amplitudes is to have two MHV corners and two

googly-MHV three-point corners, and the latter must be at opposite corners. In other words, we can only have 2-mass easy boxes where the massless corners are googly. Of course, this argument only holds for gluons in the internal and external states, but the conclusions hold in general because all non-zero amplitudes are related to the gluons-only amplitude with the same sum of helicities.



Rather than now classifying the positions of the two negative helicity external legs, we can start out by using the simple form of the MHV amplitude to write down part of the coefficients, namely the part that depends on the denominator of (2.41),

$$\begin{aligned}
& \frac{1}{2} \frac{1}{\langle(-l_1)d+1\rangle\langle d+1\cdots b-1\rangle\langle b-1l_2\rangle\langle l_2(-l_1)\rangle} \frac{1}{[(-l_2)b][bl_3][l_3(-l_2)]} \\
& \times \frac{1}{\langle(-l_3)b+1\rangle\langle b+1\cdots d-1\rangle\langle d-1l_4\rangle\langle l_4(-l_3)\rangle} \frac{1}{[(-l_4)d][dl_1][l_1(-l_4)]} \\
& = \frac{1}{2\langle\cdots\rangle} \frac{\langle dd+1\rangle}{[dl_1]\langle l_1d+1\rangle} \frac{\langle b-1b\rangle}{\langle b-1l_2\rangle[l_2b]} \frac{\langle bb+1\rangle}{[bl_3]\langle l_3b+1\rangle} \frac{\langle d-1d\rangle}{\langle d-1l_4\rangle[l_4d]} \\
& \times \frac{1}{\langle l_1l_2\rangle[l_2l_3]\langle l_3l_4\rangle[l_4l_1]}. \tag{6.1}
\end{aligned}$$

Using the solutions of the internal constraints (B.3), we can write this as

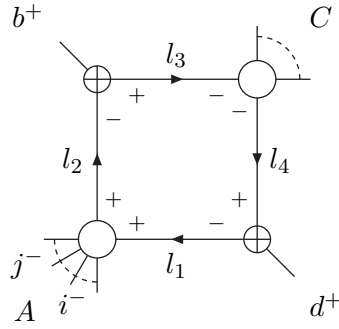
$$\begin{aligned}
& \frac{1}{2\langle\cdots\rangle} \frac{\langle db\rangle}{[dAb]} \frac{\langle bd\rangle}{\langle dAb\rangle} \frac{\langle bd\rangle}{[bCd]} \frac{\langle db\rangle}{\langle bCd\rangle} \frac{\langle bd\rangle^4}{\langle db\rangle\langle dACd\rangle\langle bd\rangle\langle bCAb\rangle} \\
& = \frac{\langle bCd\rangle\langle dAb\rangle}{2\langle\cdots\rangle} \left(\frac{\langle bd\rangle}{\langle bCd\rangle\langle dAb\rangle} \right)^4. \tag{6.2}
\end{aligned}$$

Notice that

$$\begin{aligned}
& \langle bCd\rangle\langle dAb\rangle \\
& = -\langle bC(A+b+C)Ab\rangle \\
& = -A^2\langle bCb\rangle - C^2\langle bAb\rangle - \langle bAb\rangle\langle bCb\rangle \\
& = A^2(C^2 - (b+C)^2) + C^2(A^2 - (A+b)^2) \\
& \quad - (A^2 - (A+b)^2)(C^2 - (C+b)^2) \\
& = -(A+b)^2(C+b)^2 + A^2C^2 \tag{6.3}
\end{aligned}$$

is twice the Gram determinant. Thus, the denominator consists of the Gram determinant, the conventional $\langle \dots \rangle$ spinor product, and a remaining term to the fourth power.

The term coming from the numerator depends on the position of the two external negative helicity legs. These can be placed in four distinct ways, but we will content ourselves with the calculation of two of them. The first case is when the two negative helicity legs are on the same MHV corner, say corner A ,

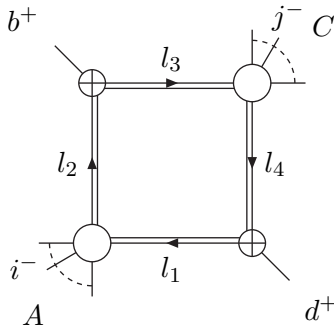


If we call them i and j , respectively, the numerator becomes

$$\begin{aligned}
 & \langle ij \rangle^4 [bl_3]^4 \langle (-l_3)l_4 \rangle^4 [(-l_4)d]^4 \\
 &= \langle ij \rangle^4 \left(\frac{[bCd] \langle bd \rangle \langle bCd \rangle}{\langle bd \rangle^2} \right)^4 \\
 &= \langle ij \rangle^4 \left(\frac{\langle bCd \rangle \langle dAb \rangle}{\langle bd \rangle} \right)^4. \tag{6.4}
 \end{aligned}$$

We see that the paranthesis cancels with the one in (6.2) and leaves only the Gram determinant times the tree amplitude.

We now turn to the case where i and j are on corners A and C , respectively. In this case, the whole $\mathcal{N} = 4$ multiplet can run in the loop which we draw as an extra internal line,



The numerator contribution from the gluons can easily be seen to be

$$\langle il_2 \rangle^4 [(-l_2)b]^4 \langle jl_4 \rangle^4 [(-l_4)d]^4 + \langle (-l_1)i \rangle^4 [bl_3]^4 \langle (-l_3)j \rangle^4 [dl_1]^4. \quad (6.5)$$

The contribution of the fermions can be computed by noting that the amplitude $A^{\text{MHV}}(g^-, f^-, f^+, \dots)$ is simply related to $A^{\text{MHV}}(g^-, g^-, \dots)$, namely by the exchange of one of the numerator factors with another. This yields

$$\begin{aligned} & -4 \left(\langle il_2 \rangle^3 \langle i(-l_1) \rangle [(-l_2)b]^3 [l_3b] \langle jl_4 \rangle^3 \langle j(-l_3) \rangle [(-l_4)d]^3 [l_1d] \right. \\ & \left. + \langle l_2i \rangle \langle (-l_1)i \rangle^3 [b(-l_2)] [bl_3]^3 \langle l_4j \rangle \langle (-l_3)j \rangle^3 [d(-l_4)] [dl_1]^3 \right), \end{aligned} \quad (6.6)$$

where the prefactor takes into account that there are four species and that they must have fermionic sign. The scalar contribution becomes

$$6 \langle il_2 \rangle^2 \langle i(-l_1) \rangle^2 [(-l_2)b]^2 [l_3b]^2 \langle jl_4 \rangle^2 \langle j(-l_3) \rangle^2 [(-l_4)d]^2 [l_1d]^2. \quad (6.7)$$

When we add these three expressions together, we see a common situation in $\mathcal{N} = 4$ SYM: the particle multiplicities make sure that the result is simplified, in this case by making it writable as a fourth power of some term:

$$\begin{aligned} & \left(\langle il_2 \rangle [(-l_2)b] \langle jl_4 \rangle [(-l_4)d] - \langle (-l_1)i \rangle [bl_3] \langle (-l_3)j \rangle [dl_1] \right)^4 \\ & = \left(\langle il_3 \rangle [l_3b] \langle jl_1 \rangle [l_1d] - \langle il_1 \rangle [l_1d] \langle jl_3 \rangle [l_3b] \right)^4 \\ & = \langle ij \rangle^4 \left(\langle l_3l_1 \rangle [l_3b] [l_1d] \right)^4 \\ & = \langle ij \rangle^4 \left(\frac{[bCd] \langle bd \rangle \langle bAd \rangle}{\langle bd \rangle^2} \right)^4 \\ & = \langle ij \rangle^4 \left(\frac{\langle bCd \rangle \langle dAb \rangle}{\langle bd \rangle} \right)^4. \end{aligned} \quad (6.8)$$

In words, the particle states of $\mathcal{N} = 4$ running in the loop conspire to make the numerator factor the same as before. It is not difficult to imagine (and true) that all four positionings of the negative helicity legs i and j give the same numerator factor.

We can now write down the complete one-loop MHV amplitude in $\mathcal{N} = 4$ SYM. It is

$$A_{\text{MHV}}^{1\text{-loop}} = c_{\Gamma} A_{\text{MHV}}^{\text{tree}} \sum_{i=1}^n \sum_{j=i+2}^{\min(n, i-2+n)} F_4(i, P_{i+1, j-1}, j). \quad (6.9)$$

This was the result for gluons in the external states, but in fact, it holds for any MHV choice of external particles. Remember from section 2.3.2 that SWI's fix all tree-level MHV amplitudes up to a constant; since the one-loop result should also respect the full $\mathcal{N} = 4$ supersymmetry, the same is the case here. Only the common factor is corrected from its tree-level value to its one-loop value.

6.2 NMHV Amplitudes

The next natural step would be to compute all NMHV amplitudes. The purely gluonic case was worked out by the unitarity methods of section 5.2 by Bern, Dixon and Kosower [37] prior to the publication of the quadruple cut method. With this method, its inventors computed the MHV constructible parts of the NMHV amplitude [59]. The case with other external particles was worked out by Bidder, Perkins and the author [127], but since the latter calculation naturally incorporates the pure gluon case, both cases will be reviewed here.

For most (but not all) of the box coefficients of the NMHV amplitude, we can again exploit MHV constructibility. Doing the same analysis of the “number of minuses” as above, we see that there are a total of seven minuses, which can be distributed among the four corner amplitudes in two ways: Either there is one googly-MHV three point corner and three MHV corners, or there are two googly-MHV three point corners, one MHV corner, and one NMHV corner. The latter solution is not MHV constructible and will be postponed until we have considered the former which is. The diagram for the calculation and the solution for the internal spinors are

$$\begin{aligned}
 l_1 &= \frac{|d\rangle\langle dCBA|}{\langle dACd\rangle} \\
 l_2 &= \frac{|BCd\rangle\langle dA|}{\langle dACd\rangle} \\
 l_3 &= \frac{|BA d\rangle\langle dC|}{\langle dACd\rangle} \\
 l_4 &= \frac{|d\rangle\langle dABC|}{\langle dACd\rangle}.
 \end{aligned} \tag{6.10}$$

6.2.1 3 Mass Boxes, Gluons Only

As in the MHV case, we start by getting the denominator factors out of the way since they are independent of the external helicities. To fix the ambiguity in scale of the spinors, we assume the convention

$$|l_1\rangle = |d\rangle, \quad |l_2\rangle = |BCd\rangle, \quad |l_3\rangle = |BA d\rangle, \quad |l_4\rangle = |d\rangle. \tag{6.11}$$

The numerators now become

$$\begin{aligned}
 & \frac{1}{2} \frac{1}{\langle(-l_1)A_1\rangle\langle A_1 \cdots A_{-1}\rangle\langle A_{-1}l_2\rangle\langle l_2(-l_1)\rangle} \\
 & \times \frac{1}{\langle(-l_2)B_1\rangle\langle B_1 \cdots B_{-1}\rangle\langle B_{-1}l_3\rangle\langle l_3(-l_2)\rangle} \\
 & \times \frac{1}{\langle(-l_3)C_1\rangle\langle C_1 \cdots C_{-1}\rangle\langle C_{-1}l_4\rangle\langle l_4(-l_3)\rangle}
 \end{aligned}$$

$$\times \frac{1}{[(-l_4)d][dl_1][l_1(-l_4)]} \quad (6.12)$$

$$= \frac{1}{2\langle \dots \rangle} \frac{\langle dA_1 \rangle \langle A_{-1}B_1 \rangle \langle B_{-1}C_1 \rangle \langle C_{-1}d \rangle}{\langle A_1l_1 \rangle [l_1l_4] \langle l_4C_{-1} \rangle [dl_4] \langle l_4l_3 \rangle \langle l_2l_1 \rangle [l_1d]}$$

$$\times \frac{1}{\langle A_{-1}l_2 \rangle \langle l_2B_1 \rangle \langle l_3l_2 \rangle \langle B_{-1}l_3 \rangle \langle l_3C_1 \rangle} \quad (6.13)$$

$$= \frac{1}{2\langle \dots \rangle} \frac{-\langle dACd \rangle^2}{\langle dCBACBAd \rangle}$$

$$\times \frac{-\langle A_{-1}B_1 \rangle \langle B_{-1}C_1 \rangle}{[dCl_3] \langle l_2Ad \rangle \langle A_{-1}l_2 \rangle \langle l_2B_1 \rangle \langle l_3l_2 \rangle \langle B_{-1}l_3 \rangle \langle l_3C_1 \rangle} \quad (6.14)$$

$$= \frac{1}{2\langle \dots \rangle} \frac{\langle dACd \rangle \langle A_{-1}B_1 \rangle \langle B_{-1}C_1 \rangle}{\langle dCBAd \rangle [dCBAd] \langle dCBAd \rangle \langle dCBBAd \rangle}$$

$$\times \frac{1}{\langle A_{-1}BCd \rangle \langle dCBB_1 \rangle \langle B_{-1}BAd \rangle \langle dABC_1 \rangle} \quad (6.15)$$

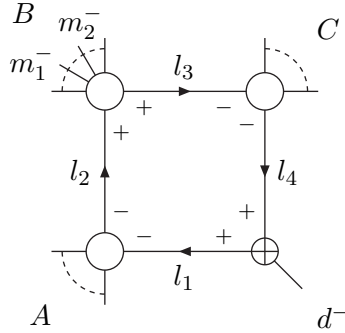
$$= \frac{\langle dCBAd \rangle}{2} \frac{1}{\langle dCBAd \rangle^4}$$

$$\times \frac{-\langle A_{-1}B_1 \rangle \langle B_{-1}C_1 \rangle}{\langle \dots \rangle P_B^2 \langle dCBA_{-1} \rangle \langle dCBB_1 \rangle \langle dABB_{-1} \rangle \langle dABC_1 \rangle}. \quad (6.16)$$

By manipulations of the same kind as (6.3) it can be shown that $\langle dCBAd \rangle / 2$ is the Gram determinant. We see the same kind of structure as for MHV: the Gram determinant, something to the power 4 (which we hope disappears) and a factor involving $\langle \dots \rangle$ which looks natural as a box coefficient.

We can now turn to the numerators. The easiest way to proceed is to consider the gluon case first and then use NMHV SWI's and the known facts about the MHV amplitude for other-than-gluons to relate them to the gluon amplitudes. There are seven distinct non-zero configurations of the three negative helicity gluons and we will show the calculations for three of them.

The first case is shown in the box diagram below

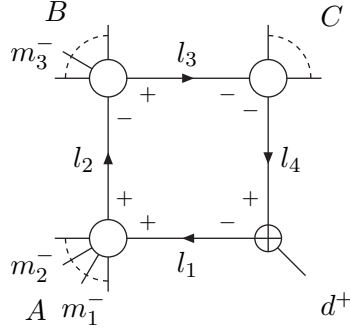


The numerator is given by

$$\left(\langle (-l_1)l_2 \rangle \langle m_1m_2 \rangle \langle (-l_3)l_4 \rangle [(-l_4)l_1] \right)^4$$

$$\begin{aligned}
&= \left(-\langle m_1 m_2 \rangle \langle l_3 l_4 \rangle [l_4 l_1] \langle l_1 l_2 \rangle \right)^4 \\
&= \left(\langle m_1 m_2 \rangle \langle l_3 d \rangle [d A l_2] \right)^4 \\
&= \left(\langle m_1 m_2 \rangle \langle d A B d \rangle \right)^4 \langle d C B A d \rangle^4.
\end{aligned} \tag{6.17}$$

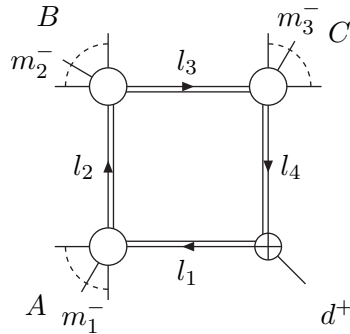
We should be happy to see the factor $\langle d C B A d \rangle^4$ appearing as it cancels the corresponding (unphysical) factor in the denominator. The second placement of the negative helicity gluons we will explore is



which has the numerator

$$\begin{aligned}
&\left(\langle m_1 m_2 \rangle \langle (-l_2) m_3 \rangle \langle (-l_4) l_3 \rangle \langle (-l_4) d \rangle \right)^4 \\
&= \left(\langle m_1 m_2 \rangle \langle l_2 m_3 \rangle \langle l_3 l_4 d \rangle \right)^4 \\
&= \left(-\langle m_1 m_2 \rangle \langle l_2 m_3 \rangle \langle l_3 C d \rangle \right)^4 \\
&= \left(\langle m_1 m_2 \rangle \langle d C B d \rangle \right)^4 \langle d A B C d \rangle^4 \\
&= \left(\langle m_1 m_2 \rangle \langle d C B d \rangle \right)^4 \langle d C B A d \rangle^4.
\end{aligned} \tag{6.18}$$

As before, we see the wanted factor to the power four. The last case is the one where the three negative helicity gluons are situated on the three massive corners,



This configuration is rather special, as the whole $\mathcal{N} = 4$ multiplet can run in the loop and we have to sum over all the particle species. The two gluon contributions

can be constructed as for the cases above,

$$\begin{aligned}
& \left(\langle m_1 l_2 \rangle \langle m_2 l_3 \rangle \langle m_3 l_4 \rangle [d(-l_4)] \right)^4 + \left(\langle m_1(-l_1) \rangle \langle m_2(-l_2) \rangle \langle m_3(-l_3) \rangle [dl_1] \right)^4 \\
&= \left(\langle m_1 B C d \rangle \langle m_2 B A d \rangle \frac{\langle m_3 d \rangle \langle d A B C d \rangle}{\langle d A C d \rangle} \right)^4 \\
&\quad + \left(- \frac{\langle m_1 d \rangle \langle d C B A d \rangle}{\langle d A C d \rangle} \langle m_2 B C d \rangle \langle m_3 B A d \rangle \right)^4 \\
&= \left[\left(\langle m_1 B C d \rangle \langle m_2 B A d \rangle \langle m_3 d \rangle \right)^4 + \left(- \langle m_1 d \rangle \langle m_2 B C d \rangle \langle m_3 B A d \rangle \right)^4 \right] \\
&\quad \times \frac{\langle d C B A d \rangle^4}{\langle d A C d \rangle^4}. \tag{6.19}
\end{aligned}$$

As in the one-loop MHV calculation above, the fermion and scalar contributions follow from the gluon ones by taking products of the two parantheses above with powers summing to four and by adjusting the prefactors. This exactly turns the final result into a complete power of four:

$$\begin{aligned}
& \left(\langle m_1 l_2 \rangle \langle m_2 l_3 \rangle \langle m_3 l_4 \rangle [d(-l_4)] + \langle m_1(-l_1) \rangle \langle m_2(-l_2) \rangle \langle m_3(-l_3) \rangle [dl_1] \right)^4 \\
&= \left(\langle m_1 B C d \rangle \langle m_2 B A d \rangle \langle m_3 d \rangle - \langle m_1 d \rangle \langle m_2 B C d \rangle \langle m_3 B A d \rangle \right)^4 \frac{\langle d C B A d \rangle^4}{\langle d A C d \rangle^4} \\
&= \left[\langle m_3 m_1 \rangle \langle d B C d \rangle \langle m_2 B A d \rangle \right. \\
&\quad \left. + \langle m_1 d \rangle \left(\langle m_3 B C d \rangle \langle m_2 B A d \rangle - \langle m_2 B C d \rangle \langle m_3 B A d \rangle \right) \right]^4 \frac{\langle d C B A d \rangle^4}{\langle d A C d \rangle^4} \\
&= \left(- \langle m_3 m_1 \rangle \langle m_2 B A d \rangle + K_B^2 \langle m_1 d \rangle \langle m_2 m_3 \rangle \right)^4 \langle d C B A d \rangle^4 \\
&= \left(\langle m_1 m_2 \rangle \langle m_3 B A d \rangle + \langle m_3 m_2 \rangle \langle m_1 B C d \rangle \right)^4 \langle d C B A d \rangle^4. \tag{6.20}
\end{aligned}$$

Again, we see the same picture emerging as before.

When doing all negative helicity gluon configurations, we finally obtain the result

$$c^{3m}(m_{1,2,3}^-) = \frac{-\langle A_{-1} B_1 \rangle \langle B_{-1} C_1 \rangle \mathcal{H}_k^4}{\langle \dots \rangle P_B^2 \langle d C B A_{-1} \rangle \langle d C B B_1 \rangle \langle d A B B_{-1} \rangle \langle d A B C_1 \rangle} \tag{6.21}$$

where k denotes the configuration and

$$\begin{aligned}
\mathcal{H}_{BBd} &= \langle m_1 m_2 \rangle \langle d A C d \rangle, \\
\mathcal{H}_{ABd} &= \langle m_1 d \rangle \langle m_2 B C d \rangle, \\
\mathcal{H}_{BCd} &= \langle m_2 d \rangle \langle m_1 B A d \rangle, \\
\mathcal{H}_{ACd} &= \langle m_1 d \rangle \langle m_2 d \rangle K_B^2, \\
\mathcal{H}_{AAB} &= \langle m_1 m_2 \rangle \langle m_3 B C d \rangle, \\
\mathcal{H}_{BCC} &= \langle m_2 m_3 \rangle \langle m_1 B A d \rangle,
\end{aligned}$$

$$\begin{aligned}
\mathcal{H}_{ABB} &= \langle m_2 m_3 \rangle \langle m_1 B C d \rangle, \\
\mathcal{H}_{BBC} &= \langle m_1 m_2 \rangle \langle m_3 B A d \rangle, \\
\mathcal{H}_{AAC} &= \langle m_1 m_2 \rangle \langle m_3 d \rangle K_B^2, \\
\mathcal{H}_{ACC} &= \langle m_2 m_3 \rangle \langle m_1 d \rangle K_B^2, \\
\mathcal{H}_{ABC} &= \langle m_1 m_2 \rangle \langle m_3 B A d \rangle + \langle m_3 m_2 \rangle \langle m_1 B C d \rangle.
\end{aligned} \tag{6.22}$$

6.2.2 NMHV SWIs

Before proceeding to the equivalent calculations with other particle content than gluons, we should consider some of the constraints on those amplitudes coming from supersymmetry. In section 2.3.2 we looked at the effective supersymmetry of tree amplitudes, supersymmetry algebras and the supersymmetric Ward identities that follow. Since we are now working with a genuinely $\mathcal{N} = 4$ supersymmetric theory we can use these considerations for loop amplitudes also. Even better, since the box functions are all independent, $\mathcal{N} = 4$ SWIs for the full amplitude imply that they must also be satisfied coefficient by coefficient. Here we will derive SWIs for amplitudes \mathcal{A} where all g^+ states are implicit.

To derive NMHV SWIs relating pure glue amplitudes to amplitudes with a pair of fermions, we start from $\mathcal{A}(g_1^-, g_i^-, g_j^-, f_{a,k}^+)$ and apply $Q_a(q, \theta)$ to find

$$\begin{aligned}
0 &= \langle 1q \rangle \mathcal{A}(f_{a,1}^-, g_i^-, g_j^-, f_{a,k}^+) + \langle iq \rangle \mathcal{A}(g_1^-, f_{a,i}^-, g_j^-, f_{a,k}^+) \\
&\quad + \langle jq \rangle \mathcal{A}(g_1^-, g_i^-, f_{a,j}^-, f_{a,k}^+) - \langle kq \rangle \mathcal{A}(g_1^-, g_i^-, g_j^-, g_k^+).
\end{aligned} \tag{6.23}$$

This relation holds irrespective of the number of supersymmetries since we are only using one. In a notation closer in spirit to what we will use here, the SWI is

$$\begin{aligned}
0 &= \langle 1q \rangle \mathcal{A}(1^{-1/2}, i^-, j^-, k^{+1/2}) + \langle iq \rangle \mathcal{A}(1^-, i^{-1/2}, j^-, k^{+1/2}) \\
&\quad + \langle jq \rangle \mathcal{A}(1^-, i^-, j^{-1/2}, k^{+1/2}) - \langle kq \rangle \mathcal{A}(1^-, i^-, j^-, k^+).
\end{aligned} \tag{6.24}$$

We can extend this to scalars in external states by starting from the amplitude $\mathcal{A}(g_1^-, g_i^-, f_{b,j}^-, s_{ab,k})$ and applying again $Q_a(q, \theta)$. Using (2.49) we get

$$\begin{aligned}
0 &= \langle 1q \rangle \mathcal{A}(f_{a,1}^-, g_i^-, f_{b,j}^-, s_{ab,k}) + \langle iq \rangle \mathcal{A}(g_1^-, f_{a,i}^-, f_{b,j}^-, s_{ab,k}) \\
&\quad + \langle jq \rangle \mathcal{A}(g_1^-, g_i^-, \tilde{s}_{ab,j}, s_{ab,k}) - \langle kq \rangle \mathcal{A}(g_1^-, g_i^-, f_{b,j}^-, f_{b,k}^-),
\end{aligned} \tag{6.25}$$

which relates amplitudes with both gluons, fermions and scalars. For this SWI we used that an amplitude involving $\mathcal{A}(\dots, s_{ab}, f_a^+)$ vanishes, something which is not immediately obvious. This follows roughly by noting that $s_{ab} \sim Q_a f_b^+ \sim Q_b f_a^+$ which can be interpreted in the way that s_{ab} contains a f_a^+ , and this sets the amplitude to zero by fermion conservation of helicity. These arguments can be made more exact by considering a superfield formulation of the theory such as Nair's [115] which plays a major role in some twistor studies.

To obtain SWIs involving amplitudes with no negative helicity gluons we can start from $\mathcal{A}(g_1^-, f_{c,i}^-, f_{b,j}^-, s_{ab,k}, f_{c,l}^+)$ and apply $Q_a(q, \theta)$ to get

$$0 = \langle 1q \rangle \mathcal{A}(f_{a,1}^-, f_{c,i}^-, f_{b,j}^-, s_{ab,k}, f_{c,l}^+) + \langle iq \rangle \mathcal{A}(g_1^-, \tilde{s}_{ac,i}, f_{b,j}^-, s_{ab,k}, f_{c,l}^+) \\ + \langle jq \rangle \mathcal{A}(g_1^-, f_{c,i}^-, \tilde{s}_{ab,j}, s_{ab,k}, f_{c,l}^+) - \langle kq \rangle \mathcal{A}(g_1^-, f_{c,i}^-, f_{b,j}^-, f_{b,k}^+, f_{c,l}^+). \quad (6.26)$$

It is possible to deduce quite a few of these NMHV SWI's and we shall not attempt to derive all of them here. The general procedure for generating them is this: Start with an amplitude which has three and a half units of negative helicity ($N^{3/2}$ MHV) and where the SUSY indices b, c and d are each maximally used once on f_a^- and \tilde{s}_{ab} states, and where the indices a, b, c and d are used maximally once on f_a^+ and s_{ab} states (and a must be used once). Then, assuming the four SUSY indices to be different, act with $Q_a(q, \theta)$ to get the SWI. Resulting amplitudes involving a twice in f_a^+ and s_{ab} states are zero for the reason discussed above.

As should be clear from the discussion of SWI's, they are not concerned with colour ordering, or numbering in general.

6.2.3 3 Mass Boxes with Two Fermions

We now want to calculate the three mass box function coefficients when we have two negative helicity gluons and a pair of fermions. We first review some general arguments and then give the full results without detailed calculation.

The easiest way of classifying the configurations is to view it as a process of moving a half unit of negative helicity from one of the m_i 's to a leg q situated on one of the four corners. Take as an example the configuration $q, m_1 \in A, m_2 \in B$ and $m_3 = d$ and move a half unit of negative helicity from m_1 on A to q which is also on A . Since this only involves corner A the ratio of the coefficients must be the ratio of the A corner amplitudes,

$$= \frac{c^{3m}(\{q^{1/2}, m_1^{-1/2}\}, \{m_2\}, \{\}, d^-)}{c^{3m}(\{m_1^-\}, \{m_2\}, \{\}, d^-)} \\ = \frac{\langle l_1 q \rangle}{\langle l_1 m_1 \rangle}$$

$$\begin{aligned}
&= \frac{\langle qd \rangle}{\langle m_1 d \rangle} \\
&= \frac{\mathcal{H}_{ABd}(q, m_2)}{\mathcal{H}_{ABd}(m_1, m_2)}. \tag{6.27}
\end{aligned}$$

If the $-1/2$ helicity came from d we could track the effect on each corner and derive the relative factor in a similar way. However, we could also use the SWI

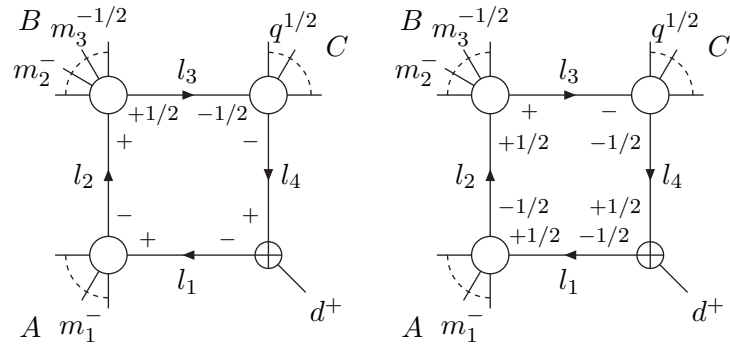
$$\begin{aligned}
&\langle q\eta \rangle c^{3m}(\{m_1^-, \{m_2^-, \{\}, d^-\}) \\
&= \langle m_1\eta \rangle c^{3m}(\{q^{1/2}, m_1^{-1/2}, \{m_2^-, \{\}, d^-\}) \\
&\quad + \langle m_2\eta \rangle c^{3m}(\{q^{1/2}, m_1^-, \{m_2^{-1/2}, \{\}, d^-\}) \\
&\quad + \langle d\eta \rangle c^{3m}(\{q^{1/2}, m_1^-, \{m_2^-, \{\}, d^{-1/2}\}), \tag{6.28}
\end{aligned}$$

and set $\eta = m_2$ to obtain

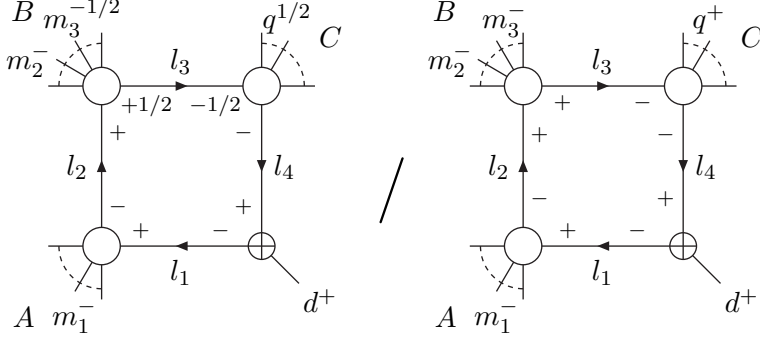
$$\begin{aligned}
&\frac{c^{3m}(\{q^{1/2}, m_1^-, \{m_2^-, \{\}, d^{-1/2}\})}{c^{3m}(\{m_1^-, \{m_2^-, \{\}, d^-\})} \\
&= \frac{\langle qm_2 \rangle}{\langle dm_2 \rangle} - \frac{\langle m_1 m_2 \rangle}{\langle dm_2 \rangle} \frac{\mathcal{H}_{ABd}(q, m_2)}{\mathcal{H}_{ABd}(m_1, m_2)} \\
&= \frac{\langle m_1 q \rangle}{\langle m_1 d \rangle} \\
&= \frac{\mathcal{H}_{AAB}(m_1, q, m_2)}{\mathcal{H}_{ABd}(m_1, m_2)}. \tag{6.29}
\end{aligned}$$

The case chosen is, of course, deceptively easy since $c^{3m}(\{q^{1/2}, m_1^-, \{m_2^{-1/2}, \{\}, d^-\}) = 0$ as can be seen by trying (and failing) to assign internal helicities in the quadruple cut. Taking the more involved road, it can also be found by using the SWI above with $\eta = m_1$.

In most cases there are no large advantages of using the one method (tracking the half unit of helicity through the vertices) over the other (SWI) but in some cases the former should definitely be avoided. Take as an example the gluon configuration $m_1 \in A$, $m_2, m_3 \in B$ and move $-1/2$ helicity from m_3 to $q \in C$. When analysing the possible internal helicity assignments we find that there are in fact *two* different ways it can be done,



Rather than calculating the result from this analysis, we can use that (including a fermionic minus)



$$\begin{aligned}
&= \frac{c^{3m}(\{m_1^{-1/2}\}, \{m_2^-, m_3^-\}, \{q^{1/2}\}, d^+)}{c^{3m}(\{m_1^-\}, \{m_2^-, m_3^-\}, \{\}, d^+)} \\
&= -\frac{\langle l_2(-l_1) \rangle}{\langle l_2 m_1 \rangle} \frac{[dl_1]}{[d(-l_4)]} \frac{\langle (-l_3)q \rangle}{\langle (-l_3)l_4 \rangle} \\
&= -\frac{\langle l_2 A d \rangle \langle l_3 q \rangle}{\langle l_2 m_1 \rangle [d C l_3]} \\
&= -\frac{\langle d A B q \rangle}{\langle d C B m_1 \rangle} \\
&= -\frac{\mathcal{H}_{BBC}(m_2, m_3, q)}{\mathcal{H}_{ABB}(m_1, m_2, m_3)} \tag{6.30}
\end{aligned}$$

and use this in the corresponding SWI with $\eta = m_2$,

$$\begin{aligned}
&\frac{c^{3m}(\{m_1^-\}, \{m_2^-, m_3^{-1/2}\}, \{q^{1/2}\}, d^+)}{c^{3m}(\{m_1^-\}, \{m_2^-, m_3^-\}, \{\}, d^+)} \\
&= \frac{\langle q m_2 \rangle}{\langle m_3 m_2 \rangle} + \frac{\langle m_1 m_2 \rangle}{\langle m_3 m_2 \rangle} \frac{\mathcal{H}_{BBC}(m_2, m_3, q)}{\mathcal{H}_{ABB}(m_1, m_2, m_3)} \\
&= \frac{\langle q m_2 \rangle \langle m_1 B C d \rangle + \langle m_1 m_2 \rangle \langle q B A d \rangle}{\langle m_3 m_2 \rangle \langle m_1 B C d \rangle} \\
&= -\frac{\mathcal{H}_{ABC}(m_1, m_2, q)}{\mathcal{H}_{ABB}(m_1, m_2, m_3)}. \tag{6.31}
\end{aligned}$$

We see the continuation of the picture that moving $-1/2$ helicity from one corner to another produces a ratio whose fourth power is the ratio for moving -2 helicity between the same legs. This holds not only when the external helicities constrain us to a single internal state in the loop, but holds when more internal states open up. The latter is a consequence of the $\mathcal{N} = 4$ supersymmetry.

This becomes a helpful realization when we want to move helicity around in the ABC gluon configuration. No matter how we do it, we will need to sum over at least eight states of the multiplet. This can of course be done (and was indeed

done in [127]) but it is simpler to note *e.g.* that

$$\begin{aligned}
\langle q\eta \rangle \mathcal{H}_{ABC}(m_1, m_2, m_3) &= \langle m_1\eta \rangle \mathcal{H}_{ABC}(q, m_2, m_3) \\
&\quad - \langle m_2\eta \rangle \mathcal{H}_{AAC}(m_1, q, m_3) \\
&\quad - \langle m_3\eta \rangle \mathcal{H}_{AAB}(m_1, q, m_2),
\end{aligned} \tag{6.32}$$

and interpret this to be 'proportional to' the corresponding SWI

$$\begin{aligned}
&\langle q\eta \rangle c^{3m}(\{m_1^-, \{m_2^-, \{m_3^-, d^+\} \\
&= \langle m_1\eta \rangle c^{3m}(\{m_1^{-1/2}, q^{1/2}, \{m_2^-, \{m_3^-, d^+\} \\
&\quad + \langle m_2\eta \rangle c^{3m}(\{m_1^-, q^{1/2}, \{m_2^{-1/2}, \{m_3^-, d^+\} \\
&\quad + \langle m_3\eta \rangle c^{3m}(\{m_1^-, q^{1/2}, \{m_2^-, \{m_3^{-1/2}, d^+\},
\end{aligned} \tag{6.33}$$

in the sense that

$$\frac{c^{3m}(\{m_1^{-1/2}, q^{1/2}, \{m_2^-, \{m_3^-, d^+\})}{c^{3m}(\{m_1^-, \{m_2^-, \{m_3^-, d^+\})} = \frac{\mathcal{H}_{ABC}(q, m_2, m_3)}{\mathcal{H}_{ABC}(m_1, m_2, m_3)}, \tag{6.34}$$

etcetera. Using the methods described in this section, one can derive all box coefficients involving two gluinos. They are reported in the tables below. The top line of each table states the gluon configuration we start from and the associated \mathcal{H} factor. Below, the first column states where the $-1/2$ unit is moved to (the position of q) and the second column states which of the negative helicity gluons it came from. The third column then states which factor the \mathcal{H} in the top line is to be replaced by to obtain the correct box coefficient. In the first three cases we have used identities such as $-\mathcal{H}_{ABd}(m_1, m_2) = \mathcal{H}_{AAB}(q, m_1, m_2)$ to abbreviate results.

AAB		$\mathcal{H}_{AAB}(m_1, m_2, m_3)$	AAC		$\mathcal{H}_{AAC}(m_1, m_2, m_3)$
A	m_1	$\mathcal{H}_{AAB}(q, m_2, m_3)$	A	m_1	$\mathcal{H}_{AAC}(q, m_2, m_3)$
$/d$	m_2	$\mathcal{H}_{AAB}(m_1, q, m_3)$	$/d$	m_2	$\mathcal{H}_{AAC}(m_1, q, m_3)$
	m_3	0		m_3	0
B	m_1	$\mathcal{H}_{ABB}(m_2, q, m_3)$	B	m_1	$-\mathcal{H}_{ABC}(q, m_2, m_3)$
	m_2	$\mathcal{H}_{ABB}(m_1, m_3, q)$		m_2	$-\mathcal{H}_{ABC}(m_1, q, m_3)$
	m_3	$\mathcal{H}_{AAB}(m_1, m_2, q)$		m_3	$-\mathcal{H}_{AAC}(m_1, m_2, q)$
C	m_1	$\mathcal{H}_{ABC}(m_2, m_3, q)$	C	m_1	$\mathcal{H}_{ACC}(m_2, q, m_3)$
	m_2	$-\mathcal{H}_{ABC}(m_1, m_3, q)$		m_2	$\mathcal{H}_{ACC}(m_1, m_3, q)$
	m_3	$-\mathcal{H}_{AAC}(m_1, m_2, q)$		m_3	$\mathcal{H}_{AAC}(m_1, m_2, q)$

ABB		$\mathcal{H}_{ABB}(m_1, m_2, m_3)$
A	m_1	$\mathcal{H}_{ABB}(q, m_2, m_3)$
	m_2	$\mathcal{H}_{AAB}(q, m_1, m_3)$
	m_3	$\mathcal{H}_{AAB}(m_1, q, m_2)$
B	m_1	0
	m_2	$\mathcal{H}_{ABB}(m_1, q, m_3)$
	m_3	$\mathcal{H}_{ABB}(m_1, m_2, q)$
C	m_1	$\mathcal{H}_{BBC}(m_2, m_3, q)$
	m_2	$\mathcal{H}_{ABC}(m_1, m_3, q)$
	m_3	$-\mathcal{H}_{ABC}(m_1, m_2, q)$

ABd		$\mathcal{H}_{ABd}(m_1, m_2)$
A	m_1	$\mathcal{H}_{ABd}(q, m_2)$
	m_2	0
	d	$\mathcal{H}_{AAB}(m_1, q, m_2)$
B	m_1	$\mathcal{H}_{BBd}(m_2, q)$
	m_2	$\mathcal{H}_{ABd}(m_1, q)$
	d	$\mathcal{H}_{ABB}(m_1, m_2, q)$
C	m_1	$-\mathcal{H}_{BCd}(m_2, q)$
	m_2	$-\mathcal{H}_{ACd}(m_1, q)$
	d	$-\mathcal{H}_{ABC}(m_1, m_2, q)$

ACd		$\mathcal{H}_{ACd}(m_1, m_2)$
A	m_1	$\mathcal{H}_{ACd}(q, m_2)$
	m_2	0
	d	$\mathcal{H}_{ACd}(m_1, q)$
B	m_1	$-\mathcal{H}_{BCd}(q, m_2)$
	m_2	$-\mathcal{H}_{ABd}(m_1, q)$
	d	$-\mathcal{H}_{ABC}(m_1, q, m_2)$
C	m_1	0
	m_2	$\mathcal{H}_{ACd}(m_1, q)$
	d	$\mathcal{H}_{ACC}(m_1, m_2, q)$

BBd		$\mathcal{H}_{BBd}(m_1, m_2)$
A	m_1	$-\mathcal{H}_{ABd}(q, m_2)$
	m_2	$-\mathcal{H}_{ABd}(m_1, q)$
	d	$-\mathcal{H}_{ABB}(q, m_1, m_2)$
B	m_1	$\mathcal{H}_{BBd}(q, m_2)$
	m_2	$\mathcal{H}_{BBd}(m_1, q)$
	d	0
C	m_1	$-\mathcal{H}_{BCd}(m_2, q)$
	m_2	$-\mathcal{H}_{BCd}(m_1, q)$
	d	$-\mathcal{H}_{BBC}(m_1, m_2, q)$

ABC		$\mathcal{H}_{ABC}(m_1, m_2, m_3)$
A	m_1	$\mathcal{H}_{ABC}(q, m_2, m_3)$
	m_2	$\mathcal{H}_{AAC}(q, m_1, m_3)$
	m_3	$\mathcal{H}_{AAB}(q, m_1, m_2)$
B	m_1	$\mathcal{H}_{BBC}(q, m_2, m_3)$
	m_2	$\mathcal{H}_{ABC}(m_1, q, m_3)$
	m_3	$\mathcal{H}_{ABB}(m_1, q, m_2)$
C	m_1	$\mathcal{H}_{BCC}(m_2, q, m_3)$
	m_2	$\mathcal{H}_{ACC}(m_1, q, m_3)$
	m_3	$\mathcal{H}_{ABC}(m_1, m_2, q)$
d	m_1	$-\mathcal{H}_{BCd}(m_2, m_3)$
	m_2	$-\mathcal{H}_{ACd}(m_1, m_3)$
	m_3	$-\mathcal{H}_{ABd}(m_1, m_2)$

6.2.4 Beyond Two Fermions

Using the same methods as above and assisted by SWI's, the analysis can be extended to other external particles than gluons and two fermions. For instance, the ratio of coefficients between a $(g^-, g^-, s_{ab}, \bar{s}_{ab})$ and a (g^-, g^-, g^-, g^+) amplitude is found by squaring the ratio between coefficients of (g^-, g^-, f^-, f^+) and a

(g^-, g^-, g^-, g^+) , e.g.

$$\begin{aligned}
& c^{3m}(\{m_1^-, m_2^-\}, \{m_3^{0-}\}, \{q^{0+}\}, d^+) \\
&= \frac{-\mathcal{H}_{AAC}(m_1, m_2, q)}{\mathcal{H}_{AAB}(m_1, m_2, m_3)} c^{3m}(\{m_1^-, m_2^-\}, \{m_3^{-1/2}\}, \{q^{1/2}\}, d^+) \\
&= \left(\frac{-\mathcal{H}_{AAC}(m_1, m_2, q)}{\mathcal{H}_{AAB}(m_1, m_2, m_3)} \right)^2 c^{3m}(\{m_1^-, m_2^-\}, \{m_3^-\}, \{q^+\}, d^+). \tag{6.35}
\end{aligned}$$

If we moved four units of $-1/2$ helicity from m_3 to q we would have to take the parenthesis to the power 4, which is of course equivalent to exchanging $\mathcal{H}_{AAB}(m_1, m_2, m_3)^4$ with $\mathcal{H}_{AAC}(m_1, m_2, q)^4$ in (6.21) as it should be.

Amplitudes with both scalars and fermions can be constructed in similar ways by viewing them as pure-gluon amplitudes where units of $-1/2$ helicity have been moved around. For each move, one of the original \mathcal{H}_k factors is removed and replaced by another which captures where the helicity was moved to. In general this does not fix the overall sign unambiguously, so we must resort to SWIs to be completely sure. As an example we can try to compute the coefficient $c^{3m}(\{m_1^-, m_2^{-1/2}\}, \{m_3^{-1/2}\}, \{q^{0+}\}, d^+)$ by noting that it comes from moving $-1/2$ helicity from m_2 to q in $c^{3m}(\{m_1^-, m_2^-\}, \{m_3^{-1/2}\}, \{q^{1/2}\}, d^+)$. This tells us that the relative factor must be $\pm \mathcal{H}_{ABC}(m_1, m_3, q) / \mathcal{H}_{AAB}(m_1, m_2, m_3)$, and that we must use a SWI of the type (6.25) which describes moving helicity from somewhere to in an AAB configuration to corner C . Such an SWI is represented in the first table above in the last three lines, namely

$$\begin{aligned}
0 &= \langle m_1 \eta \rangle \mathcal{H}_{ABC}(m_2, m_3, q) - \langle m_2 \eta \rangle \mathcal{H}_{ABC}(m_1, m_3, q) \\
&\quad - \langle m_3 \eta \rangle \mathcal{H}_{AAC}(m_1, m_2, q) - \langle q \eta \rangle \mathcal{H}_{AAB}(m_1, m_2, m_3). \tag{6.36}
\end{aligned}$$

This leads us to conclude that

$$\begin{aligned}
& c^{3m}(\{m_1^-, m_2^{-1/2}\}, \{m_3^{-1/2}\}, \{q^{0+}\}, d^+) \\
&= \frac{-\mathcal{H}_{ABC}(m_1, m_3, q)}{\mathcal{H}_{AAB}(m_1, m_2, m_3)} c^{3m}(\{m_1^-, m_2^-\}, \{m_3^{-1/2}\}, \{q^{1/2}\}, d^+) \\
&= \frac{\mathcal{H}_{ABC}(m_1, m_3, q) \mathcal{H}_{AAC}(m_1, m_2, q)}{\mathcal{H}_{AAB}(m_1, m_2, m_3)^2} c^{3m}(\{m_1^-, m_2^-\}, \{m_3^-\}, \{q^+\}, d^+). \tag{6.37}
\end{aligned}$$

With these methods, three-mass box function coefficients for any NMHV external particle configuration can be calculated.

6.2.5 Beyond Three-Mass Boxes

Up until now we completely focussed on three-mass boxes because they were MHV constructible and have a well controlled structure. Two-mass-hard boxes are also MHV constructible but they have two contributions for each coefficient

since either of the two massless corners can be the googly MHV one. We can easily obtain those coefficients, however, from the three-mass coefficients by taking massive corners to have only one momentum on them,

$$c^{2mh}(A, B, c, d) = c^{3m}(A, B, \{c\}, d) + c^{3m}(\{d\}, A, B, c). \quad (6.38)$$

The two-mass-easy boxes are not MHV constructible because the opposite massless corners are both googly MHV and the two massive corners must be MHV and NMHV, respectively. Rather than using explicit expressions for the the NMHV amplitudes, we can use the same procedure as [37] where the known structure of IR divergences in $\mathcal{N} = 4$ super-Yang-Mills tells us that

$$\mathcal{A}^{1\text{-loop}} \Big|_{1/\epsilon} = -\frac{\hat{c}_\Gamma}{\epsilon^2} \sum_{i=1}^n \left(\frac{\mu^2}{-s_{i,i+1}} \right)^\epsilon \mathcal{A}^{\text{tree}}, \quad (6.39)$$

which again translates to linear conditions on the box coefficients. These can be inverted (at least for an odd number of external particles) to produce expressions for the two-mass-easy coefficients in terms of the three-mass coefficients. Because we are considering $\mathcal{N} = 4$ supersymmetry in both external and internal states, these identities hold irrespective of the external states. Formally, the identity is

$$c^{2me}(A, b, C, d) = \sum_{d \in \hat{C}} c^{3m}(\hat{C}, \dots, \dots, b) + \sum_{b \in \hat{A}} c^{3m}(\hat{A}, \dots, \dots, d), \quad (6.40)$$

where the summations run over all three-mass box coefficients that fulfill the condition.

Just as two-mass-hard boxes were degenerate three-mass boxes, one-mass boxes can be characterized as degenerate two-mass-easy and three-mass boxes. This gives us the formula for the one-mass coefficients,

$$c^{1m}(A, b, c, d) = c^{2me}(A, b, \{c\}, d) + c^{3m}(\{d\}, A, \{b\}, c). \quad (6.41)$$

Since there are no further contributions to the one-loop amplitude, this constitutes a complete characterization of the one-loop NMHV amplitude in $\mathcal{N} = 4$ super-Yang-Mills.

Chapter 7

One-Loop Amplitudes in $\mathcal{N} = 8$ Supergravity

This chapter introduces the calculation of one-loop amplitudes in $\mathcal{N} = 8$ supergravity and the “No Triangle Hypothesis”¹ for the structure. It is based on the article [50], which extends the results of earlier work [48].

7.1 One-Loop Structure of Maximal Supergravity

The results of sections 5.1.1 and 5.1.2 apply just as well to a gravity theory as to Yang–Mills. Thus, any one-loop amplitude in four dimensions can be written as a sum of boxes, triangles, bubbles and a rational function,

$$\mathcal{M}^{1\text{-loop}} = \sum_{i \in \mathcal{C}} c_i I_4^i + \sum_{j \in \mathcal{D}} d_j I_3^j + \sum_{k \in \mathcal{E}} e_k I_2^k + R. \quad (7.1)$$

There are, however, no theorems that use supersymmetry to constrain this further as with Yang–Mills, and generically, any theory of gravity should be expected to include all types of terms.

For a low number of external gravitons, there are some results that do constrain the form. If we go back to the integrand of the loop integral, it will generally have $m \leq n$ propagator terms where n is the number of external particles. Since all Feynman vertices in gravity contain momentum squared, we should have $2m$ powers of loop momentum in the numerator. By multiplying and dividing by all propagators not in the expressions, this can be written as $2n$ powers of loop momentum in the numerator and n propagators,

$$\mathcal{M}_n \sim \int d^D l \frac{[l^\mu]^{2n}}{l_1^2 l_2^2 \cdots l_n^2} \quad (7.2)$$

¹Given the present weight of evidence it should be termed the “No Triangle Conjecture”, but the original name seems to have stuck with it. Considering what it actually says, it ought to be called the “Box Hypothesis” or something similar.

When we do Passarino–Veltman reduction on this, each propagator can be exchanged for one or two fewer powers of loop momentum. For any n , this is expected to result in a combination of all the terms appearing in (7.1). However, we should also expect that there are supersymmetry cancellations like in Yang–Mills that reduce the power $2n$. This is indeed the case in the so-called string-based approach to loop calculations [43, 80] (for the string-based approach in Yang–Mills, consult [27, 42, 45, 46]) where cancellations can be made explicit which reduce the numerator power of loop momentum by 8 in $\mathcal{N} = 8$,

$$\mathcal{M}_n^{\mathcal{N}=8} \sim \int d^D l \frac{[l^\mu]^{2n-8}}{l_1^2 l_2^2 \dots l_n^2}. \quad (7.3)$$

This explicitly tells us that four-point amplitudes (as explicitly shown by a classic string calculation [94]) can only have a box integral, five-point can have boxes and triangles, six-point can have boxes, triangles and bubbles, while seven-point and above is again unconstrained.

Somewhat surprisingly, the situation seems to be even better. It has been known since the end of the 90's [24] that five-point and six-point MHV 1-loop amplitudes consisted only of boxes and it was conjectured that this would hold for all MHV amplitudes. When it was recently found that the box function part of the NMHV six-graviton amplitude was sufficient to explain all IR, soft and collinear properties of the amplitude, it was hypothesized that all one-loop amplitudes in $\mathcal{N} = 8$ supergravity consisted of boxes only. In particular, since there this means no triangles, it was called the No-Triangle Hypothesis.

An equivalent way to express this at one-loop is that $\mathcal{N} = 8$ supergravity has the same structure as $\mathcal{N} = 4$ super Yang–Mills, in particular that there are cancellations which remove additional powers of loop momentum from the numerator of integrands to reduce it to

$$\mathcal{M}_n^{\mathcal{N}=8} \sim \int d^D l \frac{[l^\mu]^{n-4}}{l_1^2 l_2^2 \dots l_n^2}. \quad (7.4)$$

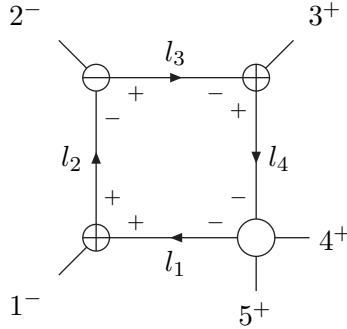
This is $n - 4$ more cancellations than $\mathcal{N} = 8$ supersymmetry is known to give and the origin is unknown. As described in the introduction, this and many other results have led to speculations that $\mathcal{N} = 8$ supergravity is perturbatively UV finite to all orders and that this may be caused by an unknown symmetry present in all gravitational theories, independent of supersymmetry, which softens the UV behaviour.

7.2 Evidence for the No-Triangle Hypothesis

The present strategy for supporting the No-Triangle Hypothesis is to determine the part of all six and seven-point amplitudes depending on box integrals and to argue that no further cut-constructible parts can be present. This leaves rational parts which are known to be absent at six-points; additional arguments are presented why these ought to vanish at seven-point and higher.

7.2.1 Box Coefficients and Soft Divergences

Box coefficients can be determined by use of the quadruple cut method of section 5.4. There are two strategies for determining these; the direct and the KLT-inspired. The latter works by using the KLT relations on all corner amplitudes of the quadruple cut to write the $\mathcal{N} = 8$ coefficient as a product of kinematic invariants and two $\mathcal{N} = 4$ coefficients [28]. As an example, the coefficient of $I_4(1^-, 2^-, 3^+, (4^+, 5^+))$ given by the quadruple cut



which can be KLT'ed to

$$\begin{aligned}
 c_{1^-, 2^-, 3^+, (4^+, 5^+)}^{\mathcal{N}=8} &= \frac{1}{2} \mathcal{M}(-l_1^+, 1^-, l_2^+) \mathcal{M}(-l_2^-, 2^-, l_3^+) \\
 &\quad \times \mathcal{M}(-l_3^-, 3^+, l_4^+) \mathcal{M}(-l_4^-, 4^+, 5^+, l_1^-) \\
 &= \frac{1}{2} \mathcal{A}(-l_1^+, 1^-, l_2^+)^2 \mathcal{A}(-l_2^-, 2^-, l_3^+)^2 \mathcal{A}(-l_3^-, 3^+, l_4^+)^2 \\
 &\quad \times s_{45} \mathcal{A}(-l_4^-, 4^+, 5^+, l_1^-) \mathcal{A}(-l_4^-, 5^+, 4^+, l_1^-) \\
 &= 2s_{45} c_{1^-, 2^-, 3^+, (4^+, 5^+)}^{\mathcal{N}=4} c_{1^-, 2^-, 3^+, (5^+, 4^+)}^{\mathcal{N}=4}. \tag{7.5}
 \end{aligned}$$

In the cases where there is a summation over the multiplet running in the loop, the rewriting will still hold because the $\mathcal{N} = 8$ multiplet is two copies of the $\mathcal{N} = 4$ multiplet, each being summed over in the two $\mathcal{N} = 4$ coefficients on the right hand side. Unfortunately, this strategy becomes increasingly cumbersome at higher points. The KLT relations become longer and involve permutations of legs which lead to the $\mathcal{N} = 4$ coefficients being the non-planar ones.

The more direct strategy is to use the expressions for $\mathcal{N} = 8$ supergravity amplitudes. These can be derived from on-shell recursion in more compact form than those given by the KLT relations, and presumably give rise to the most compact forms of the coefficients. The coefficients for general MHV amplitudes were given in [24] and the coefficients for the six-point NMHV amplitude were given in [28]. Thus, the remaining seven-point amplitudes are the NMHV ones. A large portion of these are MHV constructible (*cf.* section 6.1) but some one-mass coefficients may depend on the NMHV six-graviton tree amplitude. One even requires summation over the full multiplet, and we thus need to extend

the NMHV six-point tree amplitude to the case where two external particles are non-gravitons. This can be achieved by redoing the on-shell recursive calculation of [61] and the result is given in appendix C of [50]. The procedure like the one used in section 6.2.5 cannot be used as it relies on the previous knowledge that the amplitude contains only boxes, the fact that we are trying to establish. All the seven-point NMHV box coefficients are collected in appendix A of [50].

The results for the box coefficients constrain the rest of the amplitude because it must have the soft ($1/\epsilon$) divergence [81],

$$\mathcal{M}^{1\text{-loop}} \Big|_{\frac{1}{\epsilon}} = \frac{i}{(4\pi)^2} \left[\frac{\sum_{i<j} s_{ij} \log[-s_{ij}]}{2\epsilon} \right] \mathcal{M}^{\text{tree}}. \quad (7.6)$$

If this holds for just the box integral part of the amplitude, the triangles and bubbles must have their soft divergences add up to zero. That this is indeed the case has been checked numerically for the all amplitudes up to and including seven-point. In practise, this is done by extracting the soft parts of all the box functions and rephrasing (7.6) as identities among the box coefficients.

The soft divergences of one and two-mass triangles are best studied by rewriting them in a basis consisting of the functions

$$G(-K^2) = \frac{(-K^2)^{-\epsilon}}{\epsilon^2} = \frac{1}{\epsilon^2} - \frac{\log(-K^2)}{\epsilon} + \dots, \quad (7.7)$$

where K^2 runs over all independent kinematic invariants. Since the soft parts of this basis are independent, the vanishing of their sum amounts to requiring the vanishing of every coefficient. Going back to the basis of one and two-mass triangles this means that all coefficients of these are also zero. The three-mass triangles have no IR singularities and can thus not be ruled out in this way. The bubble functions are proportional to

$$\frac{(-K^2)^{-\epsilon}}{\epsilon} = \frac{1}{\epsilon} - \log(-K^2) + \dots, \quad (7.8)$$

so all we can say about them is that their coefficients add up to zero.

7.2.2 Ruling Out Bubbles

The safest way of ruling out bubble contributions is of course to calculate them directly. For this, the article uses two methods which are closely related. The first is the method of Britto, Buchbinder, Cachazo and Feng [58] where the unitarity cuts of amplitudes are explicitly integrated and the results compared with the cut of the expansion in terms of scalar integrals. By inspecting all unitarity cuts of seven-point NMHV amplitudes in this light, bubble integrals can indeed be ruled out.

Rather than going through this technical, albeit interesting, calculation, we will use a method which ties together the behaviour of tree amplitudes deformed by a complex parameter z as in on-shell recursion (*cf.* section 3.3) and the UV

behaviour of one-loop amplitude. This choice is made to illustrate one of the central points of this thesis, namely that properties of graviton tree amplitudes (such as $z \rightarrow \infty$ behaviour) are tightly linked with the whole perturbative expansion of $\mathcal{N} = 8$ supergravity.

Using the expansion (7.1) we can write the unitarity cut in a particular channel with momentum P and lift the momentum integration. This gives

$$\sum_{i \in \mathcal{C}'} \frac{c_i}{(l_1 - K_1(i))^2 (l_2 - K_2(i))^2} + \sum_{j \in \mathcal{D}'} \frac{d_j}{(l_1 - K_3(j))^2} + e_k + D(l_1, l_2), \quad (7.9)$$

where \mathcal{C}' and \mathcal{D}' are the sets of box and triangle functions which have a cut in the relevant channel and the $l - K_{1,2,3}$ represent the remaining propagators. Only one bubble function has the cut; this is represented by e_k . Finally, we have added a total derivative term which is set to zero by the integration. By the normal logic of unitarity, this integrand should be equal to a product of two on-shell tree amplitudes, summed over internal helicities,

$$\sum_{h_1, h_2 = \pm} \mathcal{M}(\dots, l_1^{h_1}, -l_2^{-h_2}) \mathcal{M}(\dots, l_2^{h_2}, -l_1^{-h_1}). \quad (7.10)$$

We can now deform this product in the same way as done in the BCFW construction of on-shell recursion described in section 3.3, namely by making the shift

$$|\widehat{l}_1\rangle = |l_1\rangle + z|l_2\rangle, \quad |\widehat{l}_2] = |l_2] - z|l_1]. \quad (7.11)$$

Under this shift, the integrand of boxes and triangles go as z^{-2} or z^{-1} as $z \rightarrow \infty$ and bubbles go as z^0 . This immediately suggests a condition for absence of a bubble: If (7.10) tends to zero as $z \rightarrow \infty$ (and $D(l_1, l_2)$ does as well) the bubble corresponding to the cut is absent. This condition can be related directly to an equivalent condition for vanishing of bubbles in the direct integration method mentioned above, so it is indeed an appropriate check.

The behaviour of tree amplitudes under the under above shift (7.11) is not known in general, but two things are known: For MHV amplitudes where the helicities of (l_1, l_2) are given as (h_1, h_2) , then the scaling can be derived from known expressions for the amplitude [12, 17] to be

$$\begin{aligned} \mathcal{M}^{\text{MHV}} &\sim z^{-2} && \text{when } (h_1, h_2) = (+, +), (-, -), (+, -), \\ \mathcal{M}^{\text{MHV}} &\sim z^6 && \text{when } (h_1, h_2) = (-, +), \\ \mathcal{M}^{\text{MHV}} &\sim z^{2h+2} && \text{when } (h_1, h_2) = (-h, h). \end{aligned} \quad (7.12)$$

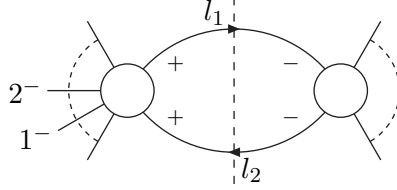
It is also known generally [14] that

$$\mathcal{M} \sim z^{-2} \quad \text{when } (h_1, h_2) = (+, -) \quad (7.13)$$

for all graviton amplitudes. Furthermore it can be verified that the two first lines of (7.12) holds for all six and seven-point tree amplitudes needed here. Thus, it is not unreasonable to assume that this is a general picture.

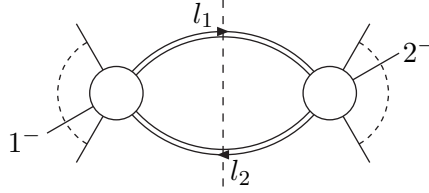
The known $z \rightarrow \infty$ behaviour of MHV amplitudes can be used immediately to derive the behaviour of the cut integrand for one-loop MHV amplitudes. A singlet cut integrand where there is only one state running in the loop has the generic form

$$\mathcal{M}(1^-, 2^-, 3^+, \dots, r^+, l_1^+, -l_2^+) \mathcal{M}(-l_1^-, l_2^-, (r+1)^+, \dots, n^+). \quad (7.14)$$



Under the shift, both tree amplitudes go as z^{-2} so the cut goes as z^{-4} , and there are no bubble contributions.

If the cut is non-singlet, the whole multiplet can run in the loop,



the integrand becomes

$$\sum_h (-1)^{2h} \binom{8}{4-2h} \times \mathcal{M}(2^-, 3^+, \dots, r^+, l_1^h, -l_2^{-h}) \mathcal{M}(-l_1^{-h}, l_2^h, (r+1)^+, \dots, n^+) \quad (7.15)$$

However, we know from SWIs that MHV amplitudes with different external particle content are related, *e.g.*,

$$\mathcal{M}(2^-, 3^+, \dots, r^+, l_1^h, -l_2^{-h}) = \left(\frac{\langle 2l_1 \rangle}{\langle 2l_2 \rangle} \right)^{4-2h} \mathcal{M}(2^-, 3^+, \dots, r^+, l_1^+, -l_2^-), \quad (7.16)$$

so we can write (7.15) as

$$\rho \times \mathcal{M}(2^-, 3^+, \dots, r^+, l_1^+, -l_2^-) \mathcal{M}(-l_1^-, l_2^+, (r+1)^+, \dots, n^+) \quad (7.17)$$

where

$$\rho = \sum_h (-1)^{2h} \binom{8}{4-2h} \left(\frac{\langle 2l_1 \rangle \langle 1l_2 \rangle}{\langle 2l_2 \rangle \langle 1l_1 \rangle} \right)^{4-2h} = \left(\frac{\langle 12 \rangle \langle l_1 l_2 \rangle}{\langle 2l_2 \rangle \langle 1l_1 \rangle} \right)^8. \quad (7.18)$$

Under the shift, the two tree amplitudes go as z^{-2} and z^6 , respectively, while ρ , whose form is a consequence of $\mathcal{N} = 8$ supersymmetry, goes as z^{-8} . In total, the integrand goes as z^{-4} which rules out bubbles in all one-loop MHV amplitudes.

For singlet NMHV cuts, the situation is quite the same as for MHV; the integrand is

$$\mathcal{M}(l_1^-, \dots, -l_2^-) \mathcal{M}(l_2^+, \dots, -l_1^+), \quad (7.19)$$

and since both tree amplitudes go as z^{-2} under the shift, the integrand goes as z^{-4} . This explicitly holds true for all cuts of six and seven-graviton amplitudes, and continues to hold for any singlet cut if the two first lines of (7.12) hold beyond MHV.

The non-singlet NMHV cuts are more involved since they require the summation over the $\mathcal{N} = 8$ multiplet. For some integrands, such as

$$\sum_h (-1)^{2h} \binom{8}{4-2h} \mathcal{M}(1^-, 2^-, 4^+, l_1^{-h}, -l_2^h) \mathcal{M}(-l_1^h, l_2^{-h}, 3^-, 5^+, 6^+), \quad (7.20)$$

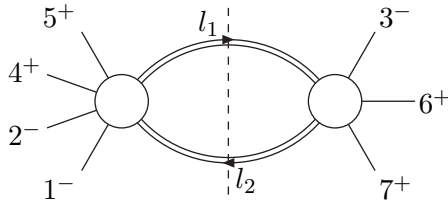
The calculation is essentially the same as for the MHV case because the left NMHV amplitude is also a googly MHV amplitude where

$$\mathcal{M}(1^-, 2^-, 4^+, l_1^{-h}, -l_2^h) = \left(-\frac{[4l_1]}{[4l_2]} \right)^{4-2h} \mathcal{M}(1^-, 2^-, 4^+, l_1^-, -l_2^+), \quad (7.21)$$

such that the integrand becomes

$$\left(\frac{\langle 3P_{124} \rangle}{\langle 3l_2 \rangle [l_2 4]} \right)^8 \mathcal{M}(1^-, 2^-, 4^+, l_1^-, -l_2^+) \mathcal{M}(-l_1^+, l_2^-, 3^-, 5^+, 6^+), \quad (7.22)$$

and goes as z^{-4} . But in the seven-point calculation we will need cuts like



with the integrand

$$\sum_h (-1)^{2h} \binom{8}{4-2h} \mathcal{M}(1^-, 2^-, 4^+, 5^+, l_1^{-h}, -l_2^h) \mathcal{M}(-l_1^h, l_2^{-h}, 3^-, 6^+, 7^+), \quad (7.23)$$

the expression depends on the six-point NMHV tree amplitude. As mentioned above, this has been calculated in the paper and is found to contain 14 terms,

of which 12 have the structure $X \times Y^{2h-4}$ and the last two only contribute at $h = \pm 2$. When this expression is inserted into (7.23) we find that it goes to zero as $z \rightarrow \infty$ *term by term* (after the h summation) although it does not go as well as z^{-4} . Again this highlights the connection between recursion relations and UV structure: Using recursion relations we can write down a form of the six-point amplitude which rules out certain bubble contributions to the seven-point one-loop amplitude without the need for further cancellations.

Since we have now calculated the $z \rightarrow \infty$ behaviour of every independent cut at six and seven-points, and found that they approach zero, we conclude that there are no bubble contributions to the one-loop amplitudes, and that the absence can be tied to recursion relations for gravity.

7.2.3 Ruling Out Three-Mass Triangles

As mentioned above, three-mass triangles have no IR singularities and have to be ruled out explicitly. This can be done by inspecting the triple cuts

$$\sum_{h_1, h_2, h_3} \int d^D l_1 \delta(l_1^2) \delta(l_2^2) \delta(l_3^2) \times \mathcal{M}(\dots, -l_1^{-h_1}, l_2^{h_2}) \mathcal{M}(\dots, -l_2^{-h_2}, l_3^{h_3}) \mathcal{M}(\dots, -l_3^{-h_3}, l_1^{h_1}), \quad (7.24)$$

and arguing that they are all results of triple cuts of the boxes,

$$\int d^D l_1 \delta(l_1^2) \delta(l_2^2) \delta(l_3^2) \sum_{i \in \mathcal{C}''} \frac{c_i}{(l_1 - K(i))^2} \quad (7.25)$$

where $l_1 - K(i)$ is the momentum of the remaining uncut propagator. The helpful fact here is that there are kinematic regimes where the three-mass triple cut is real, and thus the remaining integration can be performed numerically without appealing to complex Minkowski space methods.

The box functions that have three-mass triple cuts are the 2-mass hard, 3-mass and 4-mass boxes. Since we are only going up to seven-point amplitudes we need not worry about the last of these. The result of the cut integrations are

$$\begin{aligned} I_4(k_1, k_2, K_3, K_4) \Big|_{\text{cut}} &= \frac{\pi}{2(k_1 + k_2)^2 (k_2 + K_3)^2} \\ I_4(k_1, K_2, K_3, K_4) \Big|_{\text{cut}} &= \frac{\pi}{2 \left((k_1 + K_2)^2 (K_2 + K_3)^2 - K_2^2 K_4^2 \right)} \\ I_3(K_1, K_2, K_3) \Big|_{\text{cut}} &= \frac{\pi}{2 \sqrt{K_1^4 + K_2^4 + K_3^4 - 2(K_1^2 K_2^2 + K_2^2 K_3^2 + K_3^2 K_1^2)}} \end{aligned} \quad (7.26)$$

With the knowledge of the box coefficients we have, it is fairly straightforward to numerically integrate all the triple cuts and compare them to the expectation from the boxes at some randomly chosen kinematic points. This explicitly rules

out three-mass triangles for both six and seven-point amplitudes. For the six-point NMHV, the independent triangle coefficients are

$$\begin{aligned} d^{3m}(\{1^-, 2^-\}, \{3^-, 4^+\}, \{5^+, 6^+\}) \\ d^{3m}(\{1^-, 4^+\}, \{2^-, 5^+\}, \{3^-, 6^+\}). \end{aligned} \tag{7.27}$$

The triple cut corresponding to the latter is a non-singlet cut which requires a sum over the $\mathcal{N} = 8$ multiplet. This means that it is non-zero for $\mathcal{N} < 8$. The first triangle coefficient can be expected to be zero in any massless theory of gravity. For the seven-point NMHV, the independent three-mass triangle coefficients are

$$\begin{aligned} d^{3m}(\{1^-, 2^-\}, \{3^-, 4^+\}, \{5^+, 6^+, 7^+\}) \\ d^{3m}(\{1^-, 2^-\}, \{3^-, 4^+, 5^+\}, \{6^+, 7^+\}) \\ d^{3m}(\{1^-, 2^-, 4^+\}, \{3^-, 5^+\}, \{6^+, 7^+\}) \\ d^{3m}(\{1^-, 4^+\}, \{2^-, 5^+\}, \{3^-, 6^+, 7^+\}). \end{aligned} \tag{7.28}$$

Again, the three first correspond to singlet cuts which are only sensitive to the presence of the graviton and should be zero in any massless gravity theory, while the last is non-zero for $\mathcal{N} < 8$.

7.2.4 Factorization and Rational Terms

We have now ruled out contributions to the cut-constructible parts from anything but boxes at six and seven-point. At six-point it is already known that there are no rational parts, so this provides a verification of the No-Triangle Hypothesis in that case. For seven-point amplitudes, however, there is no general argument ruling out rational contributions.

Computing rational contributions is in general very hard in gravity theories. A strategy that works in Yang–Mills theory is to do the full calculation in $4 - 2\epsilon$ dimensions (*cf.* section 5.2.3) and extract the rational pieces by taking $\epsilon \rightarrow 0$. This works well because any massless field content can be decomposed into an $\mathcal{N} = 4$ multiplet, some number of $\mathcal{N} = 1$ chiral multiplets and some number of scalars, and because it can be proven explicitly that the two supersymmetric theories have no rational parts; only the scalar loop calculation needs to be done exactly in $4 - 2\epsilon$ dimensions. For gravity, there is no such theorem saying that supersymmetric theories have no rational contributions, so the calculation needs to be done in $4 - 2\epsilon$ dimensions for all states of the multiplet, thereby rendering most of the benefits of the spinor-helicity formalism useless.

An alternative is to use the methods of section 5.5 or, more generally, the known factorization structure of one-loop gravity amplitudes. As in the gauge case, this means in particular multiparticle, collinear and soft factorization. The multiparticle factorization is, on the grounds of general field theory arguments [30], the same as for gauge theory (5.7) with the obvious corrections for the lack of colour ordering in gravity. The collinear behaviour at one-loop is actually simpler

than in Yang–Mills (5.8) as the splitting functions have no loop corrections. This gives [24]

$$\mathcal{M}^{1\text{-loop}}(a^{h_a}, b^{h_b}, \dots) \rightarrow \sum_{h=\pm 2} \text{Split}_{-h}^{\text{grav}}(z, a^{h_a}, b^{h_b}) \mathcal{M}^{1\text{-loop}}(P^h, \dots) \quad (7.29)$$

as $a \rightarrow zP$, $b \rightarrow (1-z)P$. The splitting functions for gravitons are

$$\begin{aligned} \text{Split}_+^{\text{grav}}(z, a^+, b^+) &= 0 \\ \text{Split}_-^{\text{grav}}(z, a^+, b^+) &= -\frac{1}{z(1-z)} \frac{[ab]}{\langle ab \rangle} \\ \text{Split}_+^{\text{grav}}(z, a^-, b^+) &= -\frac{z^3}{1-z} \frac{[ab]}{\langle ab \rangle}. \end{aligned} \quad (7.30)$$

There is also a universal soft behaviour when a graviton momentum approaches zero, which also does not incur loop corrections,

$$\mathcal{M}_n^{1\text{-loop}}(s^\pm, \dots) \rightarrow \mathcal{S}_n^{\text{grav}}(s^\pm) \mathcal{M}_{n-1}^{1\text{-loop}}(\dots), \quad (7.31)$$

as $k_s \rightarrow 0$. When the graviton going soft is number n in some arbitrary ordering, the soft factor is

$$\mathcal{S}_n^{\text{grav}}(n^+) = -\frac{1}{\langle 1n \rangle \langle n(n-1) \rangle} \sum_{i=2}^{n-2} \frac{\langle 1i \rangle \langle i(n-1) \rangle [in]}{\langle in \rangle}. \quad (7.32)$$

These limits put some quite strong constraints on the possible rational parts which must have the same factorization as the cut-constructible parts. We know that the rational parts of the six-graviton amplitude are zero, so by (7.29) and (7.31) the rational part of the seven-graviton amplitude can have no collinear or soft singularities. It is hard to imagine any rational spinor expression which has none of these singularities while being of mass dimension 4 and having the right holomorphic weight of spinors as determined by their helicities. Indeed, it is hard to imagine such an expression for *any* number of external gravitons, so by “loose induction” we should expect that all rational parts are zero.

This argument could probably be formalized by using on-shell recursive methods like those of section 5.5 for gravity. Some progress has been made in this direction [53] but the approach is still too undeveloped to be used for the problem at hand.

7.3 Conclusions

Using an array of different methods, we have explicitly calculated the cut-containing parts of the NMHV six and seven graviton one-loop amplitudes in $\mathcal{N} = 8$ supergravity and found that only box integrals contribute. At six points, this determines the amplitude completely while at seven-point we have argued that an

additional rational term is highly unlikely. This proves the No-Triangle Hypothesis at six points and renders it highly credible at seven.

The methods used can be applied at any number of external particles, and it does not appear that they would suddenly start failing. This applies in particular to the ruling out of bubbles which relied on very general scaling arguments for the amplitudes, scalings that are expected to hold to any number of points. Together with the arguments that the rational parts of amplitudes are likely to be zero, this provides strong evidence that the one-loop amplitude in $\mathcal{N} = 8$ supergravity consists exclusively of boxes just as $\mathcal{N} = 4$ SYM.

As explained in the beginning of the chapter, this amounts to the cancellation of $n - 4$ powers of loop momentum in a n -point amplitude, a cancellation which is unexplained. Similar cancellations seem to occur at higher loop order also. They have been explicitly found in the four-point amplitude at two [23] and three [25] loops, where it was proven that the divergences of maximal supergravity and maximal super-Yang–Mills are the same in any dimension. This gives a strong hint that the divergences of the two theories match in general, and that $\mathcal{N} = 8$ supergravity in four dimensions is UV finite in particular. It also hints that there is some unknown symmetry or dynamical principle present in $\mathcal{N} = 8$ which is responsible, although there are no candidates for such a symmetry. There is evidence that the cancellations occur already in non-supersymmetric gravity [21], and thus the symmetry should be visible in some form without the presence of supersymmetry. The identification of such a symmetry will be of immense interest.

Chapter 8

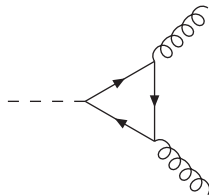
Amplitude with a Higgs

In this chapter we make the full determination of a particular one-loop helicity amplitude, $\mathcal{A}^1(\text{Higgs}, 1^-, 2^-, 3^+, 4^+)$. The chapter is based on [10] but presents the calculation in a somewhat different way. The article calculates the cut constructible parts, using the one-loop MHV rules of section 5.3, of the all- n MHV amplitude $\mathcal{A}^1(\phi, 1^-, 2^-, 3^+, \dots, n^+)$ (ϕ to be defined) and the rational part of $\mathcal{A}^1(\text{Higgs}, 1^-, 2^-, 3^+, 4^+)$ with on-shell recursion from section 5.5. In this chapter, we limit ourselves to the four-gluon case all the way through and compute the cut-constructible parts using classical unitarity as in section 5.2.

Even though the $pp \rightarrow Hjj$ process, where this amplitude is relevant, is not included in table 1.1 of wanted NLO calculations, it is generally considered of the same importance. Some semi-numerical results already exist [84], but clearer analytic results are still missing. The process forms a background to Higgs production by vector boson fusion [65].

8.1 Higgs in the Large Top Mass Limit

In the present calculation we will make the assumption that the top mass is large or, to be exact, that the kinematic scales involved in the scattering are small compared to twice the top mass. The dominant coupling of the Higgs to massless QCD particles comes through a top quark triangle loop connecting to two gluons,



In the large top mass limit, such an interaction is well approximated by an effective term in the Lagrangian [130, 132]

$$\frac{C}{2} H \text{Tr} F_{\mu\nu} F^{\mu\nu}, \quad (8.1)$$

where H is the Higgs field and C is an effective coupling constant equal to [97]

$$\frac{\alpha_s}{6\pi v} \left(1 + \frac{11\alpha_s}{4\pi} + \mathcal{O}(\alpha_s^2) \right). \quad (8.2)$$

In the addition to the Higgs, we can add a pseudoscalar Higgs A such that the total effective Lagrangian becomes

$$\frac{C}{2} \left(H \text{Tr} F_{\mu\nu} F^{\mu\nu} + iA \text{Tr} F_{\mu\nu} {}^* F^{\mu\nu} \right) \quad (8.3)$$

where

$${}^* F^{\mu\nu} = \frac{i}{2} \epsilon^{\mu\nu\kappa\lambda} F_{\kappa\lambda}. \quad (8.4)$$

If we now change variables to

$$\begin{aligned} \phi &= \frac{1}{2}(H + iA), & \phi^\dagger &= \frac{1}{2}(H - iA), \\ F_{SD}^{\mu\nu} &= \frac{1}{2}(F^{\mu\nu} + {}^* F^{\mu\nu}), & F_{ASD}^{\mu\nu} &= \frac{1}{2}(F^{\mu\nu} - {}^* F^{\mu\nu}), \end{aligned} \quad (8.5)$$

the effective Lagrangian becomes

$$C \left(\phi \text{Tr} F_{SD\mu\nu} F_{SD}^{\mu\nu} + \phi^\dagger \text{Tr} F_{ASD\mu\nu} F_{ASD}^{\mu\nu} \right), \quad (8.6)$$

and Higgs amplitudes can be recovered by

$$\mathcal{A}(H, \dots) = \mathcal{A}(\phi, \dots) + \mathcal{A}(\phi^\dagger, \dots). \quad (8.7)$$

The Higgs is colourless and does not participate in the colour ordering, but is conventionally written first.

The central observation is that tree amplitudes for ϕ and ϕ^\dagger are separately simpler than amplitudes for H or A . In particular, they follow a pattern like that of the Parke–Taylor amplitudes (2.41),

$$\begin{aligned} \mathcal{A}^0(\phi, 1^+, \dots, n^+) &= 0 \\ \mathcal{A}^0(\phi, 1^-, 2^+, \dots, n^+) &= 0 \\ \mathcal{A}^0(\phi, 1^-, 2^+, \dots, i^-, \dots, n^+) &= \frac{\langle 1i \rangle^4}{\langle 12 \rangle \langle 23 \rangle \dots \langle n1 \rangle}, \end{aligned} \quad (8.8)$$

for ϕ , and

$$\begin{aligned} \mathcal{A}^0(\phi^\dagger, 1^-, \dots, n^-) &= 0 \\ \mathcal{A}^0(\phi^\dagger, 1^+, 2^-, \dots, n^-) &= 0 \\ \mathcal{A}^0(\phi^\dagger, 1^+, 2^-, \dots, i^+, \dots, n^-) &= (-1)^n \frac{[1i]^4}{[12][23] \dots [n1]}, \end{aligned} \quad (8.9)$$

for ϕ^\dagger . Even though the amplitudes look like the MHV and googly-MHV, the condition between the gluon momenta for conservation of momentum is different because of the presence of the ϕ momentum. Notice also that parity changes the sign

of gluon helicities *and* daggers the ϕ , so there are no easy $(\phi, +, +, -, -, \dots)$ amplitudes. In fact, there is a simple ϕ -all-minus amplitude (and ϕ^\dagger -all-plus amplitude),

$$\begin{aligned}\mathcal{A}^0(\phi, 1^-, \dots, n^-) &= (-1)^n \frac{m_\phi^4}{[12][23] \cdots [n1]}, \\ \mathcal{A}^0(\phi^\dagger, 1^+, \dots, n^+) &= \frac{m_{\phi^\dagger}^4}{\langle 12 \rangle \langle 23 \rangle \cdots \langle n1 \rangle}.\end{aligned}\tag{8.10}$$

The similarity of the ϕ -MHV amplitude to the MHV amplitude have led people to develop MHV rules for amplitudes with a single ϕ , where a ϕ -MHV vertex must be used once but where the off-shell prescription is unchanged [8, 77]. The extension to one-loop amplitudes was explored in [6] and the article on which this chapter is based [10]. The former deals with the cut-constructible part of $\mathcal{A}^1(\phi, -, -, \dots, -)$.

One-loop amplitudes involving a ϕ and at most one negative helicity gluon are purely rational because the tree amplitude vanishes. All- n expressions for these amplitudes have been constructed in [20] where Schmidt's results for a Higgs and three gluons [129] is converted into the ϕ/ϕ^\dagger notation. Some of those we need are given at the relevant point below.

8.2 A One-Loop Higgs Amplitude

The methods presented in chapter 5 can be applied just as well to amplitudes containing a Higgs in the large m_t limit. Here we will apply them to the calculation of $\mathcal{A}(H, 1^-, 2^-, 3^+, 4^+)$, that is, the one-loop amplitude for a Higgs and four gluons with the 'adjacent MHV' helicity configuration. This configuration has a non-zero tree amplitude and we can thus expect cut-containing pieces at one-loop. In practice we will calculate $\mathcal{A}(\phi, 1^-, 2^-, 3^+, 4^+)$ and use that

$$\begin{aligned}\mathcal{A}(H, 1^-, 2^-, 3^+, 4^+) &= \mathcal{A}(\phi, 1^-, 2^-, 3^+, 4^+) + \mathcal{A}(\phi^\dagger, 1^-, 2^-, 3^+, 4^+) \\ &= \mathcal{A}(\phi, 1^-, 2^-, 3^+, 4^+) + \mathcal{A}(\phi, 3^-, 4^-, 1^+, 2^+)*.\end{aligned}\tag{8.11}$$

$\mathcal{A}(\phi, 1^-, 2^-, 3^+, 4^+)$ is split into its cut-containing pieces and its rational pieces. For generality we calculate the cut-containing pieces for $\mathcal{A}(\phi, 1^-, 2^-, 3^+, \dots, n^+)$. The whole calculation is done in the four-dimensional helicity (FDH) renormalization scheme.

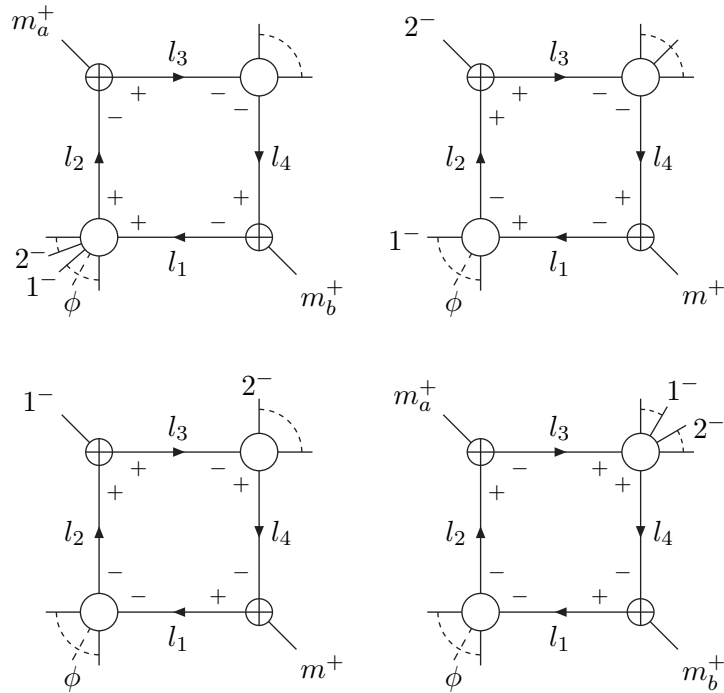
8.2.1 Cut-Constructible Pieces

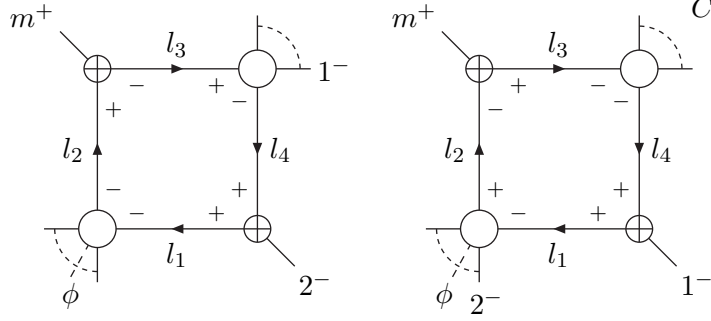
As described in section 5.1.3, the states running in the loop can be written as a linear combination of an $\mathcal{N} = 4$ multiplet, an $\mathcal{N} = 1$ chiral multiplet, and a complex scalar referred to as $\mathcal{N} = 0$. The calculation of cut-containing pieces can be performed separately for the three multiplets, and the result assembled from them.

Our plan of action is to first uncover any box functions by the use of quadruple cuts. We then consider the (two-particle) unitarity cuts where we isolate the terms coming from the (by now known) boxes and relate the remainder to triangles and bubbles.

Quadruple Cuts

If the amplitude is cut in four places, the four corners must together have six minuses (two external and four internal). These must necessarily be distributed as two three-point googly corners (opposite) and two MHV corners. Since the corner with the ϕ cannot be three-point googly, it must be one of the MHV corners. For $\mathcal{N} = 4$, which contains the gluons, this gives us the following six types of non-zero quadruple cuts:





Notice that all permitted cuts necessarily have gluons running in the loop. This immediately shows us that $\mathcal{N} = 1$ and $\mathcal{N} = 0$ cannot contribute since they do not have gluons running in loops.

The calculation of the prefactors of the box functions is almost identical to the one without the ϕ . Thus, we will only present one example calculation, namely that of the coefficient c of the box corresponding to the second cut above. From (B.3) in appendix B we derive that

$$\begin{aligned}
l_1 &= \frac{|m\rangle\langle 2P_{3,m}|}{\langle m2\rangle}, & l_2 &= \frac{|2\rangle\langle mP_{2,m-1}|}{\langle m2\rangle}, \\
l_3 &= \frac{|2\rangle\langle mP_{3,m-1}|}{\langle m2\rangle}, & l_4 &= \frac{|m\rangle\langle 2P_{3,m-1}|}{\langle m2\rangle},
\end{aligned} \tag{8.12}$$

such that

$$\begin{aligned}
c &= \frac{1}{2} \frac{\langle 1l_2 \rangle^3}{\langle l_2(-l_1) \rangle \langle (-l_1)(m+1) \rangle \langle (m+1) \cdots 1 \rangle} \frac{[l_3(-l_2)]^3}{[(-l_2)2][2l_3]} \\
&\quad \times \frac{\langle l_4(-l_3) \rangle^3}{\langle (-l_3)3 \rangle \langle 3 \cdots (m-1) \rangle \langle (m-1)l_4 \rangle} \frac{[(-l_4)m]^3}{[ml_1][l_1(-l_4)]} \\
&= \frac{1}{2} \frac{\langle 12 \rangle \langle 23 \rangle \langle (m-1)m \rangle \langle m(m+1) \rangle \langle 1l_2 \rangle^3 [l_2l_3]^3 \langle l_3l_4 \rangle^3 [l_4m]^3}{\langle \cdots \rangle \langle l_2l_1 \rangle \langle l_1(m+1) \rangle [l_22][2l_3] \langle l_33 \rangle \langle (m-1)l_4 \rangle [ml_1][l_1l_4]} \\
&= \frac{1}{2} \frac{\langle 12 \rangle \langle 23 \rangle \langle (m-1)m \rangle \langle m(m+1) \rangle \langle 12 \rangle^3 (-\langle mP_{2,m-1}P_{3,m-1}m \rangle)^3}{\langle \cdots \rangle \langle m2 \rangle^4 \langle 2m \rangle \langle m(m+1) \rangle \langle mP_{2,m-1}2 \rangle (-[2P_{3,m-1}m]) \langle 23 \rangle} \\
&\quad \times \frac{\langle 2m \rangle^3 \langle 2P_{3,m-1}m \rangle^3}{\langle (m-1)m \rangle (-[mP_{3,m}2]) (-\langle 2P_{3,m}P_{3,m-1}2 \rangle)} \\
&= \frac{\langle 12 \rangle^4}{\langle \cdots \rangle} \left(-\frac{\langle 2P_{3,m-1}m \rangle \langle mP_{3,m-1}2 \rangle}{2} \right). \tag{8.13}
\end{aligned}$$

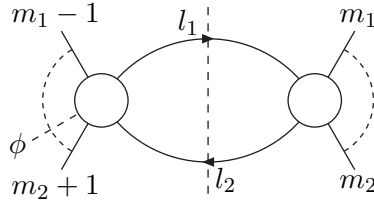
As usual for MHV amplitudes, this is just the Gram determinant times the tree amplitude. This holds for all coefficients, so the boxy part of the amplitude is given by

$$\frac{\langle 12 \rangle^4}{\langle \cdots \rangle} \sum_{m_1=1}^n \sum_{m_2=m_1+2}^{m_1-1} F_4(m_1, P_{m_1+1, m_2-1}, m_2), \tag{8.14}$$

which is a combination of 1-mass and 2-mass-easy box functions. The difference in comparison to the result without the ϕ is primarily that there are twice as many 2-mass boxes because the ϕ makes the two massive corners non-identical.

Two Particle Cuts, $\mathcal{N} = 4$ Case

By counting minuses, we can again see that the two tree amplitudes separated by the cut must be MHV and ϕ -MHV, respectively:



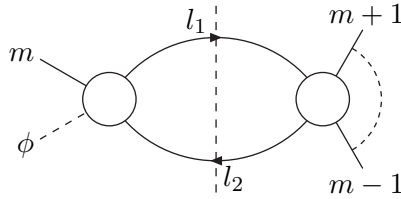
Regardless of the position of 1 and 2, the cut integrand becomes

$$\frac{\langle 12 \rangle^4 \langle (m_1 - 1)m_1 \rangle \langle l_1 l_2 \rangle \langle m_2(m_2 + 1) \rangle \langle l_2 l_1 \rangle}{\langle \dots \rangle \langle (m_1 - 1)l_1 \rangle \langle l_1 m_1 \rangle \langle m_2 l_2 \rangle \langle l_2(m_2 + 1) \rangle}. \quad (8.15)$$

For generic values of m_1 and m_2 it can be shown, analogously to the pure gluon case, that this is equivalent to the same cut of

$$\frac{\langle 12 \rangle^4}{\langle \dots \rangle} \left(F_4(m_1 - 1, P_{m_1, m_2 - 1}, m_2) + F_4(m_1 - 1, P_{m_1, m_2}, m_2 + 1) \right. \\ \left. + F_4(m_1, P_{m_1 + 1, m_2 - 1}, m_2) + F_4(m_1, P_{m_1 + 1, m_2}, m_2 + 1) \right). \quad (8.16)$$

The pure glue requirement that $m_1 - 1 \neq m_2 + 1$ is, however, not present when there is a ϕ on the left tree amplitude where the cut



must be taken into account. The decomposition is the same as above, but the box function $F_4(m_1 - 1, P_{m_1, m_2}, m_2 + 1) = F_4(m, P_{m+1, m-1}, m)$ is physically nonsensical as it stands. Luckily, its cut can be rewritten,

$$-\frac{1}{2} \frac{\langle (m_1 - 1)P_{m_1, m_2}(m_2 + 1)P_{m_1, m_2}(m_1 - 1) \rangle}{(l_1 - (m_1 - 1))^2 (l_2 + (m_2 + 1))^2}$$

$$\begin{aligned}
&= \frac{1}{2} \frac{\langle m P_{m+1, m-1} m \rangle^2}{\langle m l_1 m \rangle \langle m l_2 m \rangle} \\
&= \frac{\langle m P_{m+1, m-1} m \rangle}{2(l_1 - m)^2} + \frac{\langle m P_{m+1, m-1} m \rangle}{2(l_2 + m)^2}, \tag{8.17}
\end{aligned}$$

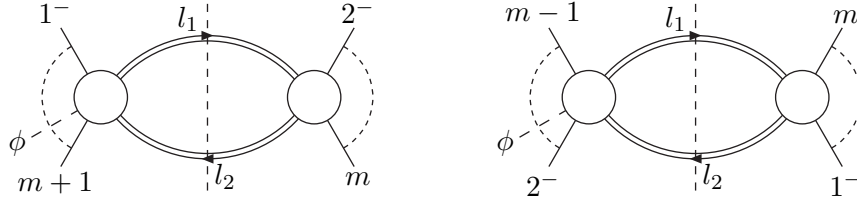
as a sum of the cuts of the two triangle functions. But since a triangle function is independent of the ordering of its momenta, these two triangles are actually the same, leaving us exactly with the cut of $F_3(m, P_{m+1, m-1})$. There are no contributions from bubble functions in the $\mathcal{N} = 4$ case.

The conclusion is, that the amplitude should have the following dependence on triangles

$$\frac{\langle 12 \rangle^4}{\langle \dots \rangle} \sum_{m=1}^n F_3(m, P_{m+1, m-1}). \tag{8.18}$$

Two Particle Cuts, $\mathcal{N} = 1$ and $\mathcal{N} = 0$ Cases

With the two particle cuts, we have a possibility to let a full multiplet run in the loop if we have 1^- and 2^- sitting on different sides of the cut, that is, in the cases



where m runs from 3 to n in both. For simplicity, we only treat the first of these.

For $\mathcal{N} = 1$, the cut is given by

$$\begin{aligned}
&\frac{\langle 1l_1 \rangle \langle 1l_2 \rangle \langle 2l_1 \rangle \langle 2l_2 \rangle \left(- \left(\langle 1l_1 \rangle \langle 2l_2 \rangle - \langle 1l_2 \rangle \langle 2l_1 \rangle \right)^2 \right)}{\langle l_1 l_2 \rangle \langle l_2(m+1) \rangle \langle (m+1) \dots 1 \rangle \langle 1l_1 \rangle \langle l_2 l_1 \rangle \langle l_1 2 \rangle \langle 2 \dots m \rangle \langle m l_2 \rangle} \\
&= \frac{\langle 12 \rangle^3 \langle m(m+1) \rangle}{\langle \dots \rangle} \frac{\langle 1l_2 \rangle \langle l_2 2 \rangle}{\langle m l_2 \rangle \langle l_2(m+1) \rangle} \\
&= \frac{\langle 12 \rangle^3}{\langle \dots \rangle} \left(\frac{\langle m 1 \rangle \langle 2l_2 \rangle}{\langle m l_2 \rangle} + \frac{\langle 1(m+1) \rangle \langle 2l_2 \rangle}{\langle (m+1) l_2 \rangle} \right) \\
&= \frac{\langle 12 \rangle^3}{\langle \dots \rangle} \left(\frac{\langle 2l_2 m \rangle \langle m 1 \rangle}{\langle m l_2 m \rangle} - \frac{\langle 2l_2(m+1) \rangle \langle (m+1) 1 \rangle}{\langle (m+1) l_2(m+1) \rangle} \right). \tag{8.19}
\end{aligned}$$

We have now written this as cuts of vector triangles. To put this into the standard basis of scalar integrals we need to perform a Passarino–Veltman reduction [121].

The details of this procedure is given in appendix C, and the result is (using $P \equiv -P_{2,m}$):

$$\frac{\langle 12 \rangle^3}{\langle \dots \rangle} \left(\frac{\langle 2P_{2,m}m1 \rangle}{\langle mP_{2,m}m \rangle} - \frac{\langle 2P_{2,m}(m+1)1 \rangle}{\langle (m+1)P_{2,m}(m+1) \rangle} \right). \quad (8.20)$$

Here we have to remember that we have suppressed the integration, so what this really tells us is that the cuts we have calculated are the cuts of

$$c_\Gamma \sum_{m=3}^n \frac{\langle 12 \rangle^3}{\langle \dots \rangle} \left(\frac{\langle 2P_{2,m}m1 \rangle}{\langle mP_{2,m}m \rangle} - \frac{\langle 2P_{2,m}(m+1)1 \rangle}{\langle (m+1)P_{2,m}(m+1) \rangle} \right) F_2(P_{2,m}). \quad (8.21)$$

Using that $F_2(P_{2,m}) - F_2(P_{2,m-1}) = -\log(P_{2,m}^2/P_{2,m-1}^2)$, we can rewrite this as

$$-c_\Gamma \frac{\langle 12 \rangle^3}{\langle \dots \rangle} \sum_{m=4}^n \frac{\langle 2P_{2,m}m1 \rangle}{\langle mP_{2,m}m \rangle} \log \left(\frac{P_{2,m}^2}{P_{2,m-1}^2} \right). \quad (8.22)$$

The contribution from the second class of diagrams is

$$c_\Gamma \sum_{m=3}^n \frac{\langle 12 \rangle^3}{\langle \dots \rangle} \left(\frac{\langle 1P_{m,1}(m-1)2 \rangle}{\langle (m-1)P_{m,1}(m-1) \rangle} - \frac{\langle 1P_{m,1}m2 \rangle}{\langle mP_{m,1}m \rangle} \right) F_2(P_{m,1}), \quad (8.23)$$

or

$$-c_\Gamma \frac{\langle 12 \rangle^3}{\langle \dots \rangle} \sum_{m=4}^n \frac{\langle 1P_{m,1}(m-1)2 \rangle}{\langle (m-1)P_{m,1}(m-1) \rangle} \log \left(\frac{P_{m,1}^2}{P_{m-1,1}^2} \right). \quad (8.24)$$

The $\mathcal{N} = 0$ case is complicated by the need for integral reduction. However, if we plunge right into it, the cut corresponding to the first diagram above is

$$\begin{aligned} & 2 \frac{\langle 1l_1 \rangle^2 \langle 1l_2 \rangle^2 \langle 2l_1 \rangle^2 \langle 2l_2 \rangle^2}{\langle l_1 l_2 \rangle \langle l_2(m+1) \rangle \langle (m+1) \dots 1 \rangle \langle 1l_1 \rangle \langle l_2 l_1 \rangle \langle l_1 2 \rangle \langle 2 \dots m \rangle \langle ml_2 \rangle} \\ &= 2 \frac{\langle 12 \rangle \langle m(m+1) \rangle}{\langle \dots \rangle} \frac{\langle 1l_1 \rangle \langle 1l_2 \rangle^2 \langle 2l_1 \rangle \langle 2l_2 \rangle^2}{\langle l_1 l_2 \rangle^2 \langle ml_2 \rangle \langle l_2(m+1) \rangle} \\ &= 2 \frac{\langle 12 \rangle}{\langle \dots \rangle} \frac{\langle 1l_1 \rangle \langle 1l_2 \rangle \langle 2l_1 \rangle \langle 2l_2 \rangle^2}{\langle l_1 l_2 \rangle^2} \left(\frac{\langle 1m \rangle}{\langle ml_2 \rangle} + \frac{\langle 1(m+1) \rangle}{\langle l_2(m+1) \rangle} \right) \\ &= 2 \frac{\langle 12 \rangle}{\langle \dots \rangle} \frac{\langle 1l_1 l_2 1 \rangle \langle 2l_1 l_2 2 \rangle}{P_{2,m}^4} \left(\frac{\langle 2l_2(m+1)1 \rangle}{\langle (m+1)l_2(m+1) \rangle} - \frac{\langle 2l_2 m 1 \rangle}{\langle ml_2 m \rangle} \right) \\ &= 2 \frac{\langle 12 \rangle}{\langle \dots \rangle} \frac{\langle 1P_{2,m}l_2 1 \rangle \langle 2P_{2,m}l_2 2 \rangle}{P_{2,m}^4} \left(\frac{\langle 2l_2(m+1)1 \rangle}{\langle (m+1)l_2(m+1) \rangle} - \frac{\langle 2l_2 m 1 \rangle}{\langle ml_2 m \rangle} \right). \quad (8.25) \end{aligned}$$

These are cuts of triangles with three-index tensors in the numerators. Again, we use the Passarino–Veltman reduction from appendix C (using $P \equiv -P_{2,m}$) to reduce

$$\frac{\langle 1P_{2,m}l_2 1 \rangle \langle 2P_{2,m}l_2 2 \rangle}{P_{2,m}^4} \frac{\langle 2l_2 m 1 \rangle}{\langle ml_2 m \rangle} \quad (8.26)$$

to

$$\begin{aligned}
& \frac{\langle 1P_{2,m}m1 \rangle \langle 2P_{2,m}m2 \rangle \langle 2P_{2,m}m1 \rangle}{3\langle mP_{2,m}m \rangle^3} - \frac{\langle 1P_{2,m}\gamma^\mu 1 \rangle \langle 2P_{2,m}m2 \rangle \langle 2\gamma_\mu m1 \rangle}{12\langle mP_{2,m}m \rangle^2} \\
& - \frac{\langle 1P_{2,m}\gamma^\mu 1 \rangle \langle 2P_{2,m}\gamma_\mu 2 \rangle \langle 2P_{2,m}m1 \rangle}{12P_{2,m}^2 \langle mP_{2,m}m \rangle} \\
= & \frac{\langle 1P_{2,m}m1 \rangle \langle 2P_{2,m}m2 \rangle \langle 2P_{2,m}m1 \rangle}{3\langle mP_{2,m}m \rangle^3} + \frac{\langle 2P_{2,m}m2 \rangle \langle 1P_{2,m}m1 \rangle \langle 12 \rangle}{6\langle mP_{2,m}m \rangle^2} \\
& - \frac{\langle 12 \rangle^2 \langle 2P_{2,m}m1 \rangle}{6\langle mP_{2,m}m \rangle} \\
= & \frac{\langle 1P_{2,m}m1 \rangle \langle 2P_{2,m}m2 \rangle \langle 2[P_{2,m}, m]1 \rangle}{6\langle mP_{2,m}m \rangle^3} - \frac{\langle 12 \rangle^2 \langle 2P_{2,m}m1 \rangle}{6\langle mP_{2,m}m \rangle}. \tag{8.27}
\end{aligned}$$

Thus, the bubble functions coming from the first diagram are

$$\begin{aligned}
c_\Gamma \frac{\langle 12 \rangle}{3\langle \dots \rangle} & \left(\frac{\langle 1P_{2,m}(m+1)1 \rangle \langle 2P_{2,m}(m+1)2 \rangle \langle 2[P_{2,m}, (m+1)]1 \rangle}{\langle (m+1)P_{2,m}(m+1) \rangle^3} \right. \\
& - \frac{\langle 12 \rangle^2 \langle 2P_{2,m}(m+1)1 \rangle}{\langle (m+1)P_{2,m}(m+1) \rangle} - \frac{\langle 1P_{2,m}m1 \rangle \langle 2P_{2,m}m2 \rangle \langle 2[P_{2,m}, m]1 \rangle}{\langle mP_{2,m}m \rangle^3} \\
& \left. + \frac{\langle 12 \rangle^2 \langle 2P_{2,m}m1 \rangle}{\langle mP_{2,m}m \rangle} \right) F_2(P_{2,m}), \tag{8.28}
\end{aligned}$$

while those coming from the second are

$$\begin{aligned}
c_\Gamma \frac{\langle 12 \rangle}{3\langle \dots \rangle} & \left(- \frac{\langle 1P_{m,1}(m-1)1 \rangle \langle 2P_{m,1}(m-1)2 \rangle \langle 2[P_{m,1}, (m-1)]1 \rangle}{\langle (m-1)P_{m,1}(m-1) \rangle^3} \right. \\
& + \frac{\langle 12 \rangle^2 \langle 1P_{m,1}(m-1)2 \rangle}{\langle (m-1)P_{m,1}(m-1) \rangle} + \frac{\langle 1P_{m,1}m1 \rangle \langle 2P_{m,1}m2 \rangle \langle 2[P_{m,1}, m]1 \rangle}{\langle mP_{m,1}m \rangle^3} \\
& \left. - \frac{\langle 12 \rangle^2 \langle 1P_{m,1}m2 \rangle}{\langle mP_{m,1}m \rangle} \right) F_2(P_{m,1}). \tag{8.29}
\end{aligned}$$

Again, these can be rewritten as

$$\begin{aligned}
c_\Gamma \frac{\langle 12 \rangle}{3\langle \dots \rangle} & \sum_{m=4}^n \left[\left(\frac{\langle 1P_{2,m}m1 \rangle \langle 2P_{2,m}m2 \rangle \langle 2[P_{2,m}, m]1 \rangle}{\langle mP_{2,m}m \rangle^3} \right. \right. \\
& \left. - \frac{\langle 12 \rangle^2 \langle 2P_{2,m}m1 \rangle}{\langle mP_{2,m}m \rangle} \right) \log \left(\frac{P_{2,m}^2}{P_{2,m-1}^2} \right) \\
& + \left(\frac{\langle 1P_{m,1}(m-1)1 \rangle \langle 2P_{m,1}(m-1)2 \rangle \langle 2[P_{m,1}, (m-1)]1 \rangle}{\langle (m-1)P_{m,1}(m-1) \rangle^3} \right. \\
& \left. - \frac{\langle 12 \rangle^2 \langle 1P_{m,1}(m-1)2 \rangle}{\langle (m-1)P_{m,1}(m-1) \rangle} \right) \log \left(\frac{P_{m,1}^2}{P_{m-1,1}^2} \right) \Big]. \tag{8.30}
\end{aligned}$$

Summing Up

We can now sum up the cut containing pieces for arbitrary fermion and scalar content. In place of the logs we use

$$L_1(s, t) = \frac{\log(s/t)}{s-t}, \quad L_3(s, t) = \frac{\log(s/t)}{(s-t)^3}. \quad (8.31)$$

The result is

$$\begin{aligned} c_\Gamma \frac{\langle 12 \rangle^4}{\langle \dots \rangle} & \left\{ \sum_{m_1=1}^n \left(F_3(m_1, P_{m_1+1, m_1-1}) + \sum_{m_2=m_1+2}^{m_1-1} F_4(m_1, P_{m_1+1, m_2-1}, m_2) \right) \right. \\ & + \sum_{m=4}^n \left[\left(1 - \frac{n_f}{N} + \frac{n_s}{N} \right) \left(\frac{\langle 1P_{2,m}m1 \rangle \langle 2P_{2,m}m2 \rangle \langle 2[P_{2,m}, m]1 \rangle}{3\langle 12 \rangle^3} L_3(P_{2,m}^2, P_{2,m-1}^2) \right. \right. \\ & - \frac{\langle 1P_{m,1}(m-1)1 \rangle \langle 2P_{m,1}(m-1)2 \rangle \langle 2[P_{m,1}, (m-1)]1 \rangle}{3\langle 12 \rangle^3} \\ & \left. \left. \times L_3(P_{m,1}^2, P_{m-1,1}^2) \right) + \left(\frac{11}{3} - \frac{2n_f}{3N} - \frac{n_s}{3N} \right) \left(\frac{\langle 2P_{2,m}m1 \rangle}{\langle 12 \rangle} L_1(P_{2,m}^2, P_{2,m-1}^2) \right. \right. \\ & \left. \left. - \frac{\langle 1P_{m,1}(m-1)2 \rangle}{\langle 12 \rangle} L_1(P_{m,1}^2, P_{m-1,1}^2) \right) \right] \left. \right\}. \quad (8.32) \end{aligned}$$

We can now specialize to $n = 4$, since this is the amplitude we ultimately want to calculate. There, the result is

$$\begin{aligned} c_\Gamma \frac{\langle 12 \rangle^4}{\langle \dots \rangle} & \sum_{m=1}^4 \left(F_4^{1m}(m, m+1, m+2) + F_4^{2me}(m, P_{m+1, m+2}, m+3) \right. \\ & \left. + F_3^{2m}(m, P_{m+1, m+3}) \right) + c_\Gamma \frac{[34]}{3\langle 34 \rangle} \left(1 - \frac{n_f}{N} + \frac{n_s}{N} \right) \left(\right. \\ & \langle 1P_{23}42 \rangle \langle 2[P_{23}, 4]1 \rangle L_3(s_{234}, s_{23}) + \langle 2P_{41}31 \rangle \langle 2[P_{41}, 3]1 \rangle L_3(s_{41}, s_{341}) \left. \right) \\ & + c_\Gamma \frac{[34]\langle 12 \rangle^2}{\langle 34 \rangle} \left(\frac{11}{3} - \frac{2n_f}{3N} - \frac{n_s}{3N} \right) \left(L_1(s_{234}, s_{23}) + L_1(s_{41}, s_{341}) \right). \quad (8.33) \end{aligned}$$

8.2.2 Rational Pieces

To compute the remaining parts of the amplitude we use the methods described in section 5.5. The total one-loop amplitude is

$$\mathcal{A}^1 = C + R, \quad (8.34)$$

but C and R contain unphysical poles which cancel against each other, but prevent us from finding R directly from recursion. Instead, we add and subtract a term CR with the same unphysical singularities as C ,

$$\mathcal{A}^1 = (C + CR) + (R - CR), \quad (8.35)$$

such that only physical poles are left in each of the parentheses. Our first observation about (8.34) will be that the unphysical poles only reside in the L_3 functions, and by rewriting it as

$$\begin{aligned} L_3(s, t) &= \frac{1}{2} \frac{\log \left[1 + (s-t)/t \right]}{(s-t)^3} + \frac{1}{2} \frac{\log \left[1 + (t-s)/s \right]}{(t-s)^3} \\ &= \frac{1}{2} \frac{1}{t(s-t)^2} - \frac{1}{4} \frac{1}{t^2(s-t)} + \frac{1}{2} \frac{1}{s(t-s)^2} - \frac{1}{4} \frac{1}{s^2(t-s)} + \mathcal{O}((s-t)^0) \\ &= \frac{1}{2} \left(\frac{1}{t} + \frac{1}{s} \right) \frac{1}{(s-t)^2} - \frac{1}{4} \frac{s^2 - t^2}{s^2 t^2 (s-t)} + \mathcal{O}((s-t)^0) \\ &= \frac{1}{2} \left(\frac{1}{t} + \frac{1}{s} \right) \frac{1}{(s-t)^2} + \mathcal{O}((s-t)^0), \end{aligned} \quad (8.36)$$

we see that CR must be constructed by replacing $L_3(s, t)$ by

$$-\frac{1}{2} \left(\frac{1}{t} + \frac{1}{s} \right) \frac{1}{(s-t)^2}. \quad (8.37)$$

Thus,

$$\begin{aligned} CR &= -\frac{c_\Gamma[34]}{6\langle 34 \rangle} \left(1 - \frac{n_f}{N} + \frac{n_s}{N} \right) \left[\frac{\langle 1P_{23}42 \rangle \langle 2[P_{23}, 4]1 \rangle}{\langle 4P_{23}4 \rangle^2} \left(\frac{1}{s_{234}} + \frac{1}{s_{23}} \right) \right. \\ &\quad \left. + \frac{\langle 2P_{41}31 \rangle \langle 2[P_{41}, 3]1 \rangle}{\langle 3P_{41}3 \rangle^2} \left(\frac{1}{s_{341}} + \frac{1}{s_{41}} \right) \right]. \end{aligned} \quad (8.38)$$

Knowing now that $R - CR$ has only physical poles, we can attack it with recursion relations. For reasons which will become clear later, we choose the recursive shift

$$|\widehat{1}\rangle = |1\rangle + z|2\rangle, \quad |\widehat{2}\rangle = |2\rangle - z|1\rangle. \quad (8.39)$$

Rather than proving that this shift has the proper $z \rightarrow \infty$ behaviour, we will note that it does indeed work without the ϕ [89], and that the tests to be explained in the next section show no signs of bad $z \rightarrow \infty$ behaviour. The results of doing recursion on CR are the overlap terms O_{23} , O_{234} , O_{41} , and O_{341} , coming from the singularities in s_{23} , *etc.* These are found by leaving the kinematic invariant, shifting its coefficient according to (8.39), and inserting the z which puts us exactly at the pole. Taking O_{23} as an example, we note that CR has a pole where

$$0 = \widehat{s}_{23} = \langle 23 \rangle [3\widehat{2}] = \langle 23 \rangle ([32] - z[31]) \quad \Rightarrow \quad z = \frac{[32]}{[31]}, \quad (8.40)$$

such that

$$|\widehat{1}\rangle = \frac{|P_{1233}\rangle}{[13]}, \quad |\widehat{2}\rangle = |3\rangle \frac{[12]}{[13]}, \quad \widehat{P}_{23} = \frac{|P_{1231}\rangle[3]}{[31]}, \quad (8.41)$$

and find that

$$\begin{aligned} O_{23} &= -\frac{c_\Gamma}{6} \left(1 - \frac{n_f}{N} + \frac{n_s}{N}\right) \frac{[34] \langle \widehat{1} P_{123} 4 2 \rangle \langle 2(34 - 4P_{123}) \widehat{1} \rangle}{\langle 34 \rangle \langle 4 \widehat{P}_{23} 4 \rangle^2 s_{23}} \\ &= -\frac{c_\Gamma}{6} \left(1 - \frac{n_f}{N} + \frac{n_s}{N}\right) \frac{[34] s_{123} [34] \langle 4 2 \rangle \left(s_{123} \langle 2 4 \rangle [43] - \langle 2 3 \rangle [34] \langle 4 P_{12} 3 \rangle \right)}{\langle 34 \rangle \langle 4 P_{23} 1 \rangle^2 [34]^2 s_{23}} \\ &= -\frac{c_\Gamma}{6} \left(1 - \frac{n_f}{N} + \frac{n_s}{N}\right) \frac{[34] s_{123} \langle 4 2 \rangle \left(s_{123} \langle 4 2 \rangle + \langle 4 P_{12} 3 \rangle \langle 3 2 \rangle \right)}{\langle 34 \rangle \langle 4 P_{23} 1 \rangle^2 s_{23}}. \end{aligned} \quad (8.42)$$

The other overlaps are

$$O_{234} = -\frac{c_\Gamma}{6} \left(1 - \frac{n_f}{N} + \frac{n_s}{N}\right) \frac{[34] s_{1234} \langle 4 2 \rangle \left(s_{1234} \langle 4 2 \rangle + \langle 4 P_{123} P_{34} 2 \rangle \right)}{\langle 34 \rangle \langle 4 P_{23} 1 \rangle^2 s_{234}}, \quad (8.43)$$

$$O_{41} = -\frac{c_\Gamma}{6} \left(1 - \frac{n_f}{N} + \frac{n_s}{N}\right) \frac{[34] \langle 1 2 \rangle^2}{\langle 34 \rangle s_{41}}, \quad (8.44)$$

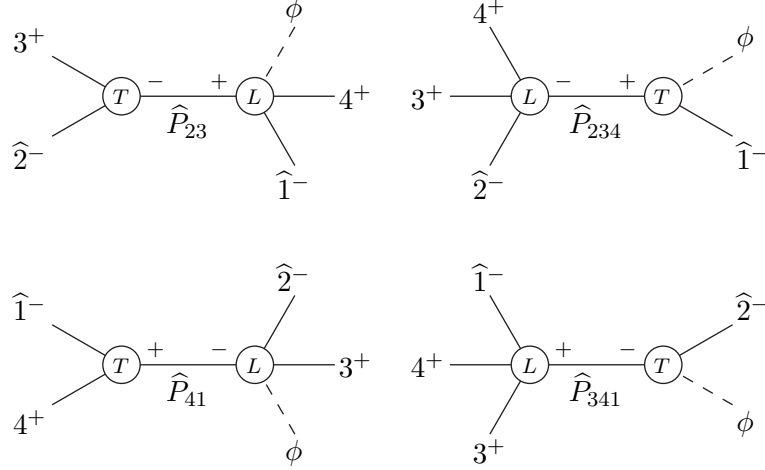
$$O_{341} = -\frac{c_\Gamma}{6} \left(1 - \frac{n_f}{N} + \frac{n_s}{N}\right) \frac{[34] \langle 2 P_{13} 4 \rangle \left(\langle 2 P_{13} 4 \rangle + \langle 2 3 \rangle [34] \right)}{\langle 34 \rangle [41]^2 s_{341}}. \quad (8.45)$$

The hattings used in these and later calculations are given in the table below:

i	$ \widehat{1}\rangle$	$ \widehat{2}\rangle$	\widehat{P}_i
23	$\frac{ P_{1233}\rangle}{[13]}$	$ 3\rangle \frac{[12]}{[13]}$	$\frac{ P_{1231}\rangle[3]}{[31]}$
234	$\frac{ P_{1234} P_{34} 2\rangle}{\langle 2 P_{34} 1 \rangle}$	$\frac{ P_{34} P_{1234} 1\rangle}{\langle 2 P_{34} 1 \rangle}$	$\frac{ P_{1234} 1\rangle \langle 2 P_{34} \rangle}{\langle 2 P_{34} 1 \rangle}$
41	$ 4\rangle \frac{\langle 2 1 \rangle}{\langle 2 4 \rangle}$	$\frac{ P_{4124}\rangle}{\langle 2 4 \rangle}$	$ 4\rangle \frac{\langle 2 P_{412} \rangle}{\langle 2 4 \rangle}$
341	$\frac{ P_{34} P_{1234} 2\rangle}{\langle 2 P_{34} 1 \rangle}$	$\frac{ P_{1234} P_{34} 1\rangle}{\langle 2 P_{34} 1 \rangle}$	$\frac{ P_{34} 1\rangle \langle 2 P_{1234} \rangle}{\langle 2 P_{34} 1 \rangle}$

We can now turn to the results of doing recursion on R . This does not give us the R since we are summing over a limited set of poles, but rather gives us the 'direct recursive' terms DR_{23} , *etc*, composed of (a sum of) an unshifted propagator times a shifted tree amplitude times a shifted rational part of a one-loop amplitude. One complication is that the three-point one-loop vertices cannot really be interpreted as the corresponding amplitudes, rather they have to be deduced from the one-loop splitting functions. In the case at hand, however, we are considering a scalar running in the loop and we have chosen our shift such that the two external gluons in a three-point vertex have opposite signs. Fortunately,

the rational parts of the corresponding splitting functions are all zero (*cf.* (5.39)) so there are no contributions in our case from three-point one-loop vertices. The non-zero diagrams are



The relevant lower-point amplitudes with a ϕ can be found in [20]

$$\begin{aligned}
A^1(\phi, 1^-, 2^-) &= \frac{1}{8\pi^2} A^0(\phi, 1^-, 2^-) \\
R(\phi, 1^-, 2^-, 3^+) &= \frac{1}{8\pi^2} A^0(\phi, 1^-, 2^-, 3^+) \\
A^1(\phi, 1^-, 2^+, 3^+) &= \frac{1}{48\pi^2} \left(1 - \frac{n_f}{N} + \frac{n_s}{N}\right) \frac{\langle 12 \rangle \langle 31 \rangle [23]}{\langle 23 \rangle^2} \\
&\quad - \frac{1}{8\pi^2} A^0(\phi^\dagger, 1^-, 2^+, 3^+)
\end{aligned} \tag{8.46}$$

while the last was calculated in [46]

$$A^1(1^-, 2^+, 3^+, 4^+) = \frac{1}{48\pi^2} \left(1 - \frac{n_f}{N} + \frac{n_s}{N}\right) \frac{\langle 24 \rangle [24]^3}{[12] \langle 23 \rangle \langle 34 \rangle [41]}. \tag{8.47}$$

This gives the direct recursive terms

$$\begin{aligned}
DR_{23} &= \mathcal{A}_3(\widehat{2}^-, 3^+, -\widehat{P}_{23}^-) \frac{1}{P_{23}^2} R_4(\phi, 4^+, \widehat{1}^-, \widehat{P}_{23}^+) \\
&= \frac{c_\Gamma}{3} \left(1 - \frac{n_f}{N} + \frac{n_s}{N}\right) \frac{[34] s_{123} [13] \langle 4P_{123} \rangle}{[12] [23] \langle 4P_{231} \rangle^2} \\
&\quad - 2c_\Gamma \mathcal{A}^0(\phi^\dagger, 1^-, 2^-, 3^+, 4^+)
\end{aligned} \tag{8.48}$$

$$\begin{aligned}
DR_{234} &= R_4(\widehat{2}^-, 3^+, 4^+, -\widehat{P}_{234}^+) \frac{1}{P_{234}^2} \mathcal{A}_3(\phi, \widehat{1}^-, \widehat{P}_{234}^-) \\
&= \frac{c_\Gamma}{3} \left(1 - \frac{n_f}{N} + \frac{n_s}{N}\right) \frac{[34] s_{1234}^2 \langle 24 \rangle^3 \langle 3P_{241} \rangle}{\langle 34 \rangle^2 s_{234} \langle 2P_{341} \rangle \langle 4P_{231} \rangle^2}
\end{aligned} \tag{8.49}$$

$$\begin{aligned}
DR_{41} &= \mathcal{A}_3(4^+, \widehat{1}^-, -\widehat{P}_{41}^+) \frac{1}{P_{41}^2} R_4(\phi, \widehat{2}^-, 3^+, \widehat{P}_{41}^-) \\
&= 2c_\Gamma \mathcal{A}^0(\phi, 1^-, 2^-, 3^+, 4^+)
\end{aligned} \tag{8.50}$$

$$\begin{aligned}
DR_{341} &= R_4(3^+, 4^+, \widehat{1}^-, -\widehat{P}_{341}^+) \frac{1}{P_{341}^2} \mathcal{A}_3(\phi, \widehat{2}^-, \widehat{P}_{341}^-) \\
&= \frac{c_\Gamma}{3} \left(1 - \frac{n_f}{N} + \frac{n_s}{N} \right) \frac{[31] \langle 2P_{134} \rangle^3}{\langle 34 \rangle s_{341} [41]^2 \langle 2P_{341} \rangle}.
\end{aligned} \tag{8.51}$$

To obtain R , we now have to add the DR terms and CR and subtract the O terms. Some lengthy but trivial manipulations give

$$\begin{aligned}
R &= 2c_\Gamma i \mathcal{A}^0(A, 1^-, 2^-, 3^+, 4^+) + CR + \frac{c_\Gamma [34]}{3 \langle 34 \rangle} \left(1 - \frac{n_f}{N} + \frac{n_s}{N} \right) \left[\right. \\
&\quad \frac{\langle 23 \rangle \langle 1P_{243} \rangle^2}{\langle 34 \rangle [43] [32] s_{234}} - \frac{\langle 41 \rangle \langle 3P_{123} \rangle}{\langle 34 \rangle [12] [32]} + \frac{\langle 14 \rangle \langle 2P_{134} \rangle^2}{\langle 34 \rangle [43] [41] s_{341}} \\
&\quad - \frac{\langle 32 \rangle \langle 4P_{124} \rangle}{\langle 34 \rangle [12] [41]} + \frac{\langle 12 \rangle \langle 2P_{134} \rangle}{2[41] s_{341}} - \frac{\langle 12 \rangle \langle 1P_{243} \rangle}{2[32] s_{234}} \\
&\quad \left. - \langle 12 \rangle^2 \left(\frac{1}{s_{34}} + \frac{1}{s_{12}} + \frac{1}{2s_{23}} + \frac{1}{2s_{41}} \right) \right].
\end{aligned} \tag{8.52}$$

It is of special interest here that the first term is present regardless of supersymmetry, where we might have expected that an amplitude with supersymmetric particle content running in the loop would be fully cut-constructible. The catch is, of course, that cut-constructibility requires also the external particles to be supersymmetric, something which is not the case with ϕ . With those arguments it may seem slightly surprising (although welcome) that it drops out of $\mathcal{A}^1(H, 1^-, 2^-, 3^+, 4^+)$ when we use (8.11). In $\mathcal{A}^1(A, 1^-, 2^-, 3^+, 4^+)$, of course, the additional rational piece stays.

8.2.3 Tests

There are a series of tests which we can perform to check that the result is correct. The first regards only the cut-containing part, in particular the IR divergences in ϵ . These are given by (*cf.* section 5.1.4)

$$\mathcal{A}^1 = -\frac{c_\Gamma}{\epsilon^2} \mathcal{A}^0 \sum_{i=1}^4 \left(\frac{\mu^2}{-s_{i,i+1}} \right)^\epsilon + \mathcal{O}(\epsilon^0). \tag{8.53}$$

This can be checked readily by taking the IR divergent parts of the box and triangle functions from appendix A and putting them into (8.33). There are no contributions from the bubble-like and rational parts.

Collinear Limits

The second test is that of collinear limits. The full checking of all collinear limits is a rather tedious exercise and will not be repeated here. It is contained in the original article in detail. Since the cut-containing parts have been fixed by unitarity, we expect the right collinear limits automatically; for the rational parts, the use of recursion amounts exactly to enforcing the correct collinear limits for gluons 4 and 1, and for gluons 2 and 3. Checking these limits provide primarily a check on the algebra.

From the perspective of on-shell recursion, the important collinear limits are the rational ones which do not participate in the direct recursive terms. If these turn out wrong, it is a sign that the use of recursion was not justified because $R(z) - CR(z)$ did not vanish as $z \rightarrow \infty$. In the case at hand, the important limits in this sense is when 1 and 2 become collinear and when 3 and 4 become collinear.

For these checks, we can use the rational parts of the splitting functions for a scalar running in the loop (5.39) along with the tree splitting functions (2.52). These predict that

$$R(\phi, 1^-, 2^-, 3^+, 4^+) \rightarrow -\frac{1}{\sqrt{z(1-z)}[12]}R(\phi, P^-, 3^+, 4^+) \quad (8.54)$$

as 1 and 2 go collinear, and

$$\begin{aligned} R(\phi, 1^-, 2^-, 3^+, 4^+) &\rightarrow \frac{1}{\sqrt{z(1-z)}\langle 34 \rangle}R(\phi, 1^-, 2^-, P^+) \\ &+ \frac{c_\Gamma}{3} \left(1 - \frac{n_f}{N} + \frac{n_s}{N} \right) \sqrt{z(1-z)} \\ &\times \left(-\frac{1}{\langle 34 \rangle} \mathcal{A}^0(\phi, 1^-, 2^-, P^+) \right. \\ &\quad \left. + \frac{[34]}{\langle 34 \rangle^2} \mathcal{A}^0(\phi, 1^-, 2^-, P^-) \right) \end{aligned} \quad (8.55)$$

as 3 and 4 go collinear. We can prove the first by first extracting the part of (8.52) that has the correct singularity,

$$\begin{aligned} R &\rightarrow 2c_\Gamma \frac{-[34]^3}{[12][23][41]} - \frac{c_\Gamma[34]}{3\langle 34 \rangle^2} \left(1 - \frac{n_f}{N} + \frac{n_s}{N} \right) \left[\frac{\langle 41 \rangle \langle 3P_{12}3 \rangle}{[12][32]} + \frac{\langle 32 \rangle \langle 4P_{12}4 \rangle}{[12][41]} \right] \\ &= \frac{-1}{\sqrt{z(1-z)}[12]} \left[-2c_\Gamma \mathcal{A}^0(\phi^\dagger, P^-, 3^+, 4^+) \right. \\ &\quad \left. + \frac{c_\Gamma[34]}{3\langle 34 \rangle^2} \left(1 - \frac{n_f}{N} + \frac{n_s}{N} \right) \langle 4P \rangle \langle P3 \rangle \right] \\ &\rightarrow \frac{-1}{\sqrt{z(1-z)}[12]} R(\phi, P^-, 3^+, 4^+), \end{aligned} \quad (8.56)$$

as wanted. For the collinear limit between 3 and 4 things are a bit more messy. Because $R(\phi, 1^-, 2^-, P^+) \sim \mathcal{A}^0(\phi, 1^-, 2^-, P^+)$, the first line of (8.55) comes from the first term of (8.52) in the same way as for 1 and 2. The remaining terms with the collinear singularity are

$$\begin{aligned}
& \frac{c_\Gamma [34]}{3 \langle 34 \rangle} \left(1 - \frac{n_f}{N} + \frac{n_s}{N} \right) \left[\frac{\langle 23 \rangle \langle 1P_{24}3 \rangle^2}{\langle 34 \rangle [43] [32] s_{234}} + \frac{\langle 14 \rangle \langle 2P_{31}4 \rangle^2}{\langle 34 \rangle [43] [41] s_{341}} \right. \\
& \quad \left. - \frac{\langle 41 \rangle \langle 3P_{12}3 \rangle}{\langle 34 \rangle [12] [32]} - \frac{\langle 32 \rangle \langle 4P_{12}4 \rangle}{\langle 34 \rangle [12] [41]} - \frac{\langle 12 \rangle^2}{\langle 34 \rangle [43]} \right] \\
& \rightarrow \frac{c_\Gamma [34]}{3 \langle 34 \rangle} \left(1 - \frac{n_f}{N} + \frac{n_s}{N} \right) \left[\frac{\langle 23 \rangle \langle 12 \rangle [23] (\langle 12 \rangle [23] + 2 \langle 14 \rangle [43])}{\langle 34 \rangle [43] [32] s_{234}} \right. \\
& \quad + \frac{\langle 14 \rangle \langle 21 \rangle [14] (\langle 21 \rangle [14] + 2 \langle 23 \rangle [34])}{\langle 34 \rangle [43] [41] s_{341}} - \frac{\langle 12 \rangle^2}{\langle 34 \rangle [43]} \\
& \quad \left. - \frac{\sqrt{z(1-z)}}{\langle 34 \rangle} \left(\frac{\langle P1 \rangle \langle PP_{12}P \rangle}{[12] [P2]} + \frac{\langle P2 \rangle \langle PP_{12}P \rangle}{[12] [P1]} \right) \right] \\
& = \frac{c_\Gamma [34]}{3 \langle 34 \rangle} \left(1 - \frac{n_f}{N} + \frac{n_s}{N} \right) \left[\frac{\langle 12 \rangle^2}{s_{34}} \left(\frac{s_{23}}{s_{234}} + \frac{s_{41}}{s_{341}} - 1 \right) + 2 \frac{\langle 12 \rangle \langle 23 \rangle \langle 41 \rangle}{\langle 34 \rangle} \right. \\
& \quad \left. \times \left(\frac{1}{s_{234}} + \frac{1}{s_{341}} \right) - \frac{\sqrt{z(1-z)}}{\langle 34 \rangle} \frac{\langle PP_{12}P \rangle^2}{[12] [2P] [P1]} \right] \\
& \rightarrow \frac{c_\Gamma [34]}{3 \langle 34 \rangle} \left(1 - \frac{n_f}{N} + \frac{n_s}{N} \right) \left[\frac{\langle 12 \rangle^3 [24] [13]}{[34] s_{234} s_{341}} + \frac{\langle 12 \rangle^2 [21] \langle 41 \rangle \langle 23 \rangle}{\langle 34 \rangle s_{234} s_{341}} \right. \\
& \quad \left. + 2 \frac{\langle 12 \rangle \langle 23 \rangle \langle 41 \rangle (\langle 3P_{12}3 \rangle + \langle 4P_{12}4 \rangle)}{\langle 34 \rangle s_{234} s_{341}} - \frac{\sqrt{z(1-z)}}{\langle 34 \rangle} \frac{\langle PP_{12}P \rangle^2}{[12] [2P] [P1]} \right] \\
& \rightarrow \frac{c_\Gamma \sqrt{z(1-z)}}{3} \left(1 - \frac{n_f}{N} + \frac{n_s}{N} \right) \left[- \frac{\langle 12 \rangle^3}{\langle 34 \rangle \langle 2P \rangle \langle P1 \rangle} - \frac{[34] m_\phi^4}{\langle 34 \rangle^2 [12] [2P] [P1]} \right] \\
& = \frac{c_\Gamma \sqrt{z(1-z)}}{3} \left(1 - \frac{n_f}{N} + \frac{n_s}{N} \right) \\
& \quad \times \left[- \frac{\mathcal{A}^0(\phi, 1^-, 2^-, P^+)}{\langle 34 \rangle} + \frac{[34] \mathcal{A}^0(\phi, 1^-, 2^-, P^-)}{\langle 34 \rangle^2} \right], \tag{8.57}
\end{aligned}$$

as wanted. Notice how we had to rewrite a contribution which superficially went as s_{34}^{-1} to one with either a $\langle 34 \rangle^{-1}$ or a $[34]^{-1}$ divergence. As noted above, the correctness of these two collinear limits are an indicative necessary condition for the recursion relation to hold.

Soft Higgs Limit

The very last test we will make is the limit as the Higgs momentum goes soft. In fact, it turns out to fail, but only because the naive expectation for the soft limit is wrong. The naive expectation comes from noting that as the Higgs momentum

goes to zero, the H field in the effective correction $CHF_{\mu\nu}F^{\mu\nu}$ becomes a constant, and the term becomes proportional to the Higgsless gluon term. This tells us that the first order term in C should be obtainable in this limit as

$$\begin{aligned}\mathcal{A}^l(k_H \rightarrow 0, n \text{ gluons}) &= Cg \frac{\partial}{\partial g} \mathcal{A}^l(n \text{ gluons}) \\ &= C(n - 2 + 2l) \mathcal{A}^l(n \text{ gluons}),\end{aligned}\tag{8.58}$$

where g is the gauge coupling and l is the number of loops. From looking at the form of the ϕ -MHV amplitude and the ϕ^\dagger -googly-MHV amplitude, it is reasonable to guess that the corresponding limits for ϕ and ϕ^\dagger are

$$\begin{aligned}\mathcal{A}^l(k_\phi \rightarrow 0, n_- g^-, n_+ g^+) &= (n_- - 1 + l) \mathcal{A}^l(n_- g^-, n_+ g^+), \\ \mathcal{A}^l(k_{\phi^\dagger} \rightarrow 0, n_- g^-, n_+ g^+) &= (n_+ - 1 + l) \mathcal{A}^l(n_- g^-, n_+ g^+).\end{aligned}\tag{8.59}$$

In other words, we should be trying to prove that

$$\mathcal{A}^1(\phi, 1^-, 2^-, 3^+, 4^+) \rightarrow 2\mathcal{A}^1(1^-, 2^-, 3^+, 4^+)\tag{8.60}$$

as $k_\phi \rightarrow 0$. $\mathcal{A}^1(1^-, 2^-, 3^+, 4^+)$ in the FDH renormalization scheme has the cut-containing and rational parts [46]

$$\begin{aligned}C(1^-, 2^-, 3^+, 4^+) &= c_\Gamma \mathcal{A}^0(1^-, 2^-, 3^+, 4^+) \left[2F_4^{0m}(1, 2, 3, 4) \right. \\ &\quad \left. - \left(\frac{11}{3} - \frac{2n_f}{3N} - \frac{n_s}{3N} \right) F_2(s_{23}) \right] \\ R(1^-, 2^-, 3^+, 4^+) &= \frac{1}{72\pi^2} \left(1 - \frac{n_f}{N} + \frac{n_s}{N} \right) \mathcal{A}^0(1^-, 2^-, 3^+, 4^+).\end{aligned}\tag{8.61}$$

The cut-containing part can be checked quite easily by taking the expression (8.33) and converting the L_k functions back into F_2 bubble functions and then treating each term in turn. In short, only the one-mass box (which becomes zero-mass) and $F_2(s_{23})$ survive the limit, and for the bubble functions it is only the last line of (8.33) that survives.

The limit of the rational part is in principle done in the same way. The term proportional to $\mathcal{A}^0(A, 1^-, 2^-, 3^+, 4^+)$ vanishes in the limit, and there are several terms which must be considered together if the limit has to be taken consistently. In the end we find that

$$R(\phi, 1^-, 2^-, 3^+, 4^+) \rightarrow -\frac{1}{48\pi^2} \left(1 - \frac{n_f}{N} + \frac{n_s}{N} \right) \mathcal{A}^0(1^-, 2^-, 3^+, 4^+),\tag{8.62}$$

as $k_\phi \rightarrow 0$. The corresponding ϕ^\dagger rational part has the soft limit

$$\begin{aligned}R(\phi^\dagger, 1^-, 2^-, 3^+, 4^+) &= R(\phi, 1^+, 2^+, 3^-, 4^-)^* \\ &\rightarrow -\frac{1}{48\pi^2} \left(1 - \frac{n_f}{N} + \frac{n_s}{N} \right) \mathcal{A}^0(1^+, 2^+, 3^-, 4^-)^* \\ &= -\frac{1}{48\pi^2} \left(1 - \frac{n_f}{N} + \frac{n_s}{N} \right) \mathcal{A}^0(1^-, 2^-, 3^+, 4^+),\end{aligned}\tag{8.63}$$

such that the Higgs soft limit is

$$R(H, 1^-, 2^-, 3^+, 4^+) \rightarrow -\frac{1}{24\pi^2} \left(1 - \frac{n_f}{N} + \frac{n_s}{N} \right) \mathcal{A}^0(1^-, 2^-, 3^+, 4^+), \quad (8.64)$$

which is a factor $-1/3$ away from the expectation. This sort of violation was anticipated already in [20] where it was pointed out that the Higgs momentum can act as a kind of effective infrared regulator and that this would cause an exchange-of-limits problem with the dimensional regularization. Thus, we conclude that our results are indeed correct.

Appendix A

Integral Functions

The box, triangle and bubble integrals used in this thesis can be obtained from [34], though with slightly different conventions. The boxes are given by

$$I_4(K_1, K_2, K_3, K_4) = -i\mu^{2\epsilon} \int \frac{d^{4-2\epsilon}L}{(2\pi)^{4-2\epsilon}} \frac{1}{L^2(L+K_1)^2(L+K_1+K_2)^2(L-K_4)^2} \quad (\text{A.1})$$

where the usual $i\epsilon$ prescription is understood. The integrals are classified according to which of the momenta are massive and which are massless. 1-mass integrals have one massive momentum, 4-mass integrals have four. There are two different 2-mass configurations; if the massive momenta are opposite it is called the 2-mass-easy and if they are adjacent it is called the 2-mass-hard.

We give the integrals in terms of the box functions $F_4(\dots)$ which are dimensionless because they are multiplied by the Gram determinant \mathcal{G} of that integral. We also take out a factor r_Γ coming from dimensional reduction,

$$I_4(\dots) = \frac{c_\Gamma}{\mathcal{G}} F_4(\dots) \quad (\text{A.2})$$

where

$$c_\Gamma = \frac{1}{(4\pi)^{2-\epsilon}} \frac{\Gamma(1+\epsilon)\Gamma^2(1-\epsilon)}{\Gamma(1-2\epsilon)} = \frac{1}{16\pi^2} + \mathcal{O}(\epsilon). \quad (\text{A.3})$$

We also define the kinematic invariants

$$s = (K_1 + K_2)^2, \quad t = (K_2 + K_3)^2. \quad (\text{A.4})$$

The box functions through 3-mass are,

$$\begin{aligned} & F_4^{0m}(k_1, k_2, k_3, k_4) \\ &= -\frac{1}{\epsilon^2} \left[\left(\frac{\mu^2}{-s} \right)^\epsilon + \left(\frac{\mu^2}{-t} \right)^\epsilon \right] + \log^2 \left(\frac{-s}{-t} \right) + \pi^2 \\ & F_4^{1m}(k_1, k_2, k_3, K_4) \end{aligned} \quad (\text{A.5})$$

$$\begin{aligned}
&= -\frac{1}{\epsilon^2} \left[\left(\frac{\mu^2}{-s} \right)^\epsilon + \left(\frac{\mu^2}{-t} \right)^\epsilon - \left(\frac{\mu^2}{-K_4^2} \right)^\epsilon \right] \\
&\quad + \text{Li}_2 \left(1 - \frac{K_4^2}{s} \right) + \text{Li}_2 \left(1 - \frac{K_4^2}{t} \right) + \frac{1}{2} \log^2 \left(\frac{-s}{-t} \right) + \frac{\pi^2}{6} \quad (\text{A.6})
\end{aligned}$$

$$\begin{aligned}
&F_4^{2me}(k_1, K_2, k_3, K_4) \\
&= -\frac{1}{\epsilon^2} \left[\left(\frac{\mu^2}{-s} \right)^\epsilon - \left(\frac{\mu^2}{-K_4^2} \right)^\epsilon + \left(\frac{\mu^2}{-t} \right)^\epsilon - \left(\frac{\mu^2}{-K_2^2} \right)^\epsilon - \left(\frac{\mu^2}{-K_4^2} \right)^\epsilon \right] \\
&\quad + \text{Li}_2 \left(1 - \frac{K_2^2}{s} \right) + \text{Li}_2 \left(1 - \frac{K_2^2}{t} \right) + \text{Li}_2 \left(1 - \frac{K_4^2}{s} \right) \\
&\quad + \text{Li}_2 \left(1 - \frac{K_4^2}{t} \right) - \text{Li}_2 \left(1 - \frac{K_2^2 K_4^2}{st} \right) + \frac{1}{2} \log^2 \left(\frac{s}{t} \right) \quad (\text{A.7})
\end{aligned}$$

$$\begin{aligned}
&F_4^{2mh}(k_1, k_2, K_3, K_4) \\
&= -\frac{1}{\epsilon^2} \left[\left(\frac{\mu^2}{-s} \right)^\epsilon + \left(\frac{\mu^2}{-t} \right)^\epsilon - \left(\frac{\mu^2}{-K_3^2} \right)^\epsilon - \left(\frac{\mu^2}{-K_4^2} \right)^\epsilon + \frac{1}{2} \left(-\frac{\mu^2 s}{K_3^2 K_4^2} \right)^\epsilon \right] \\
&\quad + \text{Li}_2 \left(1 - \frac{K_3^2}{t} \right) + \text{Li}_2 \left(1 - \frac{K_4^2}{t} \right) + \frac{1}{2} \log^2 \left(\frac{s}{t} \right) \quad (\text{A.8})
\end{aligned}$$

$$\begin{aligned}
&F_4^{3m}(k_1, K_2, K_3, K_4) \\
&= -\frac{1}{\epsilon^2} \left[\left(\frac{\mu^2}{-s} \right)^\epsilon + \left(\frac{\mu^2}{-t} \right)^\epsilon - \left(\frac{\mu^2}{-K_2^2} \right)^\epsilon - \left(\frac{\mu^2}{-K_3^2} \right)^\epsilon - \left(\frac{\mu^2}{-K_4^2} \right)^\epsilon \right. \\
&\quad \left. + \frac{1}{2} \left(-\frac{\mu^2 t}{K_2^2 K_3^2} \right)^\epsilon + \frac{1}{2} \left(-\frac{\mu^2 s}{K_3^2 K_4^2} \right)^\epsilon \right] + \text{Li}_2 \left(1 - \frac{K_2^2}{s} \right) \\
&\quad + \text{Li}_2 \left(1 - \frac{K_4^2}{t} \right) - \text{Li}_2 \left(1 - \frac{K_2^2 K_4^2}{st} \right) + \frac{1}{2} \log^2 \left(\frac{s}{t} \right) \quad (\text{A.9})
\end{aligned}$$

The Gram determinants are given by

$$\mathcal{G}^{0m} = \mathcal{G}^{1m} = \mathcal{G}^{2mh} = -\frac{1}{2} st, \quad (\text{A.10})$$

$$\mathcal{G}^{2me} = \mathcal{G}^{3m} = -\frac{1}{2} \left(st - K_2^2 K_4^2 \right). \quad (\text{A.11})$$

Triangles are defined by the integral

$$I_3(K_1, K_2, K_3) = i\mu^2 \int \frac{d^{4-2\epsilon} L}{(2\pi)^{4-2\epsilon}} \frac{1}{L^2 (L + K_1)^2 (L - K_3)^2}, \quad (\text{A.12})$$

again with $i\epsilon$ understood. They have the same classification in terms of massive corners as the boxes. As in the box case, we can take factors out of the integral and define triangle functions

$$I_3 = \frac{c_\Gamma}{\mathcal{G}} F_3. \quad (\text{A.13})$$

The triangle functions are (omitting the 3-mass)

$$F_3^{1m}(K_1, k_2, k_3) = \frac{1}{\epsilon^2} \left(\frac{\mu^2}{-K_1^2} \right)^\epsilon \quad (\text{A.14})$$

$$F_3^{2m}(K_1, K_2, k_3) = \frac{1}{\epsilon^2} \left[\left(\frac{\mu^2}{-K_1^2} \right)^\epsilon - \left(\frac{\mu^2}{-K_2^2} \right)^\epsilon \right] \quad (\text{A.15})$$

where

$$\begin{aligned} \mathcal{G}^{1m} &= -K_1^2 \\ \mathcal{G}^{2m} &= -K_1^2 + K_2^2. \end{aligned} \quad (\text{A.16})$$

The bubble integral is given by

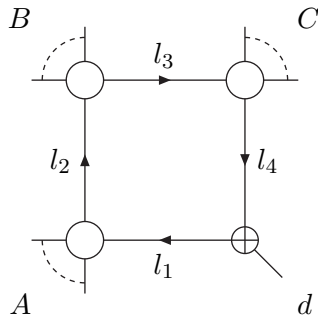
$$\begin{aligned} I_2(K) &= -i\mu^{2\epsilon} \int \frac{d^{4-2\epsilon}L}{(2\pi)^{4-2\epsilon}} \frac{1}{L^2(L+K)^2} \\ &= \frac{c_\Gamma}{\epsilon(1-2\epsilon)} \left(\frac{\mu^2}{-K^2} \right)^\epsilon \\ &= c_\Gamma \left[\frac{1}{\epsilon} + \log \left(\frac{\mu^2}{-K^2} \right) + 2 \right] + \mathcal{O}(\epsilon) \\ &\equiv c_\Gamma F_2(K^2). \end{aligned} \quad (\text{A.17})$$

Appendix B

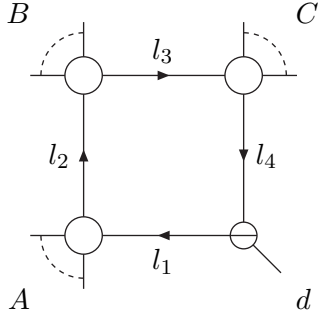
Solutions of Quadruple Cut Constraints

This appendix lists the solutions to the cut constraints in a quadruple cut of a one-loop amplitude. For each number of massive corners there are two solutions which are distinguished by which massless corners are MHV and which are googly-MHV. The two solutions will always be related by flipping ($|\cdot\rangle \leftrightarrow |\cdot\rangle$) but they are all included for clarity. The four-mass cut is not used in this thesis and the reader is referred to the original article for those solutions [59]. It should also be noted that all the solutions here follow from the three-mass cases (which follow from four-mass) by taking external momenta lightlike, but again, all cases are included to benefit maximally from the masslessness of some corners.

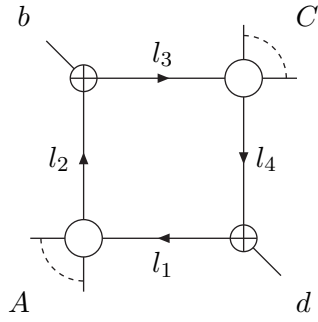
Our conventions are to denote the internal on-shell momenta l_1 through l_4 starting from the bottom of the diagram and moving clockwise around the loop. These momenta point in the clockwise direction. The corners are denoted by A through D starting in the lower left corner. The outgoing momenta at those corners are denoted by the corresponding letter in uppercase when it is massive and in lowercase when it is massless. Massless corners are denoted by \ominus when they are MHV and by \oplus when they are googly-MHV.



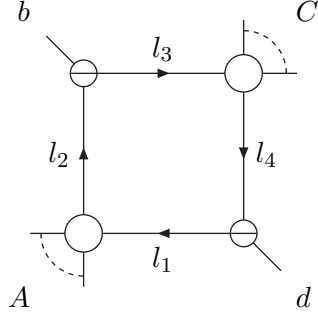
$$\begin{aligned}
 l_1 &= \frac{|d\rangle\langle dCBA|}{\langle dACd\rangle} \\
 l_2 &= \frac{|BCd\rangle\langle dA|}{\langle dACd\rangle} \\
 l_3 &= \frac{|BA d\rangle\langle dC|}{\langle dACd\rangle} \\
 l_4 &= \frac{|d\rangle\langle dABC|}{\langle dACd\rangle}
 \end{aligned}
 \tag{B.1}$$



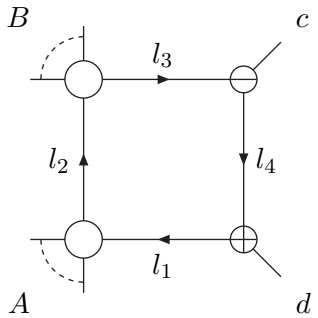
$$\begin{aligned}
 l_1 &= \frac{|ABCd][d|}{[dCA d]} \\
 l_2 &= \frac{|Ad][dCB|}{[dCA d]} \\
 l_3 &= \frac{|Cd][dAB|}{[dCA d]} \\
 l_4 &= \frac{|CBAd][d|}{[dCA d]}
 \end{aligned} \tag{B.2}$$



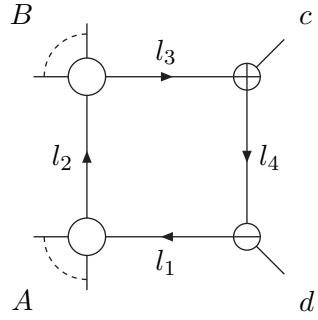
$$\begin{aligned}
 l_1 &= \frac{|d\rangle\langle bA|}{\langle bd\rangle} \\
 l_2 &= \frac{|b\rangle\langle dA|}{\langle bd\rangle} \\
 l_3 &= \frac{|b\rangle\langle dC|}{\langle db\rangle} \\
 l_4 &= \frac{|d\rangle\langle bC|}{\langle db\rangle}
 \end{aligned} \tag{B.3}$$



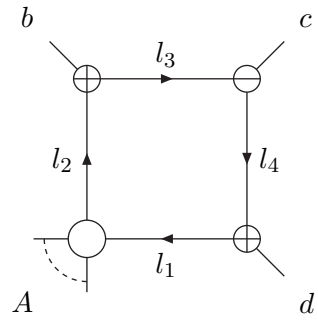
$$\begin{aligned}
 l_1 &= \frac{|Ab][d|}{[db]} \\
 l_2 &= \frac{|Ad][b|}{[db]} \\
 l_3 &= \frac{|Cd][b|}{[bd]} \\
 l_4 &= \frac{|Cb][d|}{[bd]}
 \end{aligned} \tag{B.4}$$



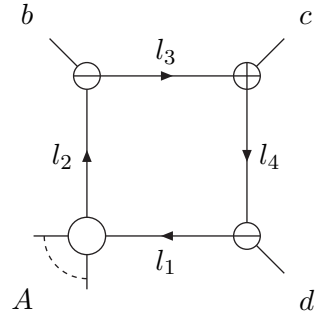
$$\begin{aligned}
 l_1 &= \frac{|d\rangle[cBA|}{\langle dBc\rangle} \\
 l_2 &= \frac{|Bc\rangle\langle dA|}{\langle dAc\rangle} \\
 l_3 &= \frac{|BA d\rangle[c|}{\langle dBc\rangle} \\
 l_4 &= |d\rangle \frac{(B+c)^2}{\langle dAc\rangle} [c|
 \end{aligned} \tag{B.5}$$



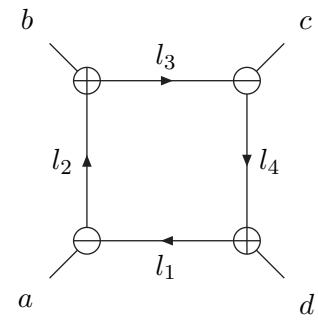
$$\begin{aligned}
 l_1 &= \frac{|ABc\rangle[d]}{\langle cBd\rangle} \\
 l_2 &= \frac{|Ad\rangle\langle cB|}{\langle cAd\rangle} \\
 l_3 &= \frac{|c\rangle[dAB]}{\langle cBd\rangle} \\
 l_4 &= |c\rangle \frac{(B+c)^2}{\langle cAd\rangle} [d]
 \end{aligned} \tag{B.6}$$



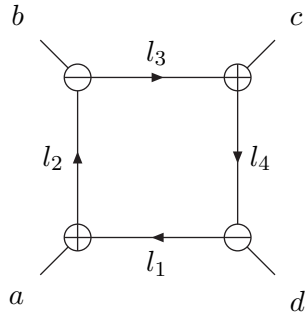
$$\begin{aligned}
 l_1 &= \frac{|d\rangle\langle bA|}{\langle bd\rangle} \\
 l_2 &= \frac{|b\rangle\langle dA|}{\langle bd\rangle} \\
 l_3 &= |b\rangle \frac{\langle dc\rangle}{\langle db\rangle} [c] \\
 l_4 &= |d\rangle \frac{\langle bc\rangle}{\langle db\rangle} [c]
 \end{aligned} \tag{B.7}$$



$$\begin{aligned}
 l_1 &= \frac{|Ab\rangle[d]}{[db]} \\
 l_2 &= \frac{|Ad\rangle[b]}{[db]} \\
 l_3 &= |c\rangle \frac{[cd]}{[bd]} [b] \\
 l_4 &= |c\rangle \frac{[cb]}{[bd]} [d]
 \end{aligned} \tag{B.8}$$



$$\begin{aligned}
 l_1 &= |d\rangle \frac{\langle ba\rangle}{\langle bd\rangle} [a] \\
 l_2 &= |b\rangle \frac{\langle da\rangle}{\langle bd\rangle} [a] \\
 l_3 &= |b\rangle \frac{\langle dc\rangle}{\langle db\rangle} [c] \\
 l_4 &= |d\rangle \frac{\langle bc\rangle}{\langle db\rangle} [c]
 \end{aligned} \tag{B.9}$$



$$\begin{aligned}
 l_1 &= |a\rangle \frac{[ab]}{\langle db\rangle} [d] \\
 l_2 &= |a\rangle \frac{[ad]}{\langle db\rangle} [b] \\
 l_3 &= |c\rangle \frac{[cd]}{[bd]} [b] \\
 l_4 &= |c\rangle \frac{[cb]}{[bd]} [d]
 \end{aligned}$$

(B.10)

Appendix C

Passarino–Veltman Reduction of Cuts

This appendix deals with the reduction of cut integrals which have loop momentum dependence in their numerators. Those needed for this thesis are:

$$I_0 = \int d\mu, \quad I_1^\mu = \int l^\mu d\mu, \quad I_2^{\mu\nu} = \int l^\mu l^\nu d\mu, \quad (\text{C.1})$$

$$J_0 = \int \frac{d\mu}{\langle mlm \rangle}, \quad J_1^\mu = \int \frac{l^\mu}{\langle mlm \rangle} d\mu, \quad J_2^{\mu\nu} = \int \frac{l^\mu l^\nu}{\langle mlm \rangle} d\mu, \quad (\text{C.2})$$

$$J_3^{\mu\nu\kappa} = \int \frac{l^\mu l^\nu l^\kappa}{\langle mlm \rangle} d\mu, \quad (\text{C.3})$$

where

$$d\mu = \delta(l^2) \delta((l-P)^2) d^4l. \quad (\text{C.4})$$

The goal is to express all of these integrals in terms of m^μ , P^μ , $g^{\mu\nu}$, I_0 , and J_0 . The method can be illustrated for J_1^μ by noting Lorentz invariance forces it to take on the structure

$$J_1^\mu = P^\mu I' + m^\mu I'', \quad (\text{C.5})$$

where I' and I'' are scalar integrals. These can be determined from the equations

$$\langle m J_1 m \rangle = \int \frac{\langle m l m \rangle}{\langle m l m \rangle} d\mu = I_0 = \langle m P m \rangle I' \quad (\text{C.6})$$

and

$$2P \cdot J_1 = \int \frac{2P \cdot l}{\langle m l m \rangle} d\mu = P^2 J_0 = 2P^2 I' + \langle m P m \rangle I''. \quad (\text{C.7})$$

Similarly, $I_2^{\mu\nu}$ can be computed by noting that it must take on the form

$$I_2^{\mu\nu} = g^{\mu\nu} I' + P^\mu P^\nu I'' \quad (\text{C.8})$$

and using the contractions

$$I_{2\mu}^\mu = \int l^2 d\mu = 0 = 4I' + P^2 I'', \quad (\text{C.9})$$

and

$$2P^\nu I_2^{\mu\nu} = \int (2P \cdot l) l^\mu d\mu = P^2 I_1^\mu = 2P^\mu I' + 2P^2 P^\mu I'', \quad (\text{C.10})$$

which relate I' and I'' to I_1^μ . This procedure will allow us to construct the required integrals recursively. Rather than deriving the results in detail, we will just note that they are

$$I_1^\mu = \frac{1}{2} P^\mu I_0 \quad (\text{C.11})$$

$$I_2^{\mu\nu} = -\frac{P^2}{12} I_0 + \frac{1}{3} P^\mu P^\nu I_0 \quad (\text{C.12})$$

$$J_1^\mu = \frac{P^\mu}{\langle mPm \rangle} I_0 + m^\mu \left(-\frac{2P^2}{\langle mPm \rangle^2} I_0 + \frac{P^2}{\langle mPm \rangle} J_0 \right) \quad (\text{C.13})$$

$$J_2^{\mu\nu} = -\frac{g^{\mu\nu} P^2}{4\langle mPm \rangle} I_0 + \frac{P^\mu P^\nu}{2\langle mPm \rangle} I_0 + \frac{(m^\mu P^\nu + P^\mu m^\nu) P^2}{2\langle mPm \rangle^2} I_0 \\ + m^\mu m^\nu \left(-\frac{3P^4}{\langle mPm \rangle^3} I_0 + \frac{P^4}{\langle mPm \rangle^2} J_0 \right), \quad (\text{C.14})$$

$$J_3^{\mu\nu\kappa} = -\frac{(g^{\mu\nu} P^\kappa + g^{\nu\kappa} P^\mu + g^{\kappa\mu} P^\nu) P^2}{12\langle mPm \rangle} I_0 + \frac{P^\mu P^\nu P^\kappa}{3\langle mPm \rangle} I_0 \quad (\text{C.15})$$

$$+ \frac{(P^\mu P^\nu m^\kappa + m^\mu P^\nu P^\kappa + P^\mu m^\kappa P^\nu) P^2}{6\langle mPm \rangle^2} I_0 \quad (\text{C.16})$$

$$+ \frac{(m^\mu m^\nu P^\kappa + P^\mu m^\nu m^\kappa + m^\mu P^\nu m^\kappa) P^4}{3\langle mPm \rangle^3} I_0 \quad (\text{C.17})$$

$$- \frac{(g^{\mu\nu} m^\kappa + g^{\nu\kappa} m^\mu + g^{\kappa\mu} m^\nu) P^4}{12\langle mPm \rangle^2} I_0 \quad (\text{C.18})$$

$$+ m^\mu m^\nu m^\kappa \left(-\frac{11}{9} \frac{P^6}{\langle mPm \rangle^4} I_0 + \frac{P^6}{3\langle mPm \rangle^3} J_0 \right). \quad (\text{C.19})$$

Bibliography

- [1] Mohab Abou-Zeid, Christopher M. Hull, and Lionel J. Mason. Einstein supergravity and new twistor string theories. [hep-th/0606272], 2006.
- [2] C. Anastasiou, Z. Bern, Lance J. Dixon, and D. A. Kosower. Planar amplitudes in maximally supersymmetric Yang–Mills theory. *Phys. Rev. Lett.*, 91:251602, 2003.
- [3] Charalampos Anastasiou, Ruth Britto, Bo Feng, Zoltan Kunszt, and Pierpaolo Mastrolia. D-dimensional unitarity cut method. *Phys. Lett.*, B645:213–216, 2007.
- [4] Charalampos Anastasiou, Ruth Britto, Bo Feng, Zoltan Kunszt, and Pierpaolo Mastrolia. Unitarity cuts and reduction to master integrals in d dimensions for one-loop amplitudes. *JHEP*, 03:111, 2007.
- [5] Nima Arkani-Hamed and Jared Kaplan. On tree amplitudes in gauge theory and gravity. [arXiv:0801.2385].
- [6] S. D. Badger and E. W. Nigel Glover. One-loop helicity amplitudes for $H \rightarrow$ gluons: The all-minus configuration. *Nucl. Phys. Proc. Suppl.*, 160:71–75, 2006.
- [7] S. D. Badger, E. W. Nigel Glover, V. V. Khoze, and P. Svrček. Recursion relations for gauge theory amplitudes with massive particles. *JHEP*, 07:025, 2005.
- [8] S. D. Badger, E. W. Nigel Glover, and Valentin V. Khoze. MHV rules for Higgs plus multi-parton amplitudes. *JHEP*, 03:023, 2005.
- [9] S. D. Badger, E. W. Nigel Glover, and Valentin V. Khoze. Recursion relations for gauge theory amplitudes with massive vector bosons and fermions. *JHEP*, 01:066, 2006.
- [10] S. D. Badger, E. W. Nigel Glover, and Kasper Risager. One-loop phi-MHV amplitudes using the unitarity bootstrap. *JHEP*, 07:066, 2007.

- [11] James Bedford, Andreas Brandhuber, Bill J. Spence, and Gabriele Travaglini. Non-supersymmetric loop amplitudes and MHV vertices. *Nucl. Phys.*, B712:59–85, 2005.
- [12] James Bedford, Andreas Brandhuber, Bill J. Spence, and Gabriele Travaglini. A recursion relation for gravity amplitudes. *Nucl. Phys.*, B721:98–110, 2005.
- [13] James Bedford, Andreas Brandhuber, Bill J. Spence, and Gabriele Travaglini. A twistor approach to one-loop amplitudes in N=1 supersymmetric Yang–Mills theory. *Nucl. Phys.*, B706:100–126, 2005.
- [14] Paolo Benincasa, Camille Boucher-Veronneau, and Freddy Cachazo. Taming tree amplitudes in general relativity. [hep-th/0702032], 2007.
- [15] Paolo Benincasa and Freddy Cachazo. Consistency conditions on the S-matrix of massless particles. [arXiv:0705.4305], 2007.
- [16] Frits A. Berends and W. T. Giele. Recursive calculations for processes with n gluons. *Nucl. Phys.*, B306:759, 1988.
- [17] Frits A. Berends, W. T. Giele, and H. Kuijf. On relations between multi-gluon and multigraviton scattering. *Phys. Lett.*, B211:91, 1988.
- [18] C. F. Berger, Z. Bern, L. J. Dixon, F. Febres Cordero, D. Forde, H. Ita, D. A. Kosower, and D. Maître. An automated implementation of on-shell methods for one-loop amplitudes. [arXiv:0803.4180].
- [19] Carola F. Berger, Zvi Bern, Lance J. Dixon, Darren Forde, and David A. Kosower. Bootstrapping one-loop QCD amplitudes with general helicities. *Phys. Rev.*, D74:036009, 2006.
- [20] Carola F. Berger, Vittorio Del Duca, and Lance J. Dixon. Recursive construction of Higgs+multiparton loop amplitudes: The last of the phi-nite loop amplitudes. *Phys. Rev.*, D74:094021, 2006. Erratum *ibid.* D76:099901, 2007.
- [21] Z. Bern, J. J. Carrasco, D. Forde, H. Ita, and H. Johansson. Unexpected cancellations in gravity theories. [arXiv:0707.1035], 2007.
- [22] Z. Bern, A. De Freitas, and H. L. Wong. On the coupling of gravitons to matter. *Phys. Rev. Lett.*, 84:3531, 2000.
- [23] Z. Bern, Lance J. Dixon, D. C. Dunbar, M. Perelstein, and J. S. Rozowsky. On the relationship between Yang–Mills theory and gravity and its implication for ultraviolet divergences. *Nucl. Phys.*, B530:401–456, 1998.

- [24] Z. Bern, Lance J. Dixon, M. Perelstein, and J. S. Rozowsky. Multi-leg one-loop gravity amplitudes from gauge theory. *Nucl. Phys.*, B546:423–479, 1999.
- [25] Z. Bern et al. Three-loop superfiniteness of N=8 supergravity. *Phys. Rev. Lett.*, 98:161303, 2007.
- [26] Z. Bern and A. G. Morgan. Massive loop amplitudes from unitarity. *Nucl. Phys.*, B467:479–509, 1996.
- [27] Zvi Bern. A compact representation of the one loop N gluon amplitude. *Phys. Lett.*, B296:85–94, 1992.
- [28] Zvi Bern, N. E. J. Bjerrum-Bohr, and David C. Dunbar. Inherited twistor-space structure of gravity loop amplitudes. *JHEP*, 05:056, 2005.
- [29] Zvi Bern, N. E. J. Bjerrum-Bohr, David C. Dunbar, and Harald Ita. Recursive calculation of one-loop QCD integral coefficients. *JHEP*, 11:027, 2005.
- [30] Zvi Bern and Gordon Chalmers. Factorization in one loop gauge theory. *Nucl. Phys.*, B447:465–518, 1995.
- [31] Zvi Bern, Vittorio Del Duca, Lance J. Dixon, and David A. Kosower. All non-maximally-helicity-violating one-loop seven-gluon amplitudes in N=4 super-Yang–Mills theory. *Phys. Rev.*, D71:045006, 2005.
- [32] Zvi Bern, Vittorio Del Duca, William B. Kilgore, and Carl R. Schmidt. The infrared behavior of one-loop QCD amplitudes at next-to-next-to-leading order. *Phys. Rev.*, D60:116001, 1999.
- [33] Zvi Bern, Lance J. Dixon, David C. Dunbar, and David A. Kosower. One loop n point gauge theory amplitudes, unitarity and collinear limits. *Nucl. Phys.*, B425:217–260, 1994.
- [34] Zvi Bern, Lance J. Dixon, David C. Dunbar, and David A. Kosower. Fusing gauge theory tree amplitudes into loop amplitudes. *Nucl. Phys.*, B435:59–101, 1995.
- [35] Zvi Bern, Lance J. Dixon, David C. Dunbar, and David A. Kosower. One-loop self-dual and N=4 superYang–Mills. *Phys. Lett.*, B394:105–115, 1997.
- [36] Zvi Bern, Lance J. Dixon, and David A. Kosower. Dimensionally regulated pentagon integrals. *Nucl. Phys.*, B412:751–816, 1994.
- [37] Zvi Bern, Lance J. Dixon, and David A. Kosower. All next-to-maximally helicity-violating one-loop gluon amplitudes in N=4 super-Yang–Mills theory. *Phys. Rev.*, D72:045014, 2005.

- [38] Zvi Bern, Lance J. Dixon, and David A. Kosower. The last of the finite loop amplitudes in QCD. *Phys. Rev.*, D72:125003, 2005.
- [39] Zvi Bern, Lance J. Dixon, and David A. Kosower. On-shell recurrence relations for one-loop QCD amplitudes. *Phys. Rev.*, D71:105013, 2005.
- [40] Zvi Bern, Lance J. Dixon, and David A. Kosower. Bootstrapping multiparton loop amplitudes in QCD. *Phys. Rev.*, D73:065013, 2006.
- [41] Zvi Bern, Lance J. Dixon, and Vladimir A. Smirnov. Iteration of planar amplitudes in maximally supersymmetric Yang–Mills theory at three loops and beyond. *Phys. Rev.*, D72:085001, 2005.
- [42] Zvi Bern and David C. Dunbar. A mapping between Feynman and string motivated one loop rules in gauge theories. *Nucl. Phys.*, B379:562–601, 1992.
- [43] Zvi Bern, David C. Dunbar, and Tokuzo Shimada. String based methods in perturbative gravity. *Phys. Lett.*, B312:277–284, 1993.
- [44] Zvi Bern, Darren Forde, David A. Kosower, and Pierpaolo Mastrolia. Twistor-inspired construction of electroweak vector boson currents. *Phys. Rev.*, D72:025006, 2005.
- [45] Zvi Bern and David A. Kosower. Efficient calculation of one loop QCD amplitudes. *Phys. Rev. Lett.*, 66:1669–1672, 1991.
- [46] Zvi Bern and David A. Kosower. The computation of loop amplitudes in gauge theories. *Nucl. Phys.*, B379:451–561, 1992.
- [47] N. E. J. Bjerrum-Bohr, John F. Donoghue, and Barry R. Holstein. Quantum gravitational corrections to the nonrelativistic scattering potential of two masses. *Phys. Rev.*, D67:084033, 2003.
- [48] N. E. J. Bjerrum-Bohr, David C. Dunbar, and Harald Ita. Six-point one-loop N=8 supergravity NMHV amplitudes and their IR behaviour. *Phys. Lett.*, B621:183–194, 2005.
- [49] N. E. J. Bjerrum-Bohr, David C. Dunbar, Harald Ita, Warren B. Perkins, and Kasper Risager. MHV-vertices for gravity amplitudes. *JHEP*, 01:009, 2006.
- [50] N. E. J. Bjerrum-Bohr, David C. Dunbar, Harald Ita, Warren B. Perkins, and Kasper Risager. The no-triangle hypothesis for N=8 supergravity. *JHEP*, 12:072, 2006.
- [51] N. E. J. Bjerrum-Bohr, David C. Dunbar, and Warren B. Perkins. Analytic structure of three-mass triangle coefficients. [arXiv:0709.2086], 2007.

- [52] Rutger Boels, Lionel Mason, and David Skinner. From twistor actions to MHV diagrams. *Phys. Lett.*, B648:90–96, 2007.
- [53] Andreas Brandhuber, Simon McNamara, Bill Spence, and Gabriele Travaglini. Recursion relations for one-loop gravity amplitudes. *JHEP*, 03:029, 2007.
- [54] Andreas Brandhuber, Simon McNamara, Bill J. Spence, and Gabriele Travaglini. Loop amplitudes in pure Yang–Mills from generalised unitarity. *JHEP*, 10:011, 2005.
- [55] Andreas Brandhuber, Bill Spence, and Gabriele Travaglini. From trees to loops and back. *JHEP*, 01:142, 2006.
- [56] Andreas Brandhuber, Bill Spence, Gabriele Travaglini, and Konstantinos Zoubos. One-loop MHV rules and pure Yang–Mills. *JHEP*, 07:002, 2007.
- [57] Andreas Brandhuber, Bill J. Spence, and Gabriele Travaglini. One-loop gauge theory amplitudes in N=4 super Yang–Mills from MHV vertices. *Nucl. Phys.*, B706:150–180, 2005.
- [58] Ruth Britto, Evgeny Buchbinder, Freddy Cachazo, and Bo Feng. One-loop amplitudes of gluons in SQCD. *Phys. Rev.*, D72:065012, 2005.
- [59] Ruth Britto, Freddy Cachazo, and Bo Feng. Generalized unitarity and one-loop amplitudes in N=4 super-Yang–Mills. *Nucl. Phys.*, B725:275–305, 2005.
- [60] Ruth Britto, Freddy Cachazo, and Bo Feng. New recursion relations for tree amplitudes of gluons. *Nucl. Phys.*, B715:499–522, 2005.
- [61] Ruth Britto, Freddy Cachazo, Bo Feng, and Edward Witten. Direct proof of tree-level recursion relation in Yang–Mills theory. *Phys. Rev. Lett.*, 94:181602, 2005.
- [62] Ruth Britto and Bo Feng. Unitarity cuts with massive propagators and algebraic expressions for coefficients. *Phys. Rev.*, D75:105006, 2007.
- [63] Ruth Britto, Bo Feng, and Pierpaolo Mastrolia. The cut-constructible part of QCD amplitudes. *Phys. Rev.*, D73:105004, 2006.
- [64] Evgeny I. Buchbinder and Freddy Cachazo. Two-loop amplitudes of gluons and octa-cuts in N=4 super Yang–Mills. *JHEP*, 11:036, 2005.
- [65] C. Buttar et al. Les houches physics at TeV colliders 2005, standard model, QCD, EW, and Higgs working group: Summary report. 2006.
- [66] Freddy Cachazo and David Skinner. On the structure of scattering amplitudes in N=4 super Yang–Mills and N=8 supergravity. 2008. [arXiv:0801.4574].

- [67] Freddy Cachazo and Peter Svrček. Lectures on twistor strings and perturbative Yang–Mills theory. *PoS*, RTN2005:004, 2005.
- [68] Freddy Cachazo and Peter Svrček. Tree level recursion relations in general relativity. [hep-th/0502160], 2005.
- [69] Freddy Cachazo, Peter Svrček, and Edward Witten. MHV vertices and tree amplitudes in gauge theory. *JHEP*, 09:006, 2004.
- [70] John M. Campbell, R. Keith Ellis, and Giulia Zanderighi. Next-to-leading order predictions for $WW + 1$ jet distributions at the LHC. 2007.
- [71] Stefano Catani. The singular behaviour of QCD amplitudes at two-loop order. *Phys. Lett.*, B427:161–171, 1998.
- [72] E. Cremmer and B. Julia. The N=8 supergravity theory. 1. The Lagrangian. *Phys. Lett.*, B80:48, 1978.
- [73] E. Cremmer and B. Julia. The SO(8) supergravity. *Nucl. Phys.*, B159:141, 1979.
- [74] E. Cremmer, B. Julia, and Joel Scherk. Supergravity theory in 11 dimensions. *Phys. Lett.*, B76:409–412, 1978.
- [75] S. Dittmaier, S. Kallweit, and P. Uwer. NLO QCD corrections to WW +jet production at hadron colliders. *Phys. Rev. Lett.*, 100:062003, 2008.
- [76] Lance J. Dixon. Calculating scattering amplitudes efficiently. [hep-ph/9601359], 1996.
- [77] Lance J. Dixon, E. W. Nigel Glover, and Valentin V. Khoze. MHV rules for Higgs plus multi-gluon amplitudes. *JHEP*, 12:015, 2004.
- [78] John F. Donoghue. General relativity as an effective field theory: The leading quantum corrections. *Phys. Rev.*, D50:3874–3888, 1994.
- [79] John F. Donoghue. Leading quantum correction to the Newtonian potential. *Phys. Rev. Lett.*, 72:2996–2999, 1994.
- [80] David C. Dunbar and Paul S. Norridge. Calculation of graviton scattering amplitudes using string based methods. *Nucl. Phys.*, B433:181–208, 1995.
- [81] David C. Dunbar and Paul S. Norridge. Infinities within graviton scattering amplitudes. *Class. Quant. Grav.*, 14:351–365, 1997.
- [82] G. Duplanić and B. Nizić. Dimensionally regulated one loop box scalar integrals with massless internal lines. *Eur.Phys.J.*, C20:357-370, 2001. [arXiv:hep-ph/0006249].

- [83] R.J. Eden, P.V. Landshoff, and D.I. Olive. The Analytic S-Matrix. Cambridge: Cambridge University Press (1966).
- [84] R. Keith Ellis, W. T. Giele, and G. Zanderighi. Virtual QCD corrections to Higgs boson plus four parton processes. *Phys. Rev.*, D72:054018, 2005.
- [85] R. K. Ellis, W. T. Giele, and Z. Kunszt. A numerical unitarity formalism for evaluating one-loop amplitudes. *JHEP*, 0803:003, 2008. [arXiv:0708.2398].
- [86] James H. Eittle and Tim R. Morris. Structure of the MHV-rules Lagrangian. *JHEP*, 08:003, 2006.
- [87] R. P. Feynman and (ed.) Brown, L. M. Selected papers of Richard Feynman: With commentary. Singapore, Singapore: World Scientific (2000) 999 p.
- [88] Darren Forde. Direct extraction of one-loop integral coefficients. *Phys. Rev.*, D75:125019, 2007.
- [89] Darren Forde and David A. Kosower. All-multiplicity one-loop corrections to MHV amplitudes in QCD. *Phys. Rev.*, D73:061701, 2006.
- [90] George Georgiou, E. W. Nigel Glover, and Valentin V. Khoze. Non-MHV tree amplitudes in gauge theory. *JHEP*, 07:048, 2004.
- [91] George Georgiou and Valentin V. Khoze. Tree amplitudes in gauge theory as scalar MHV diagrams. *JHEP*, 05:070, 2004.
- [92] W. T. Giele and E. W. Nigel Glover. Higher order corrections to jet cross-sections in $e^+ e^-$ annihilation. *Phys. Rev.*, D46:1980–2010, 1992.
- [93] A. Gorsky and A. Rosly. From Yang–Mills Lagrangian to MHV diagrams. *JHEP*, 0601:101, 2006. [arXiv:hep-th/0510111].
- [94] Michael B. Green, John H. Schwarz, and Lars Brink. N=4 Yang–Mills and N=8 supergravity as limits of string theories. *Nucl. Phys.*, B198:474–492, 1982.
- [95] Marcus T. Grisaru and H. N. Pendleton. Some properties of scattering amplitudes in supersymmetric theories. *Nucl. Phys.*, B124:81, 1977.
- [96] Marcus T. Grisaru, H. N. Pendleton, and P. van Nieuwenhuizen. Supergravity and the S matrix. *Phys. Rev.*, D15:996, 1977.
- [97] Takeo Inami, Takahiro Kubota, and Yasuhiro Okada. Effective gauge theory and the effect of heavy quarks in Higgs boson decays. *Z. Phys.*, C18:69, 1983.

- [98] Aggeliki Kanaki and Costas G. Papadopoulos. HELAC: A package to compute electroweak helicity amplitudes. *Comput. Phys. Commun.*, 132:306–315, 2000.
- [99] H. Kawai, D. C. Lewellen, and S. H. H. Tye. A relation between tree amplitudes of closed and open strings. *Nucl. Phys.*, B269:1, 1986.
- [100] J. R. Klauder. Magic without magic - John Archibald Wheeler. A collection of essays in honor of his 60th birthday. San Francisco 1972, 491p.
- [101] Ronald Kleiss and Hans Kuijf. Multi-gluon cross-sections and five jet production at hadron colliders. *Nucl. Phys.*, B312:616, 1989.
- [102] David A. Kosower. Next-to-maximal helicity violating amplitudes in gauge theory. *Phys. Rev.*, D71:045007, 2005.
- [103] F. Krauss, R. Kuhn, and G. Soff. AMEGIC++ 1.0: A matrix element generator in C++. *JHEP*, 02:044, 2002.
- [104] Z. Kunszt. Combined use of the Calkul method and N=1 supersymmetry to calculate QCD six parton processes. *Nucl. Phys.*, B271:333, 1986.
- [105] Zoltan Kunszt, Adrian Signer, and Zoltan Trocsanyi. Singular terms of helicity amplitudes at one loop in QCD and the soft limit of the cross-sections of multiparton processes. *Nucl. Phys.*, B420:550–564, 1994.
- [106] A. Lazopoulos, K. Melnikov and F. Petriello. QCD corrections to tri-boson production. *Phys.Rev.*, D76:014001, 2007. [arXiv:hep-ph/0703273].
- [107] Ming-xing Luo and Cong-kao Wen. Compact formulas for all tree amplitudes of six partons. *Phys. Rev.*, D71:091501, 2005.
- [108] Ming-xing Luo and Cong-kao Wen. Recursion relations for tree amplitudes in super gauge theories. *JHEP*, 03:004, 2005.
- [109] D. Maître and P. Mastrolia. S@M, a Mathematica implementation of the spinor-helicity formalism. [arXiv:0710.5559], 2007.
- [110] Fabio Maltoni and Tim Stelzer. MadEvent: Automatic event generation with MadGraph. *JHEP*, 02:027, 2003.
- [111] Michelangelo L. Mangano, Mauro Moretti, Fulvio Piccinini, Roberto Pittau, and Antonio D. Polosa. ALPGEN, a generator for hard multiparton processes in hadronic collisions. *JHEP*, 07:001, 2003.
- [112] Michelangelo L. Mangano and Stephen J. Parke. Multiparton amplitudes in gauge theories. *Phys. Rept.*, 200:301–367, 1991.
- [113] Paul Mansfield. The Lagrangian origin of MHV rules. *JHEP*, 03:037, 2006.

- [114] Pierpaolo Mastrolia. On triple-cut of scattering amplitudes. *Phys. Lett.*, B644:272–283, 2007.
- [115] V. P. Nair. A current algebra for some gauge theory amplitudes. *Phys. Lett.*, B214:215, 1988.
- [116] V. P. Nair. A note on graviton amplitudes for new twistor string theories. [arXiv:0710.4961], 2007.
- [117] K. J. Ozeren and W. J. Stirling. MHV techniques for QED processes. *JHEP*, 11:016, 2005.
- [118] Giovanni Ossola, Costas G. Papadopoulos, and Roberto Pittau. Reducing full one-loop amplitudes to scalar integrals at the integrand level. *Nucl.Phys.*, B763:147-169, 2007. [arXiv:hep-ph/0609007].
- [119] Stephen J. Parke and T. R. Taylor. Perturbative QCD utilizing extended supersymmetry. *Phys. Lett.*, B157:81, 1985.
- [120] Stephen J. Parke and T. R. Taylor. An amplitude for n gluon scattering. *Phys. Rev. Lett.*, 56:2459, 1986.
- [121] G. Passarino and M. J. G. Veltman. One loop corrections for $e^+ e^-$ annihilation into $\mu^+ \mu^-$ in the Weinberg model. *Nucl. Phys.*, B160:151, 1979.
- [122] Michael E. Peskin and D. V. Schroeder. An Introduction to Quantum Field Theory. Reading, USA: Addison-Wesley (1995) 842 p.
- [123] A. Pukhov et al. CompHEP: A package for evaluation of Feynman diagrams and integration over multi-particle phase space. User’s manual for version 33. 1999.
- [124] Callum Quigley and Moshe Rozali. One-loop MHV amplitudes in supersymmetric gauge theories. *JHEP*, 01:053, 2005.
- [125] Callum Quigley and Moshe Rozali. Recursion relations, helicity amplitudes and dimensional regularization. *JHEP*, 03:004, 2006.
- [126] Kasper Risager. A direct proof of the CSW rules. *JHEP*, 12:003, 2005.
- [127] Kasper Risager, Steven J. Bidder, and Warren B. Perkins. One-loop NMHV amplitudes involving gluinos and scalars in $N=4$ gauge theory. *JHEP*, 10:003, 2005.
- [128] Radu Roiban, Marcus Spradlin and Anastasia Volovich. Dissolving $N=4$ loop amplitudes into QCD tree amplitudes. *Phys. Rev. Lett.*, 94:102002, 2005.

- [129] Carl R. Schmidt. $H \rightarrow g g g$ ($g q$ anti- q) at two loops in the large- $M(t)$ limit. *Phys. Lett.*, B413:391–395, 1997.
- [130] Mikhail A. Shifman, A. I. Vainshtein, M. B. Voloshin, and Valentin I. Zakharov. Low-energy theorems for Higgs boson couplings to photons. *Sov. J. Nucl. Phys.*, 30:711–716, 1979.
- [131] Steven Weinberg. Phenomenological Lagrangians. *Physica*, A96:327, 1979.
- [132] Frank Wilczek. Decays of heavy vector mesons into Higgs particles. *Phys. Rev. Lett.*, 39:1304, 1977.
- [133] Edward Witten. Perturbative gauge theory as a string theory in twistor space. *Commun. Math. Phys.*, 252:189–258, 2004.
- [134] Jun-Bao Wu and Chuan-Jie Zhu. MHV vertices and fermionic scattering amplitudes in gauge theory with quarks and gluinos. *JHEP*, 09:063, 2004.
- [135] Jun-Bao Wu and Chuan-Jie Zhu. MHV vertices and scattering amplitudes in gauge theory. *JHEP*, 07:032, 2004.
- [136] Chuan-Jie Zhu. The googly amplitudes in gauge theory. *JHEP*, 04:032, 2004.